

Heterogeneous integration and applications in electronics



T. Baron,

Grenoble Alpes University

CNRS/LTM

thierry.baron@cea.fr



What kind of functionalities can be addresses by nanomaterials and nanostructures grown on a substrate ?

How to integrate nanomaterials in devices with an added value ?



OUTLINE

- ❑ Nanocrystals for memory devices
- ❑ Nanowires for low power devices, capacitors and sensors
- ❑ Thin films : SiGe (D. Dutartre) and III-V (B. Kunert) on a Si platform for NMOS and PMOS FET



OUTLINE

- ❑ Nanocrystals for memory devices
 - Principle
 - Nanocrystal growth
 - Integration in devices

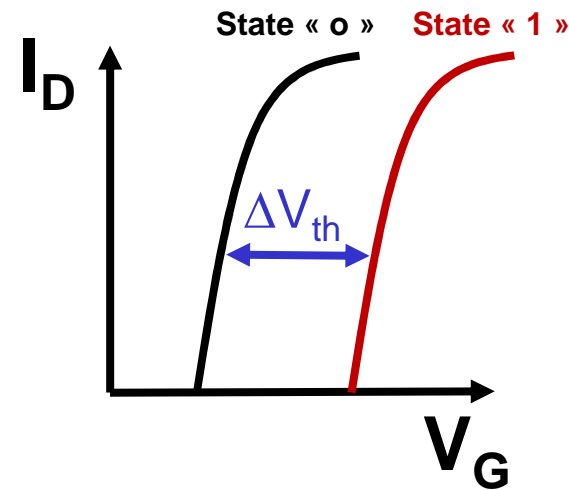
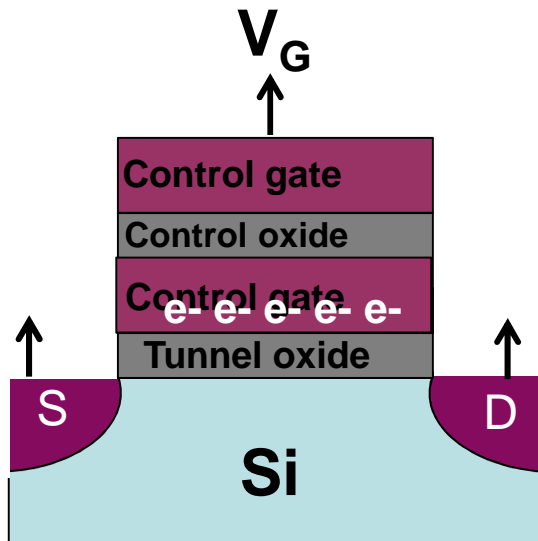
- ❑ Nanowires for low power devices, capacitors and sensors

- ❑ SiGe and InGaAs thin films for NMOS and PMOS FET



Principles

- Flash memory = MOSFET + floating gate
- Electron storage in floating gate → shift I_D - V_G characteristic

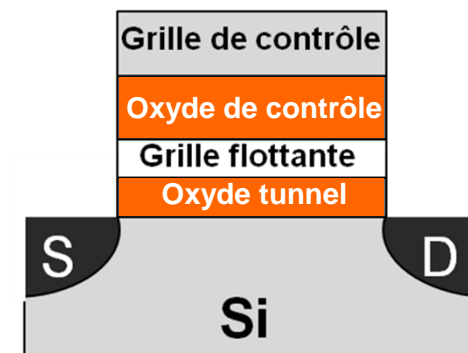


- Two different states due to the presence of charges in the floating gate

Standard Flash memories :

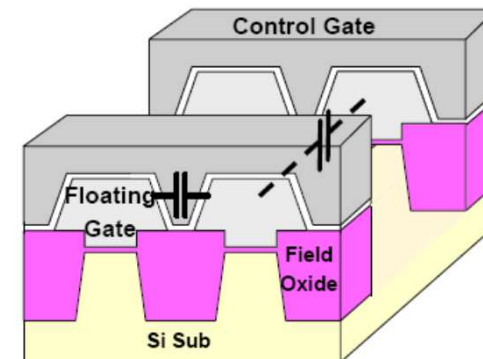
□ Limitation of reducing the thicknesses of dielectric [1] :

- ✓ tunnel oxide $t > 6\text{nm}$ (SILC)
- ✓ Control oxide EOT $> 10\text{nm}$

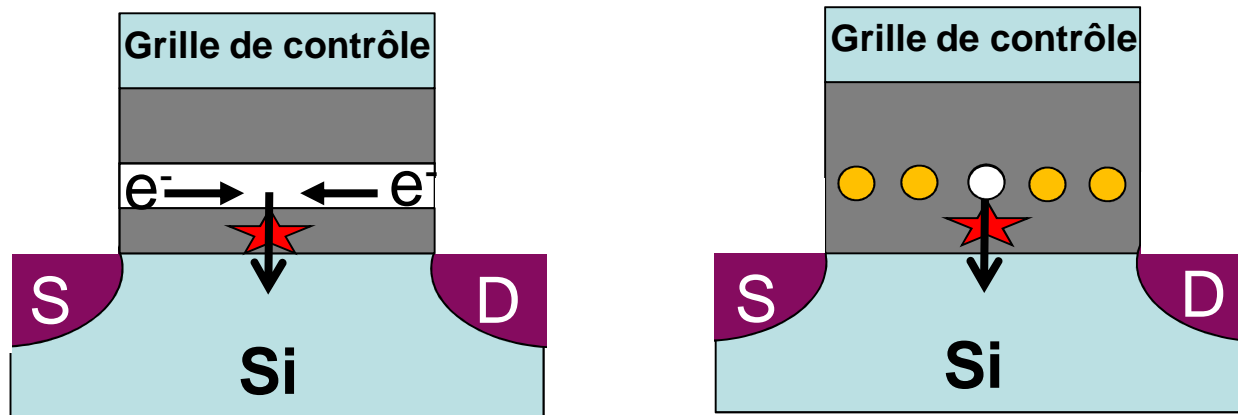


□ Spacing reduction between memory cells :

- ✓ Parasitic coupling between floating gate [2]
- ✓ Decrease of the capacitive coupling between the floating gate and the channel (lateral extension of the gate)



- Decrease of the tunnel oxide without compromise with charge retention :



- Decrease of the parasitic capacitive coupling between cells [1]
- Multilevels storage
- Decrease of the fabrication cost by decreasing the number of lithographic masks needed
- **NC advantages : more robust devices against defects**



OUTLINE

- ❑ Nanocrystals for memory devices
 - Principle
 - Nanocrystal growth
 - Integration in devices

- ❑ Nanowires for low power devices, capacitors and sensors

- ❑ SiGe and InGaAs thin films for NMOS and PMOS FET



Choice of CVD for nanocrystal growth

- ❑ Uniform distribution over large areas
- ❑ Uniform thickness and composition over large areas
- ❑ Selective area deposition because of different activation energies for reaction with different surfaces
- ❑ Objectives : high nc density and low size dispersion
 - For high charge storage and low device variability



CVD

Thermal
CVD

APCVD
LPCVD
HTCVD
MTCVD

Plasma
CVD

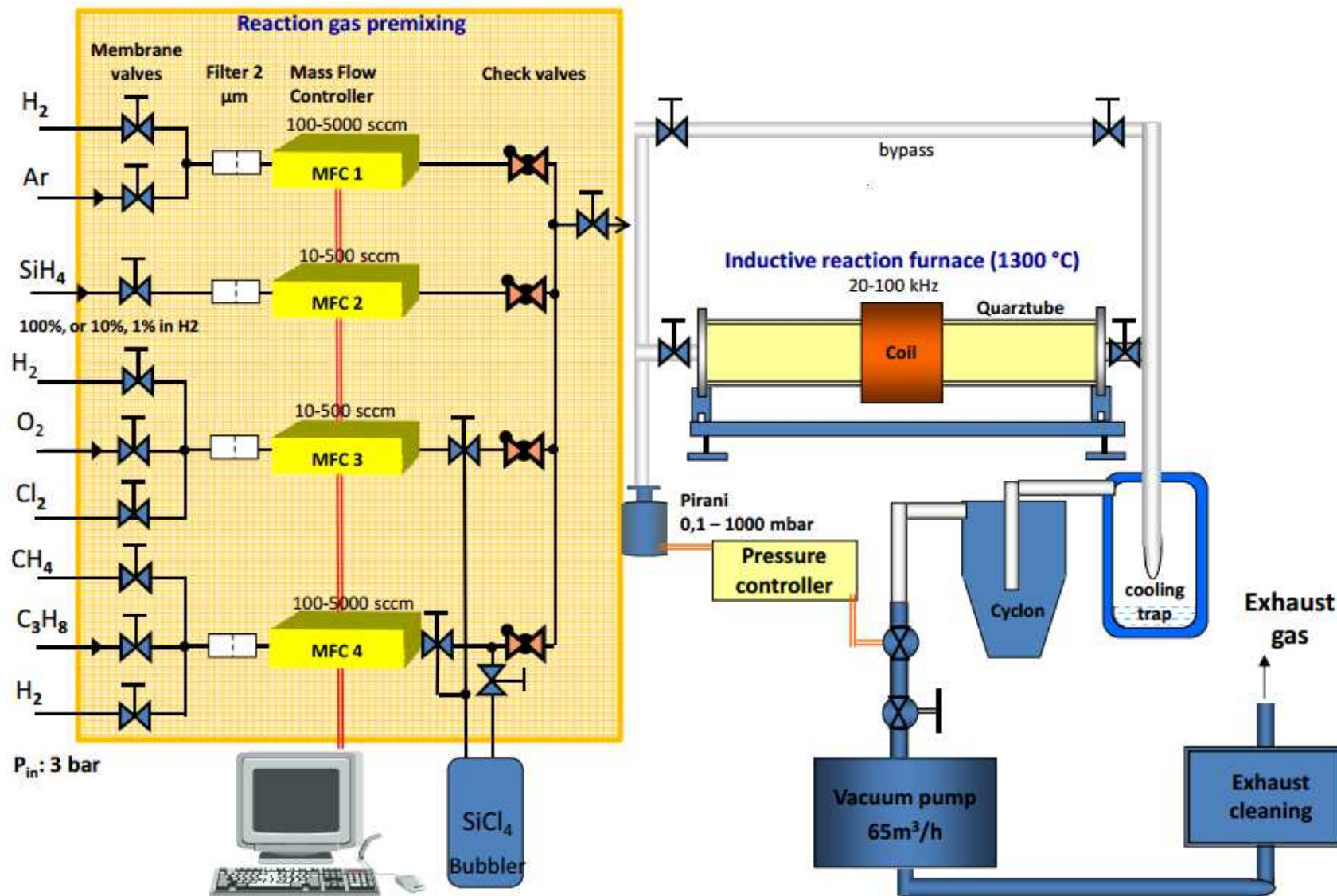
PECVD
DC CVD
RF CVD
MW CVD

Photo
CVD

Catalytic
CVD

Hot-wire
CNT

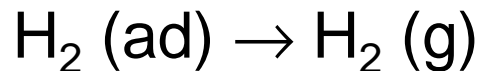
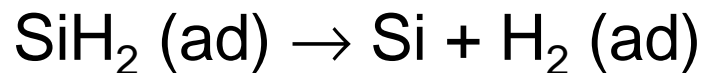
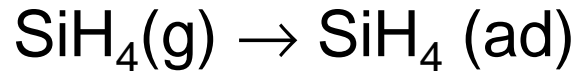
CVI





Si deposition by CVD on amorphous substrates

□ Silane dissociation reactions :



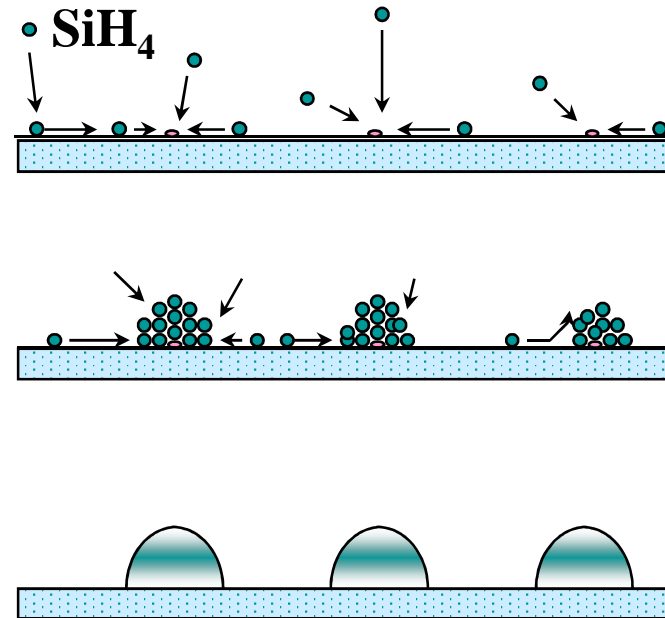
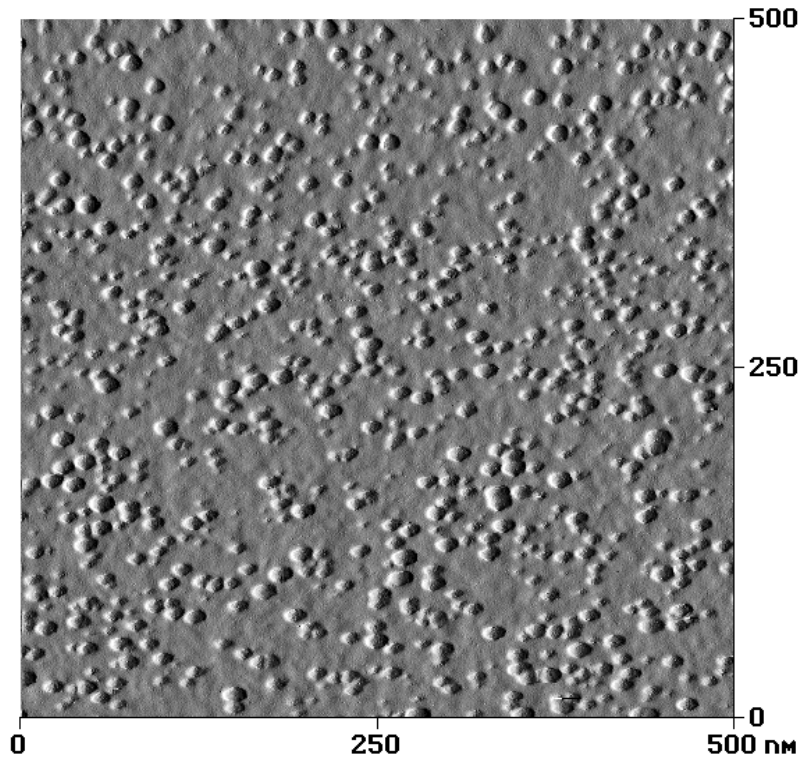
□ $V_{\text{dépôt}} = C P^a \exp(-E_a/kT)$

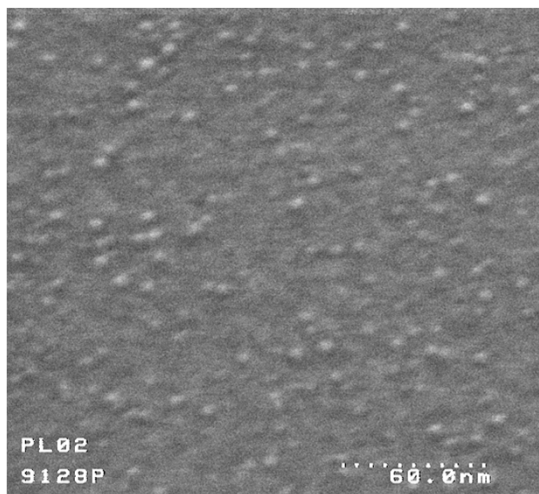
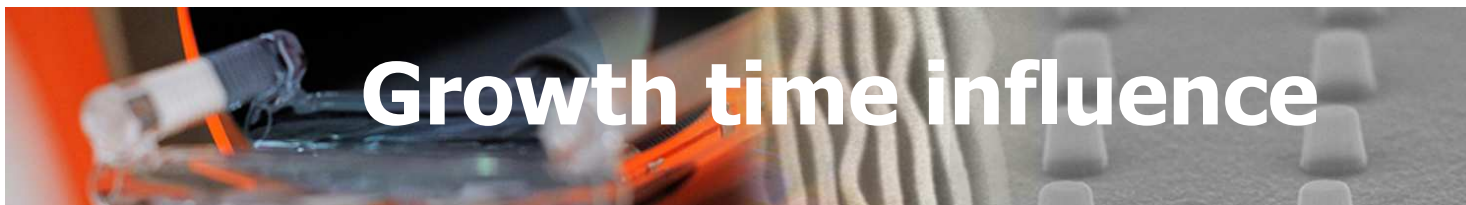
□ Si nanocrystals nucleation study on amorphous substrate:

➤ Experimental parameters (T , P_{SiH_4})

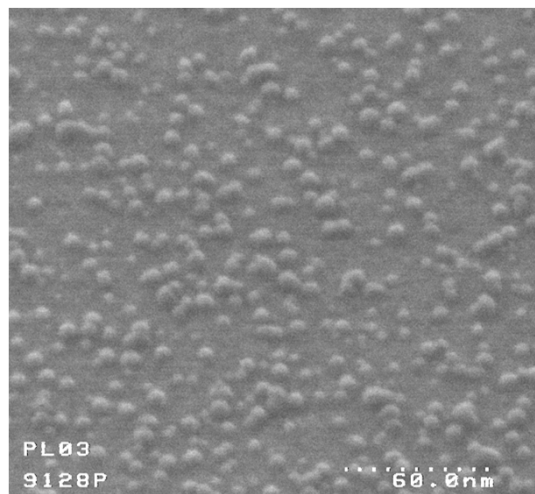
➤ Chemical nature of the substrate (SiO_2 , Si_3N_4 , Al_2O_3)

Volmer Weber 3D growth mode

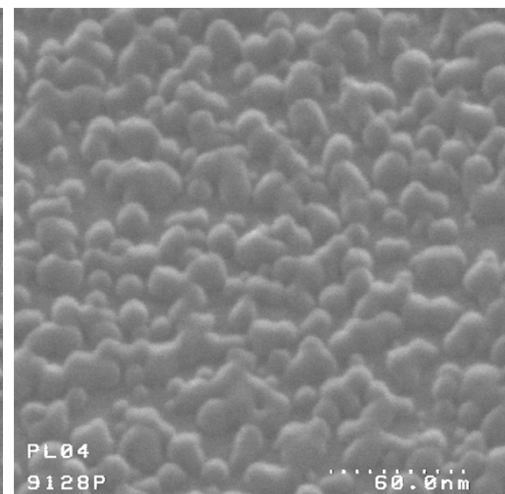




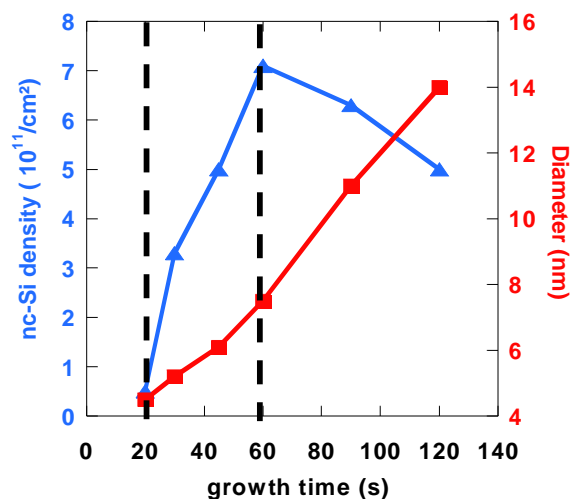
T = 30s



60s

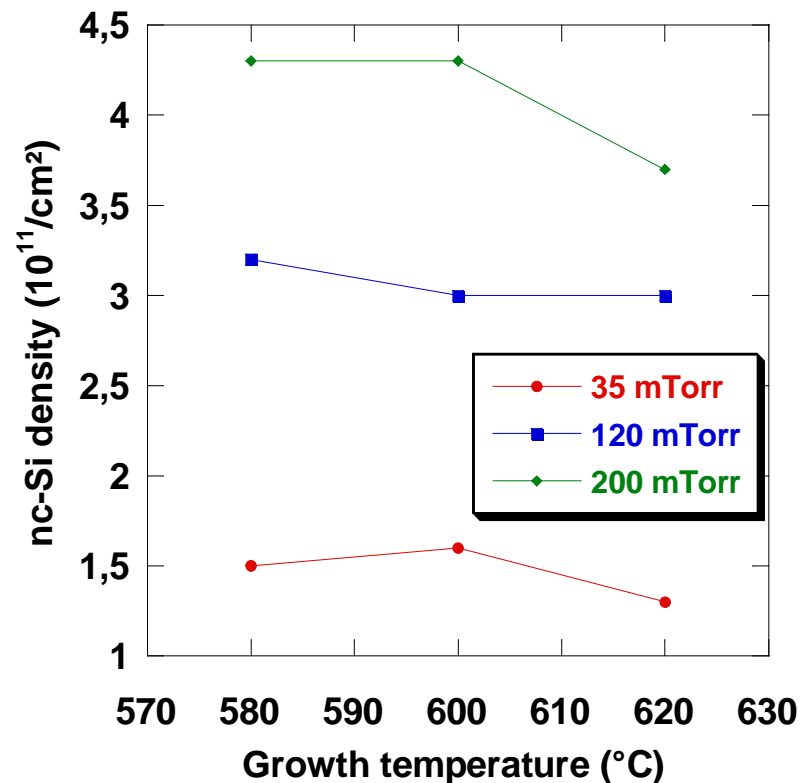
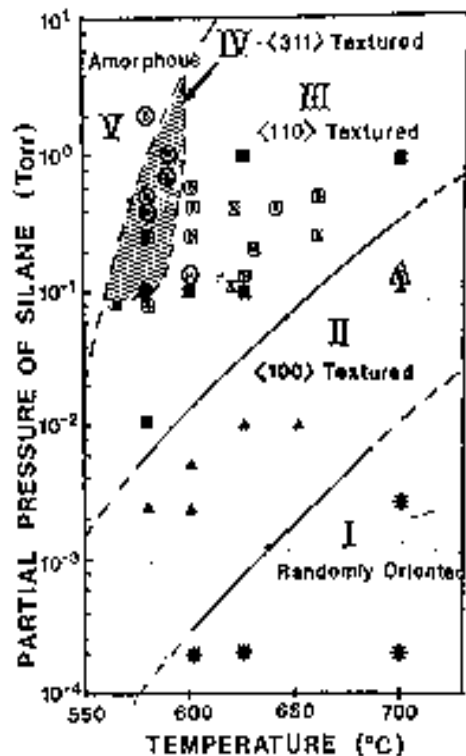


120s

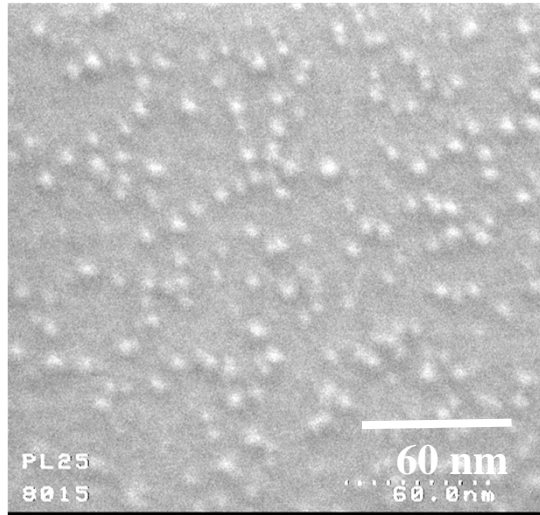


P_{SiH_4} and growth temperature constants

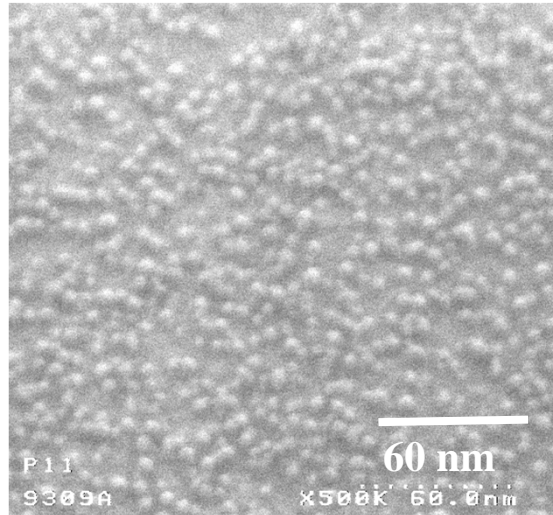
1. Nucleation
2. Growth
3. Coalescence
4. Formation of continuous Si film



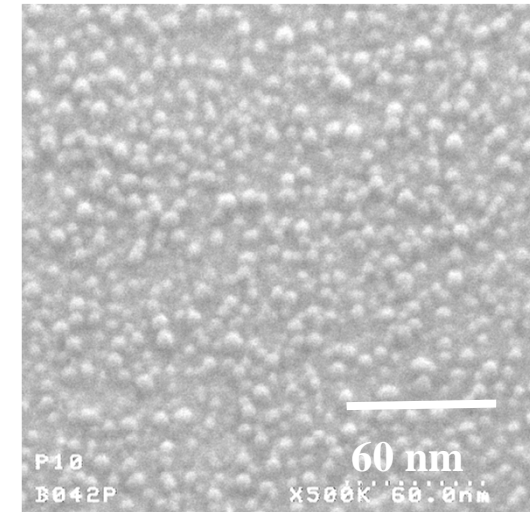
- Low effect of temperature on Si nucleation (range 570-620 $^{\circ}\text{C}$)
- P_{SiH_4} promotes Si nucleation



SiO₂
3x10¹¹ Si-Ncs/cm²

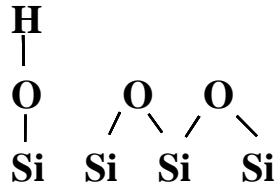


Si₃N₄
9.5x10¹¹ Si-Ncs/cm²

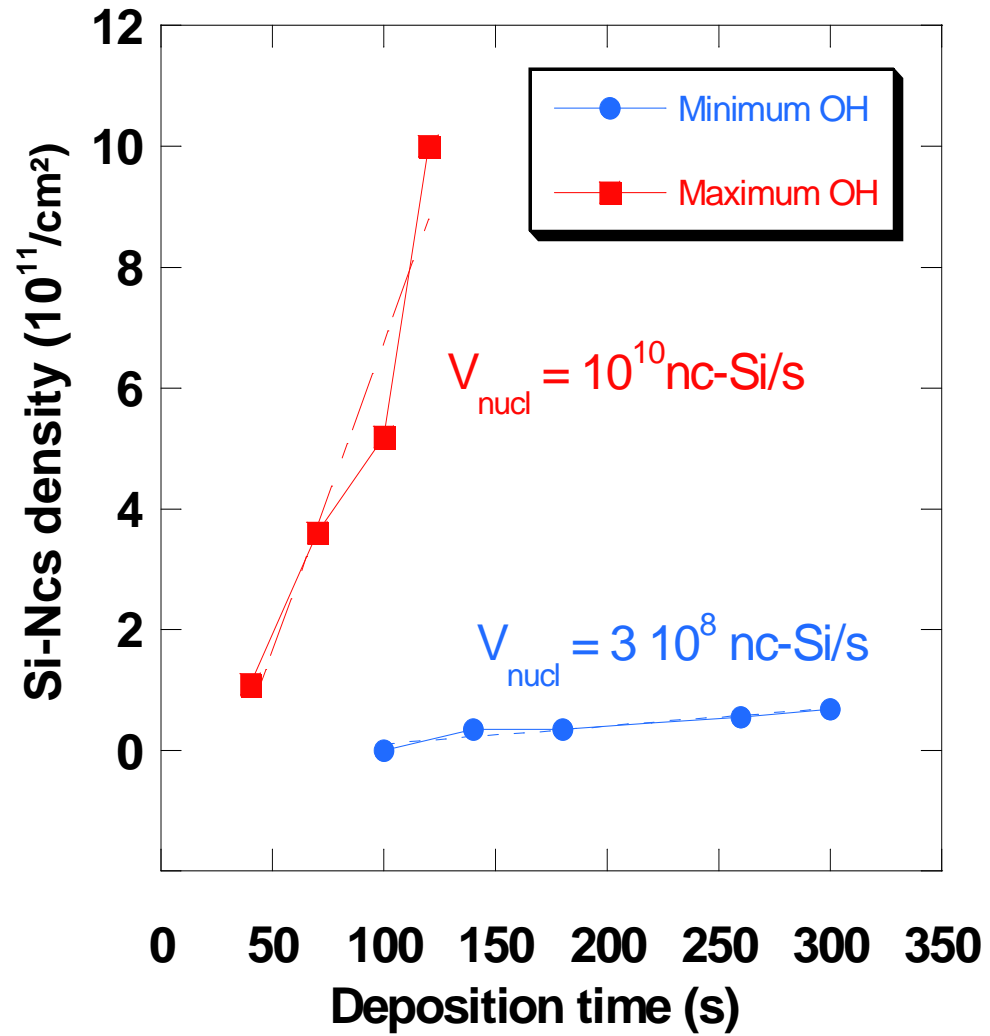
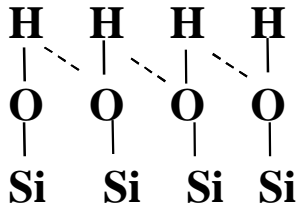


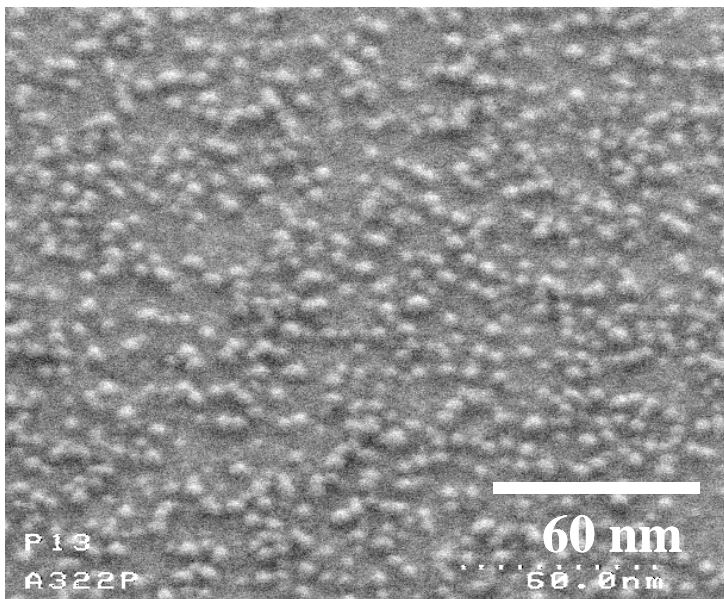
Al₂O₃ (ALD)
10¹² Si-Ncs/cm²

- ❑ Thermal SiO₂ is not favourable for a high Si-Ncs density (strong Si-O bonds)
- ❑ On deposited Si₃N₄, strong nucleation (rugosity, defects...)
- ❑ On Al₂O₃ deposited by Atomic Layer Deposition, OH groups favour Si nucleation



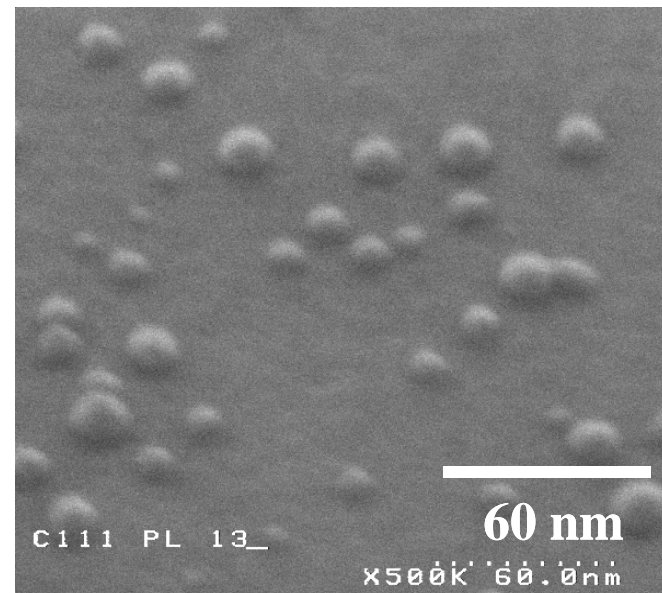
HF 0.05%





HF treatment

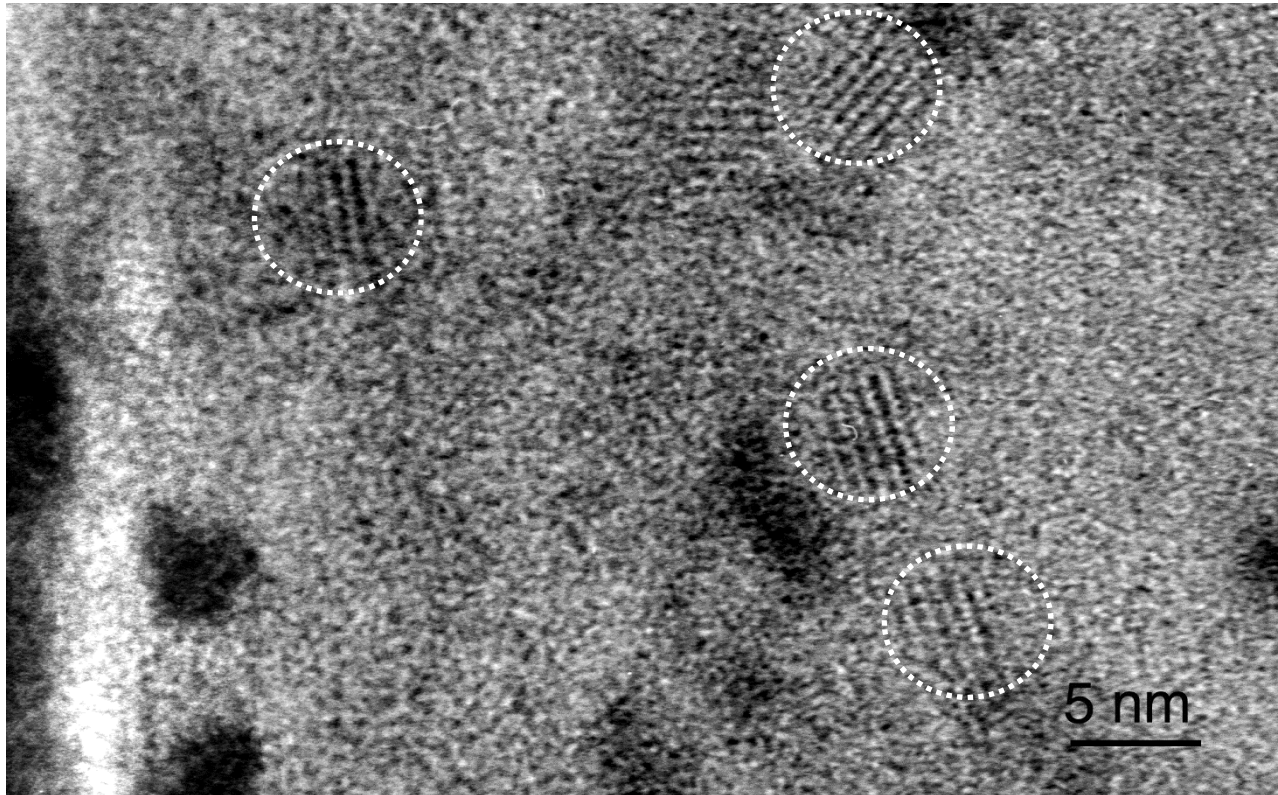
Density : 10^{12} Si-Ncs/cm²



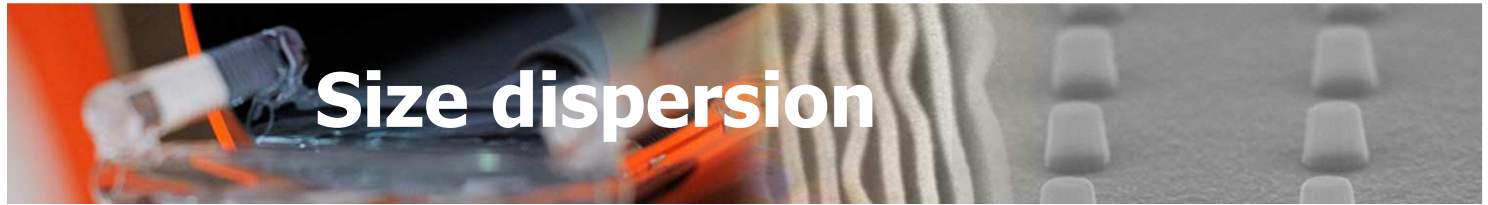
As grown SiO₂

Density : $7 \cdot 10^{10}$ Si-Ncs/cm²

□ **Si-OH groups govern the Si nucleation on SiO₂**

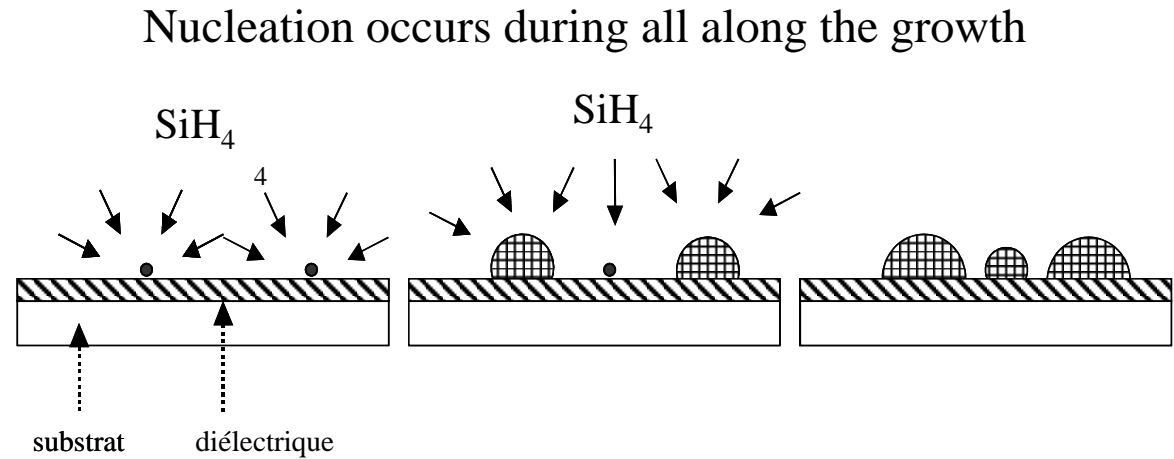
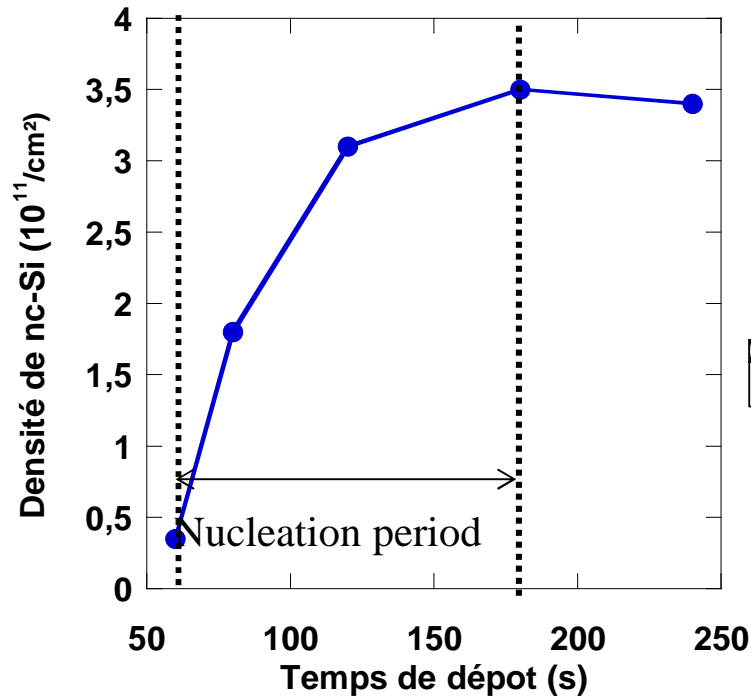


□ nc-Si are crystalline

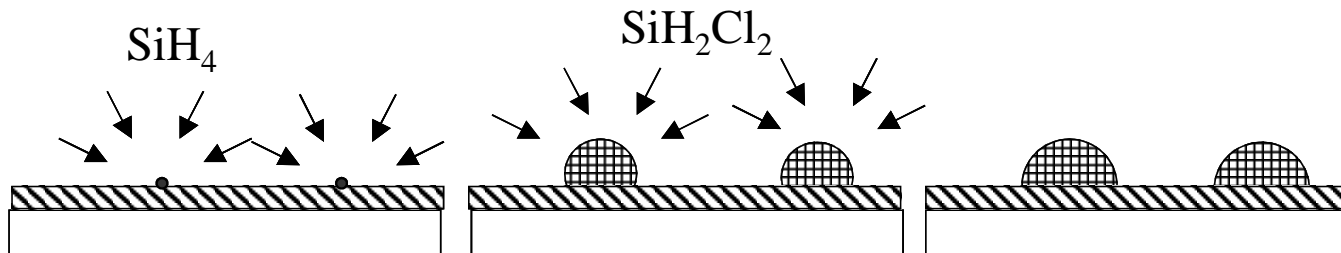


Size dispersion

Large size dispersion for nanocrystals = 30%

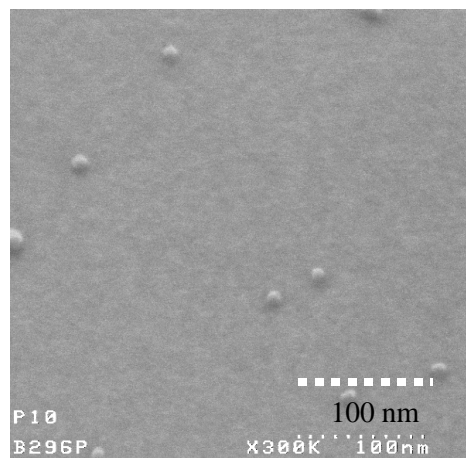


Solution : separate nucleation and growth steps



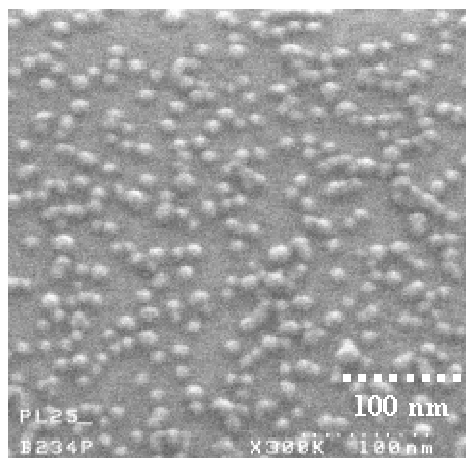


60 mTorr SiH₄



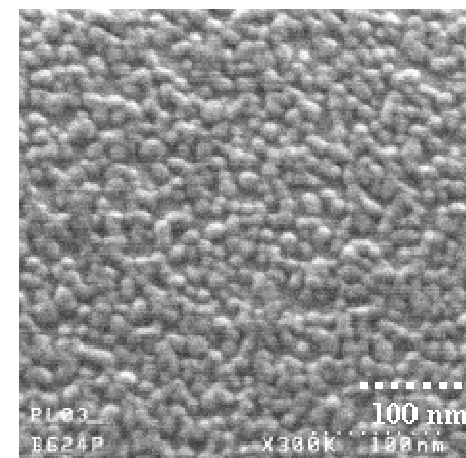
5×10^9 nc-Si/cm²

200 mTorr SiH₄



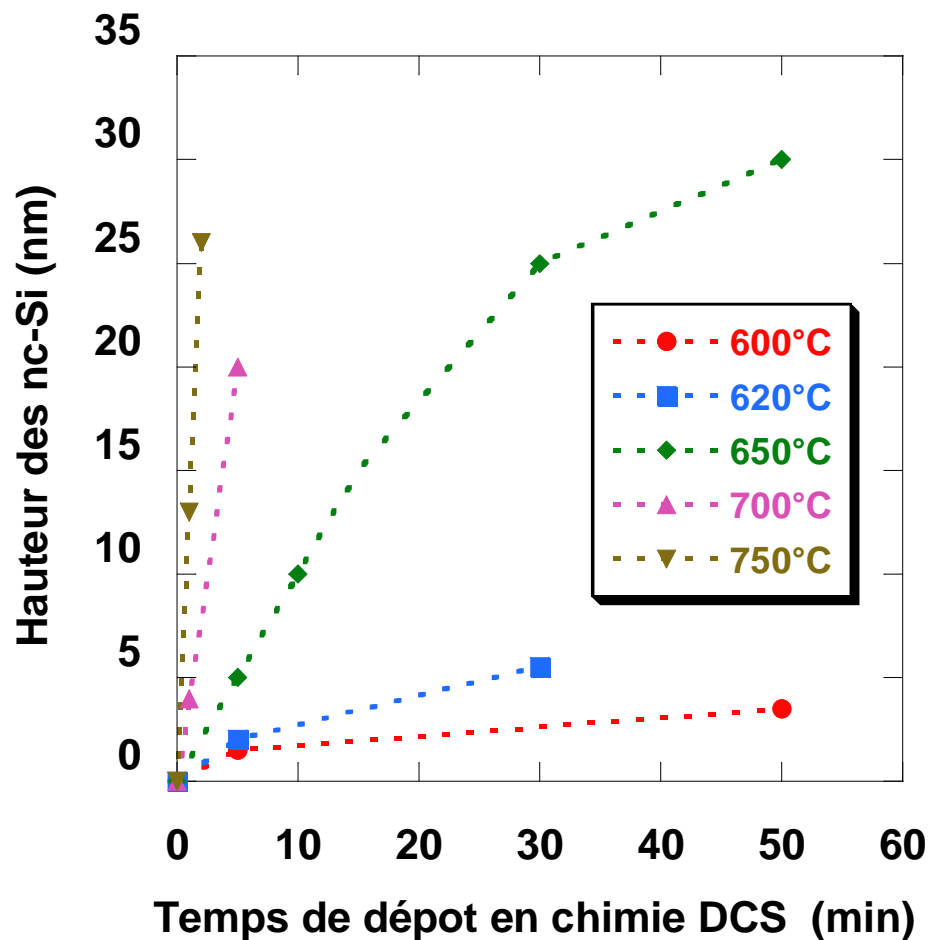
3×10^{11} nc-Si/cm²

200 mTorr SiH₄
With HF treatment

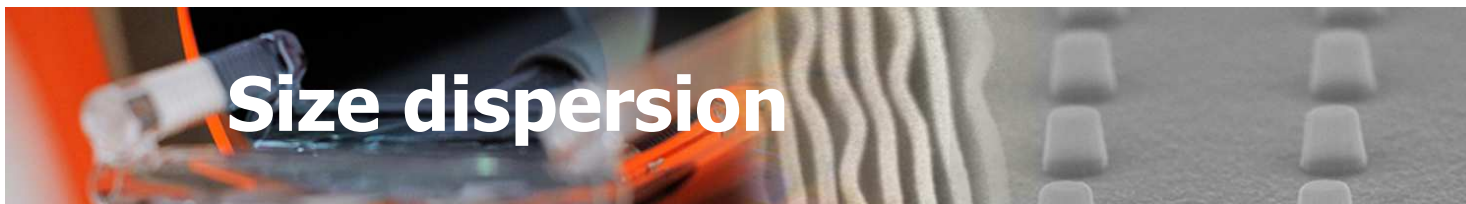


7×10^{11} nc-Si/cm²

Step 1, exposition of the surface to SiH₄ for a short time, control the nanocrystal density



Step 2, exposition of the Si nuclei to SiH_2Cl_2 control the growth rate and hence the size of the nc (0.001 à 13 nm/minute)

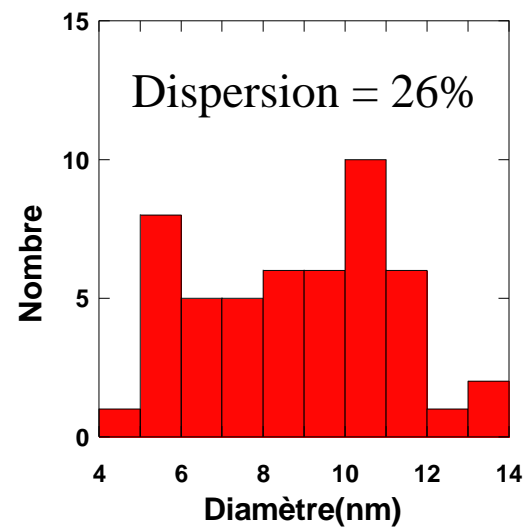
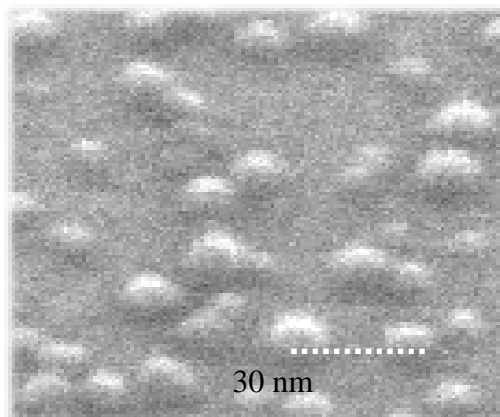


Size dispersion

1 step SiH_4

Density: $2.8 \cdot 10^{11}/\text{cm}^2$

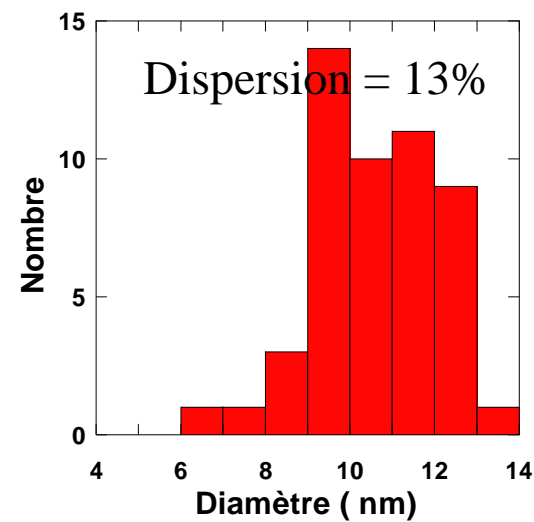
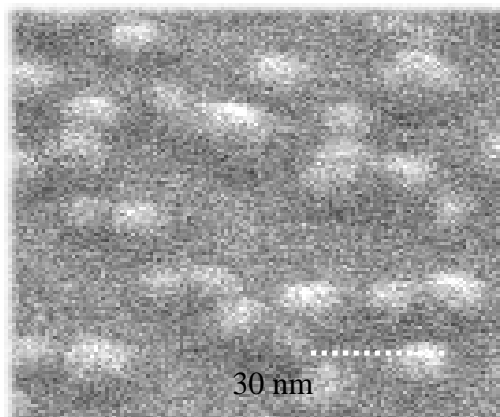
Diameter : 9 nm



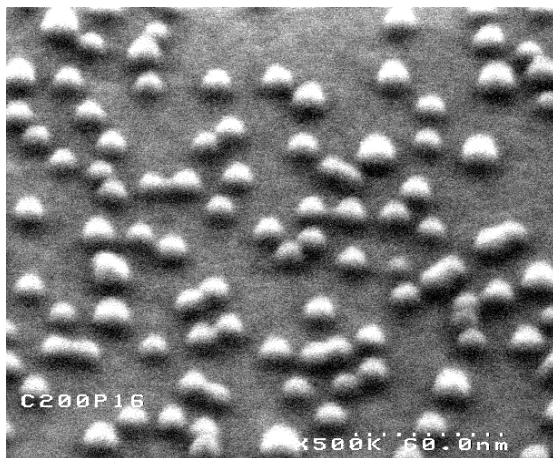
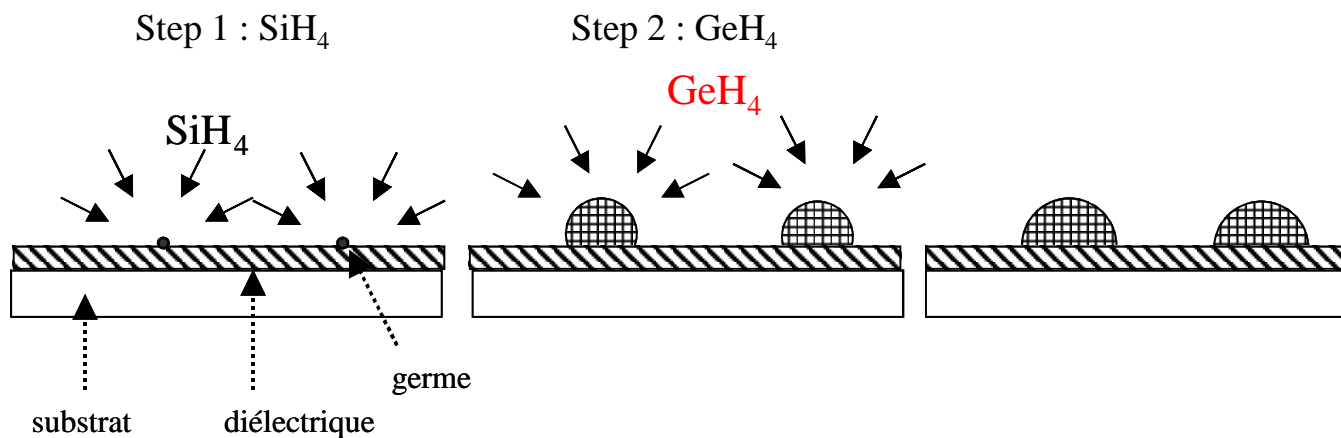
2 steps $\text{SiH}_4 + \text{SiH}_2\text{Cl}_2$

Density: $3.1 \cdot 10^{11}/\text{cm}^2$

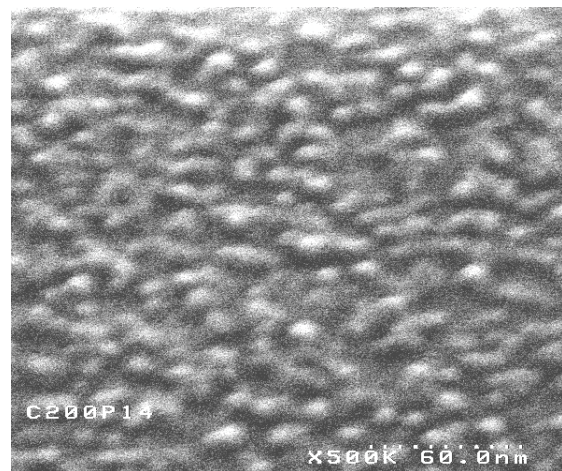
Diameter : 11 nm



GeH_4 : almost no Ge nucleation on SiO_2

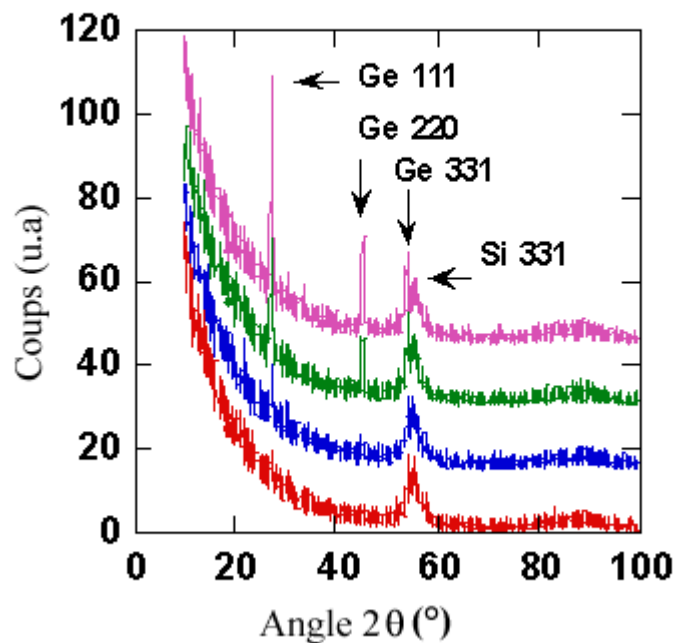


Density : 2×10^{11}
 Diameter : 12 nm



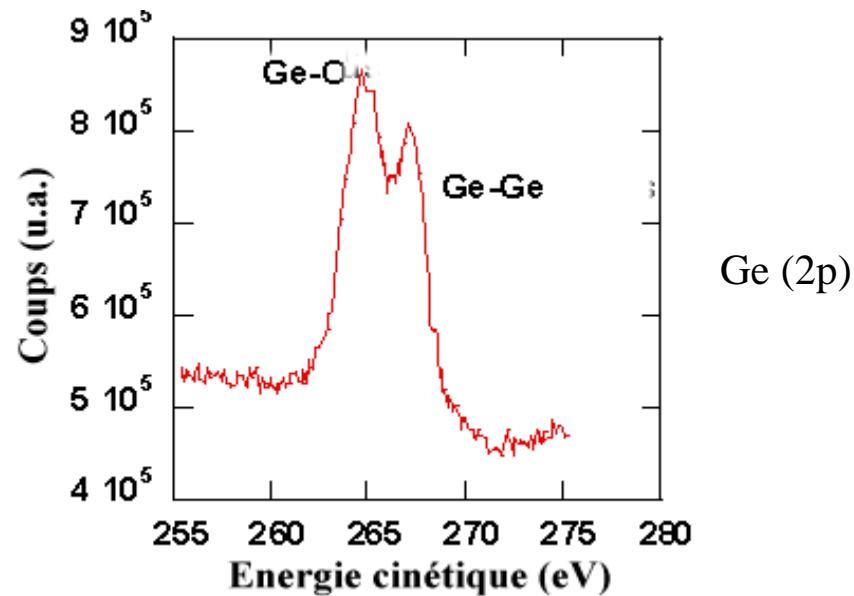
Density : 6×10^{11}
 Diameter : 7 nm

XRD

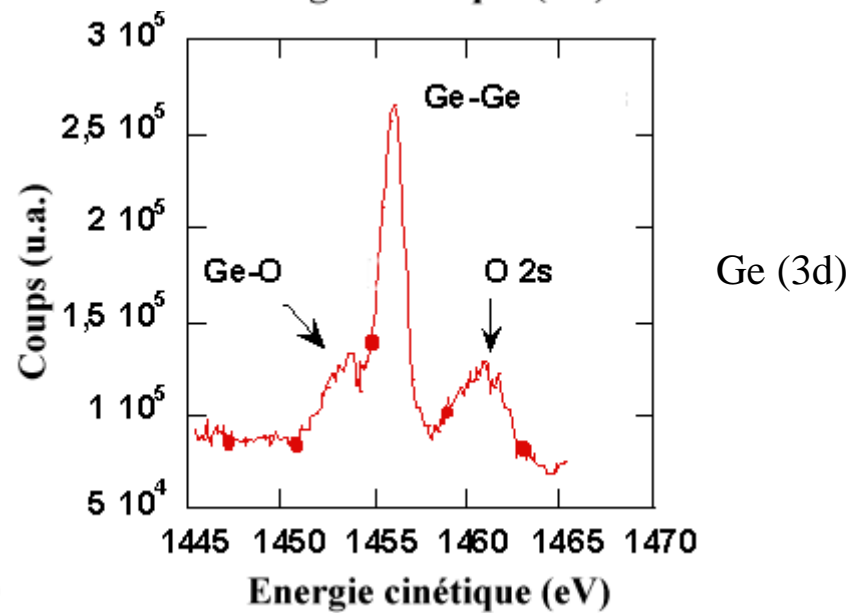


Nc-Ge cristallins with GeO_x shell

XPS

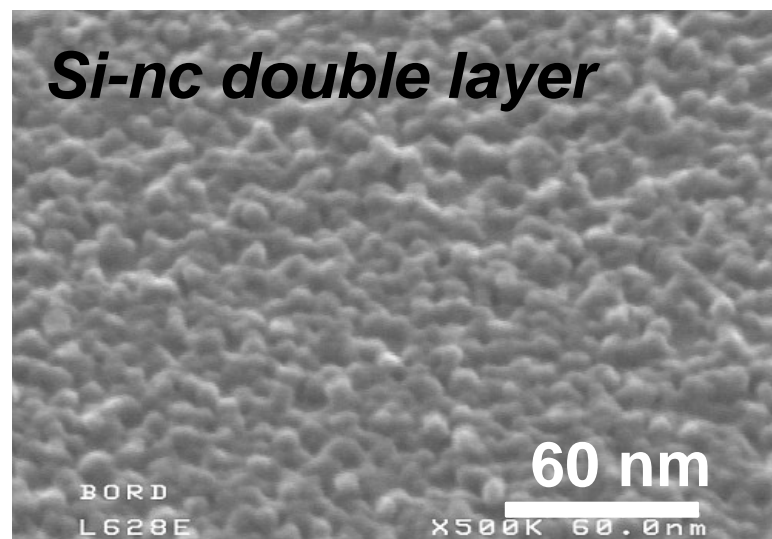
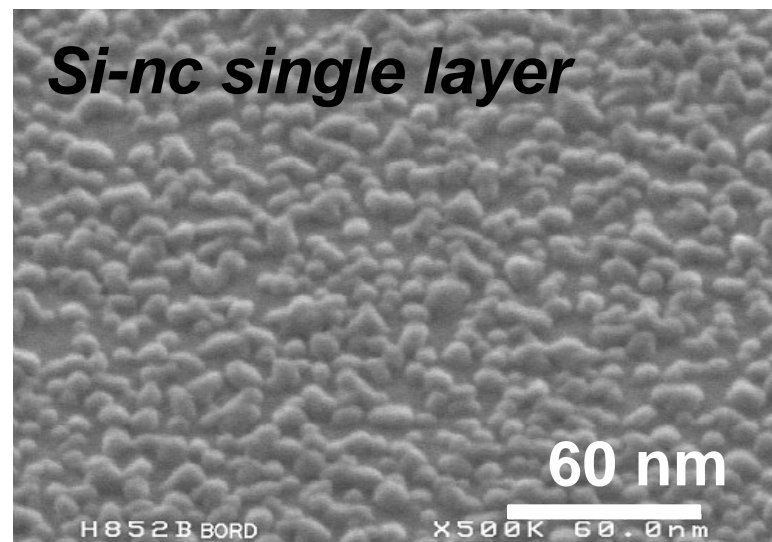
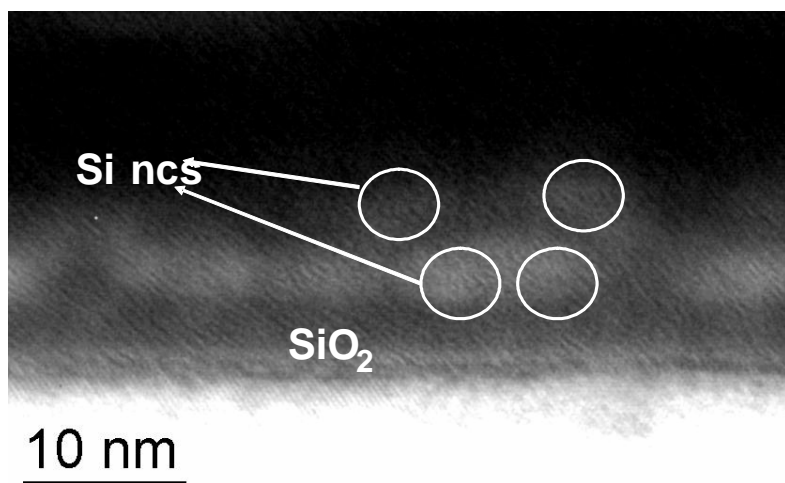
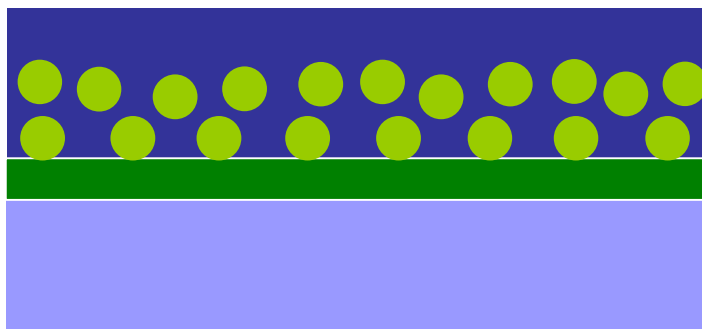


Ge (2p)



Ge (3d)

Objective: deposition of 2 layers of Si-ncs to improve the nc-Si density





OUTLINE

- ❑ Nanocrystals for memory devices
 - Principle
 - Nanocrystal growth
 - Integration in devices

- ❑ Nanowires for low power devices, capacitors and sensors

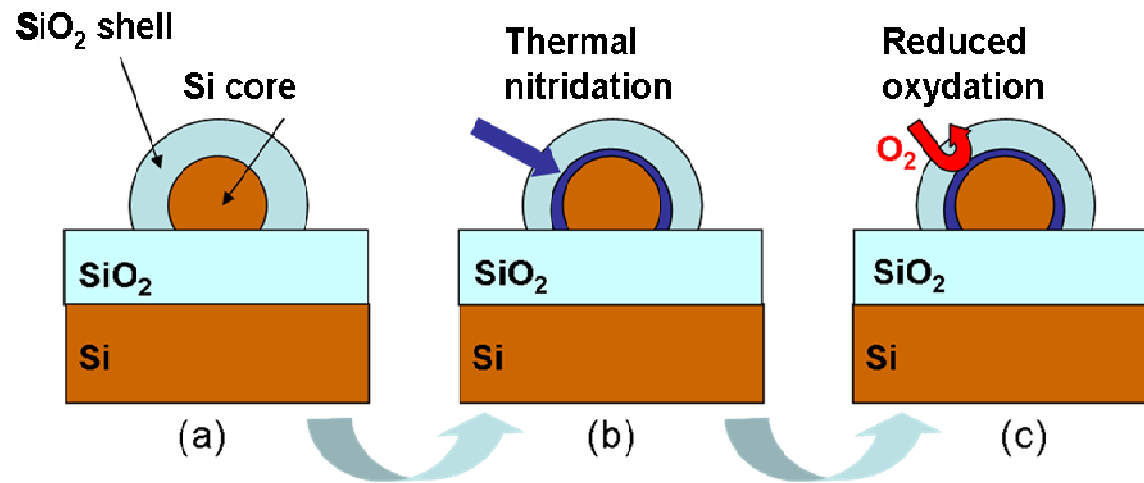
- ❑ SiGe and InGaAs thin films for NMOS and PMOS FET



Passivation of Si-nc by nitridation

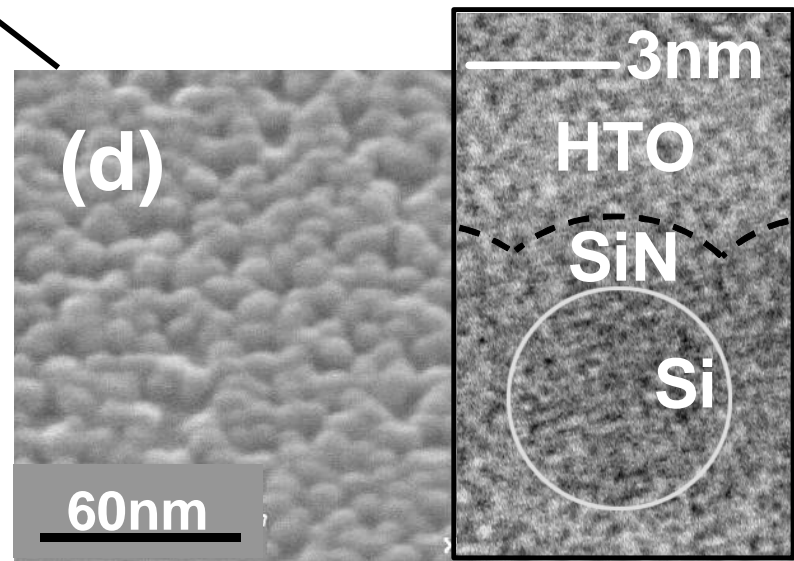
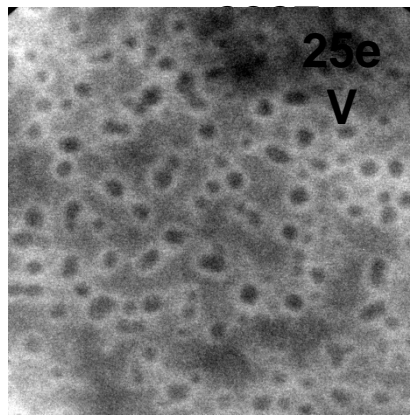
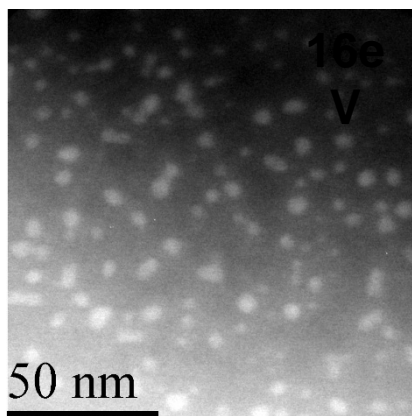
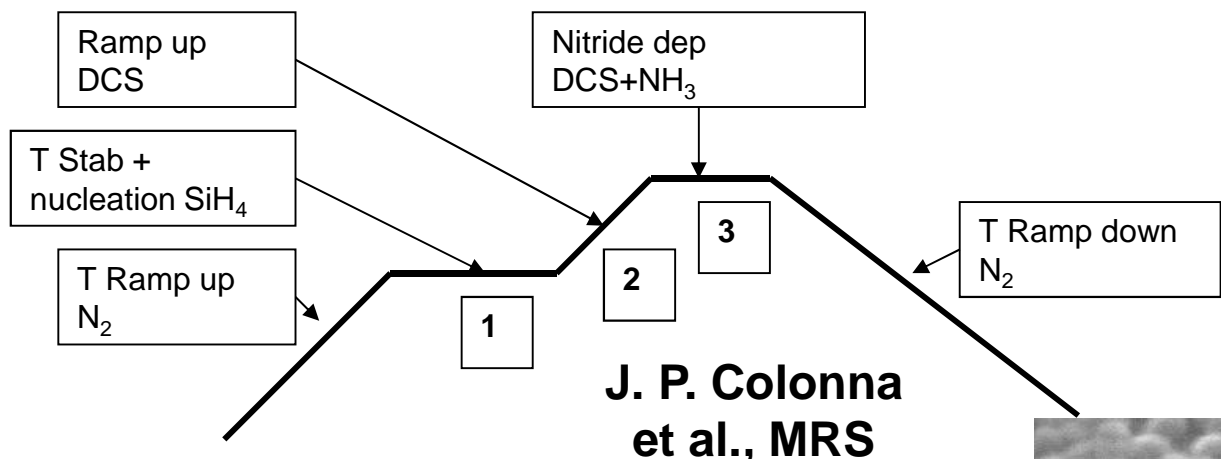
□ Nitridation effects

- Si_3N_4 O_2 diffusion¹ is limited
- NO et NH_3



¹ M.L. Green *et al.*, APL 67(11), p 1600, (1995)

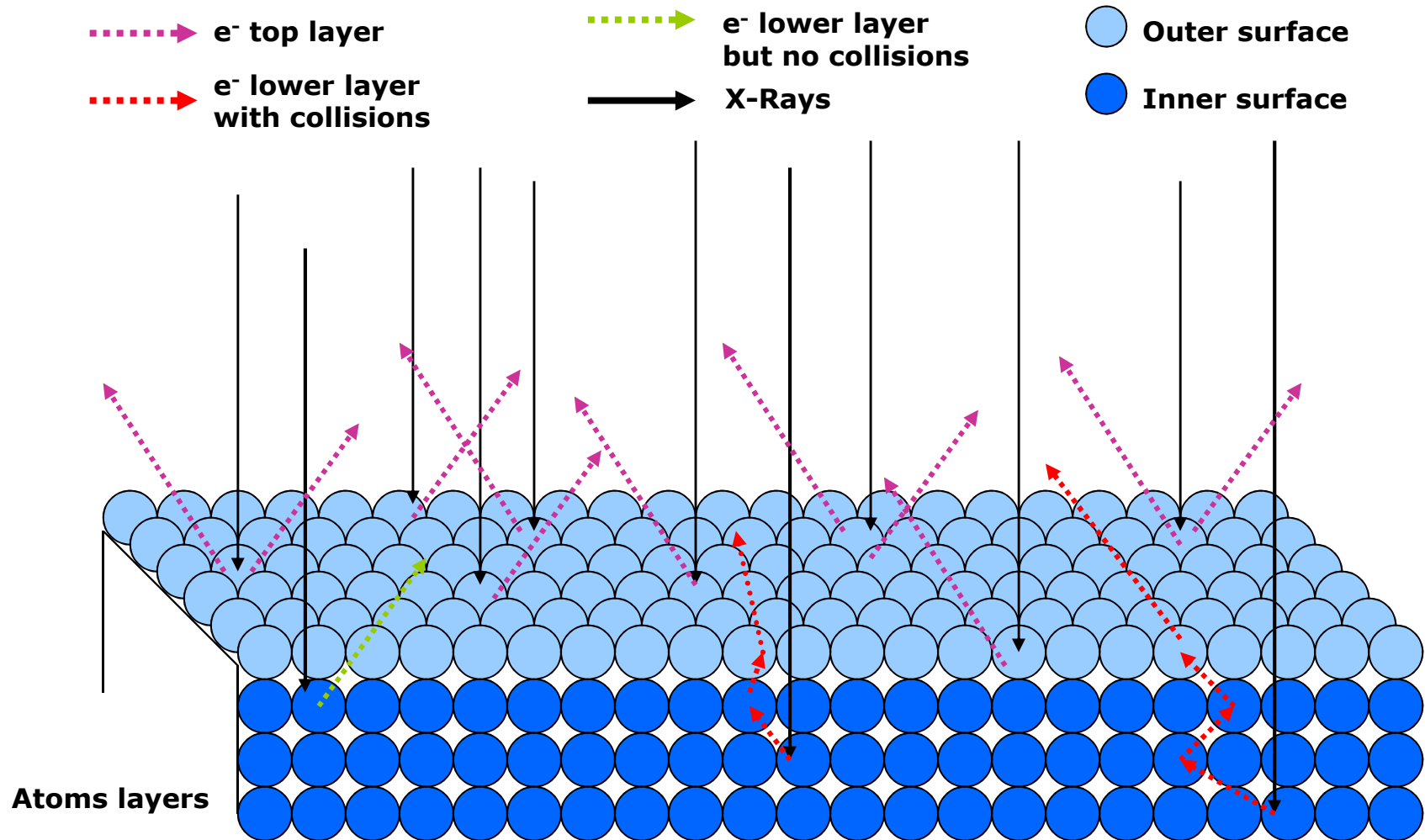
² K. C. Scheer *et al.*, APL 93 (9), p 5637, (2003)



Si-ncs capped with SiN shell : hybrid Si-nc SiN trapping layer



XPS simple description



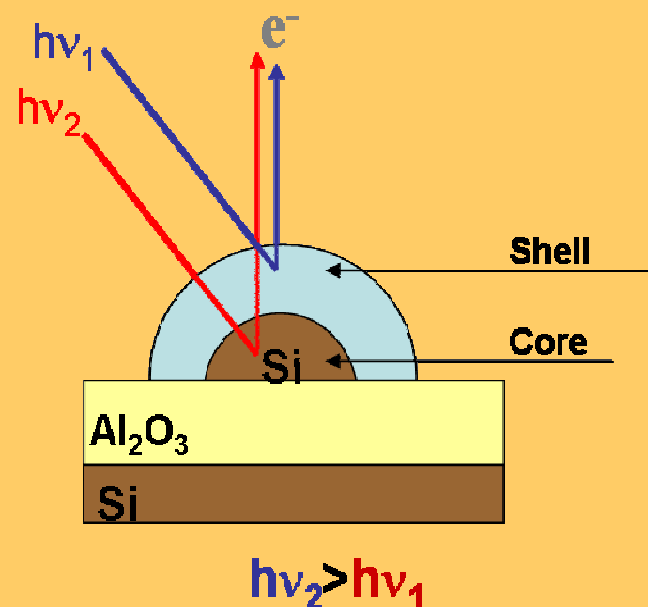


□ XPS VUV ELETTRA Synchrotron :

- Energy resolution (0.05 eV/0.5 eV for laboratory equipment)
- Energy screening (depth profil)

➤ Analysis condition :

- Shell : Si(2p) e- $h\nu=160\text{eV}$
N(1s) e- $h\nu=400\text{eV}$
- Core + shell : Si(2p) e- $h\nu=250\text{eV}$
N(1s) e- $h\nu=700\text{eV}$



➤ Samples :

Density : $8\text{E}11 \text{ cm}^{-2}$ $\varnothing = 8\text{nm}$

#1 = REF

Si dots (CVD)

+

Chemical SiO_2 (O_3)

#2 = NIT° 650°C

REF

+

Nitridation NH_3 650°C

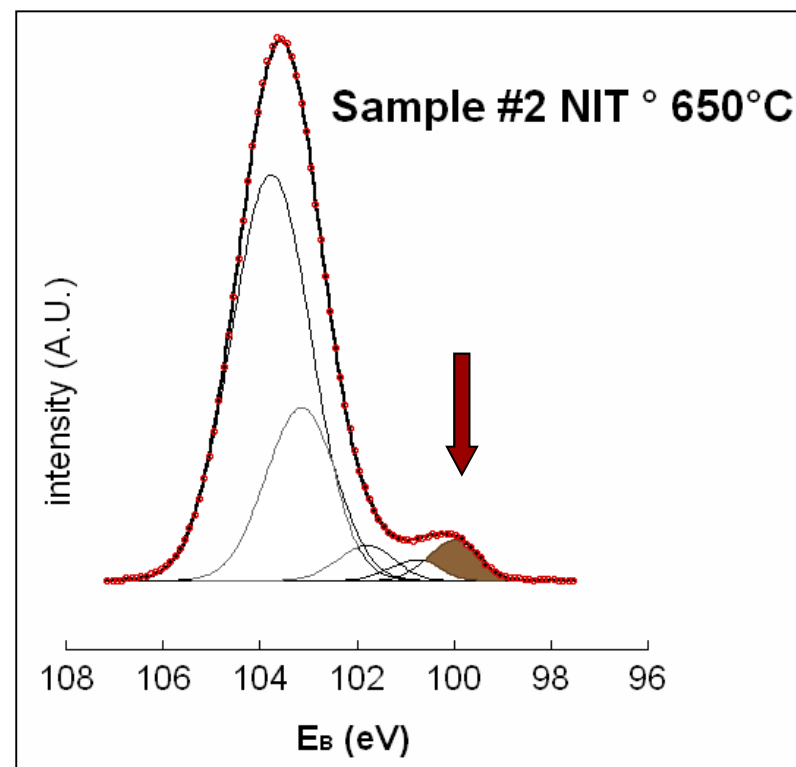
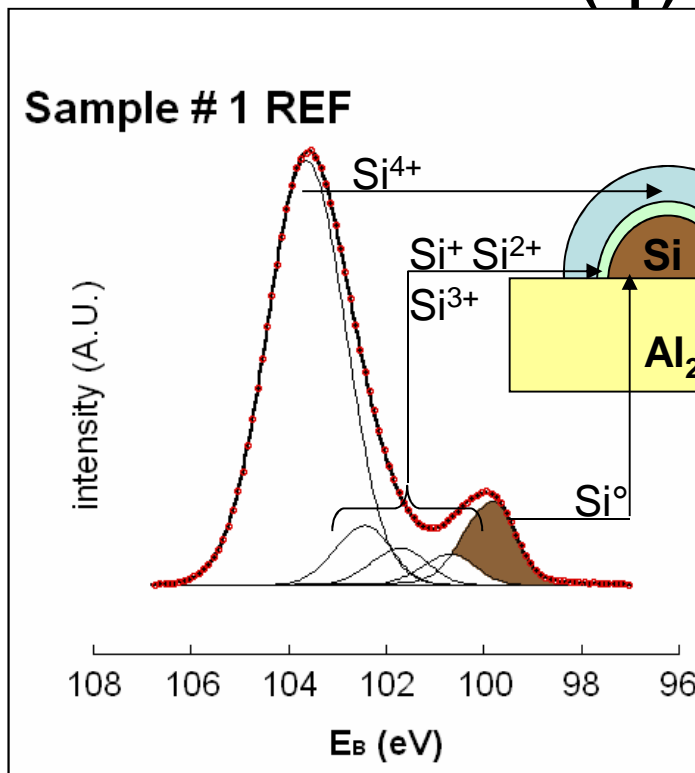
#3 = NIT° 750°C

REF

+

Nitridation NH_3 750°C

Si (2p) e-, hv = 160 eV



REF * :

Si° : core
 Si^{+} Si^{2+} Si^{3+} : Interface
 core/shell
 Si^{4+} : shell SiO_2

Nitrated sample at 650°C :
 ⇒ Shell growth
 ⇒ presence of Si core

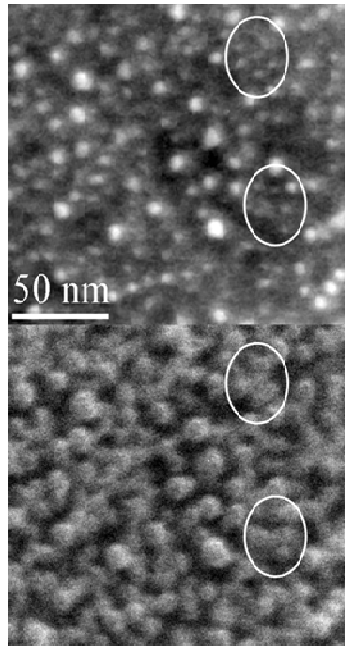
* O. Renault et al., APL **87**, 163119 (2005)

Density : $8 \times 10^{11} \text{ cm}^{-2}$,

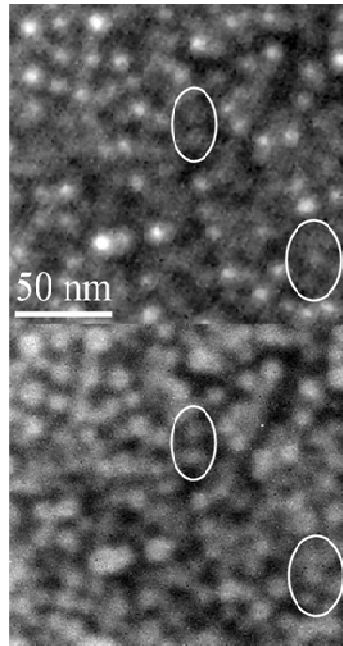
$4 \times 10^{11} \text{ cm}^{-2}$

S. Lombardo et al., IMM

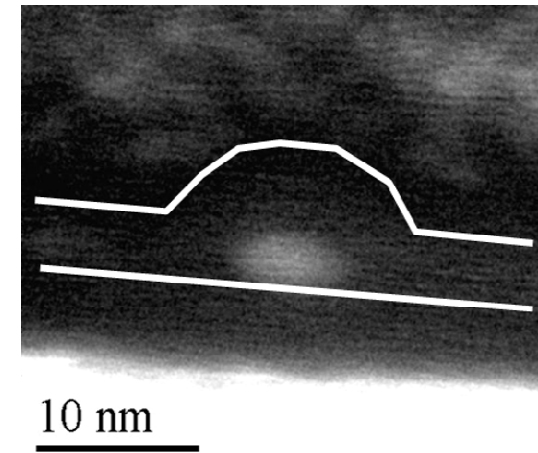
EFTEM



Reference,



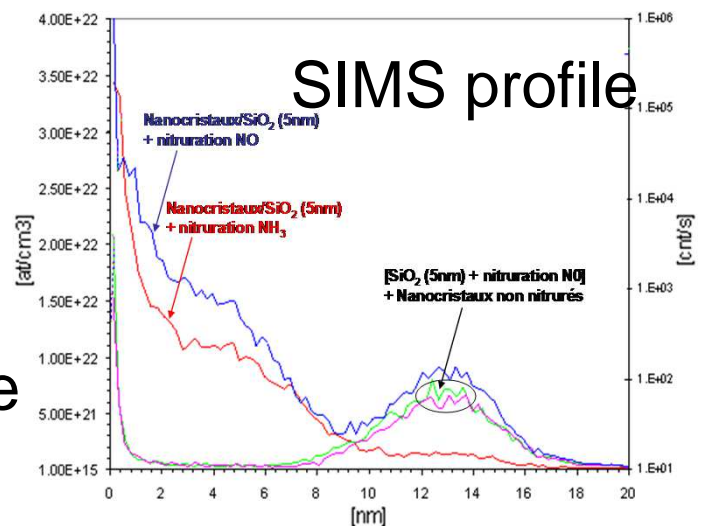
nitridation at 750°C



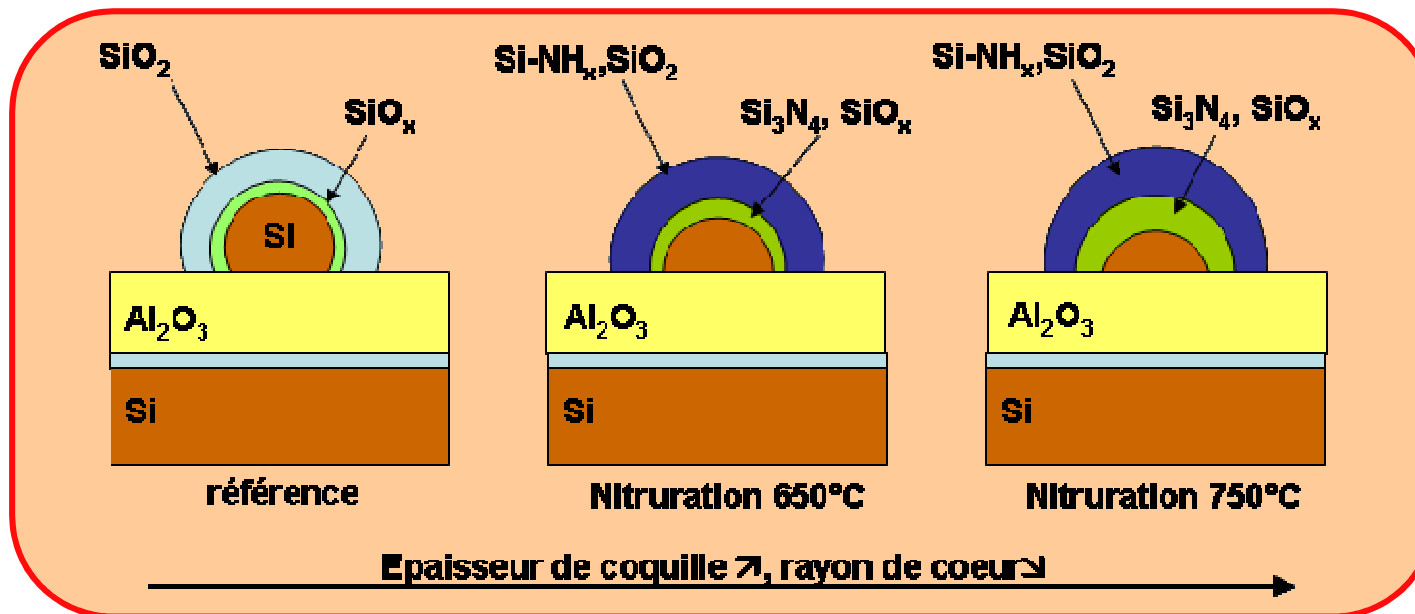
Cross section TEM

Conclusion :

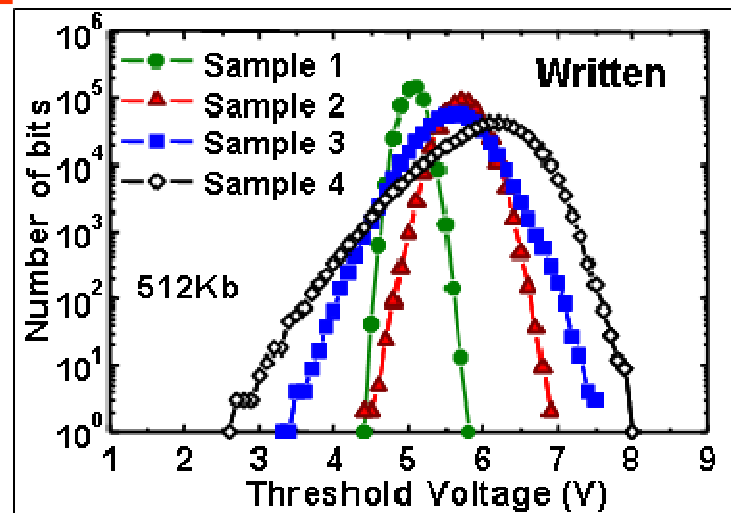
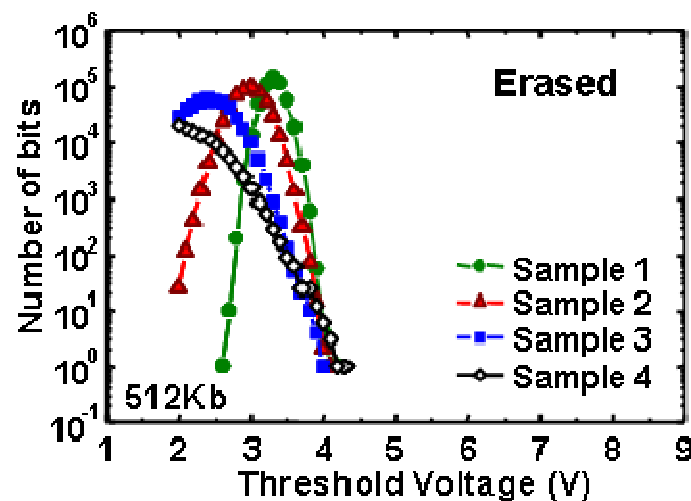
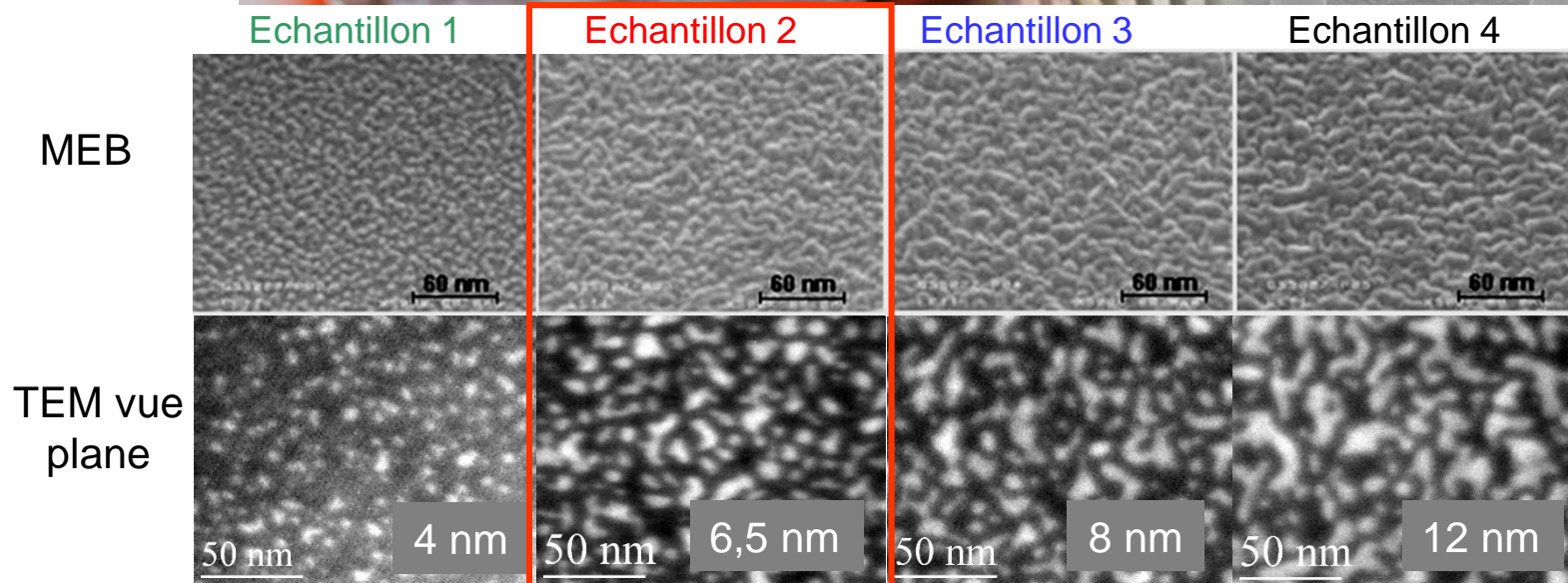
- Si nanocrystals density reduction
- N located preferentially at the surface



SIMS profile

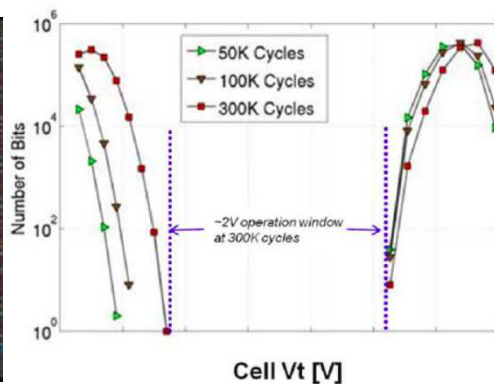
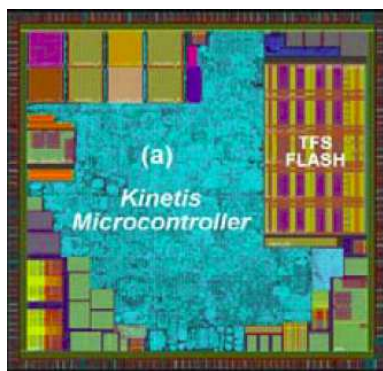


32Mbits memory devices 130 nm node



Freescape

Split gate structure



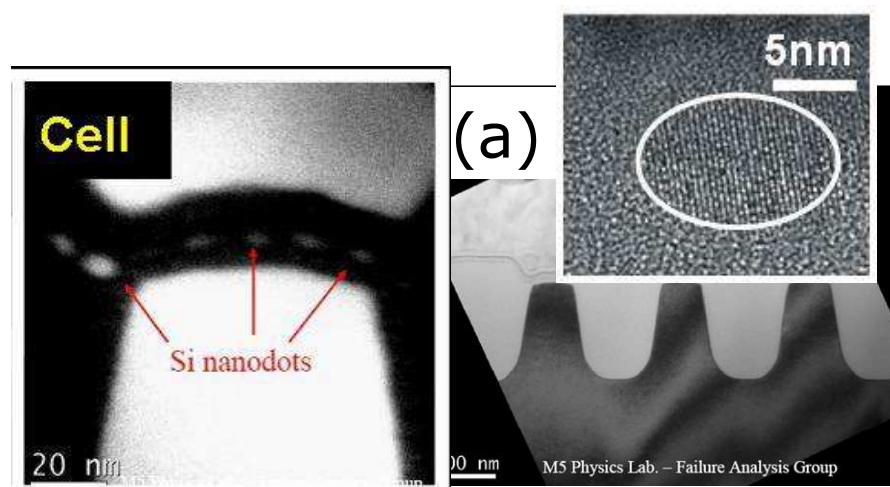
Kang et al., VLSI 2008, IMW 2009, IMW 2012

Commercial products:

Embedded memories for
microcontrollers in 90nm technology

STMicroelectronics

Architecture NOR 4Mb

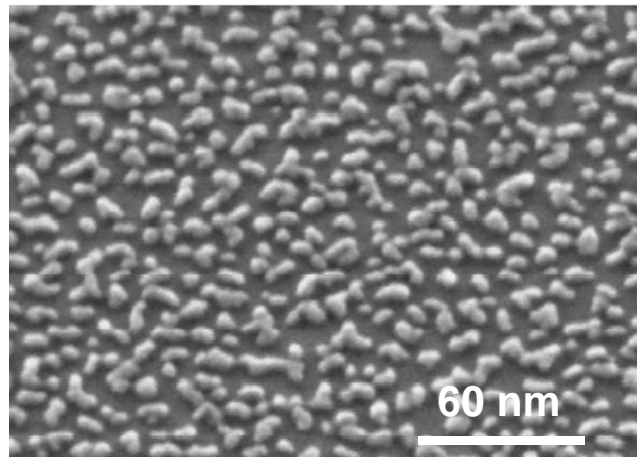
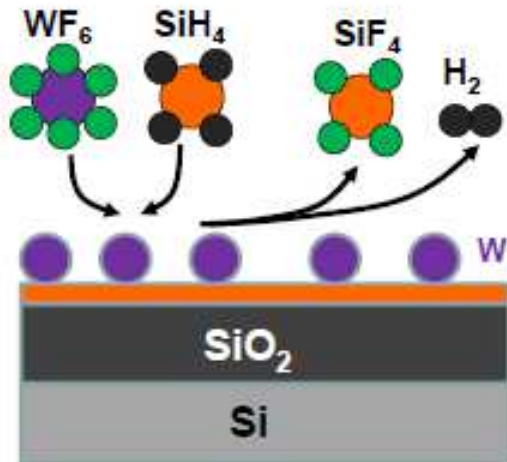


Gerardi et al., IEDM2008

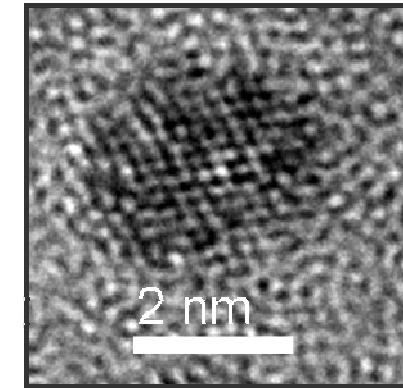
□ **W** advantages :

- ✓ refractory material ($T_{\text{fusion}} = 3410^{\circ}\text{C}$)
- ✓ Stable with SiO_2

□ Precursors : WF_6 (g) et SiH_4 (g)



MEB, tilt 40°



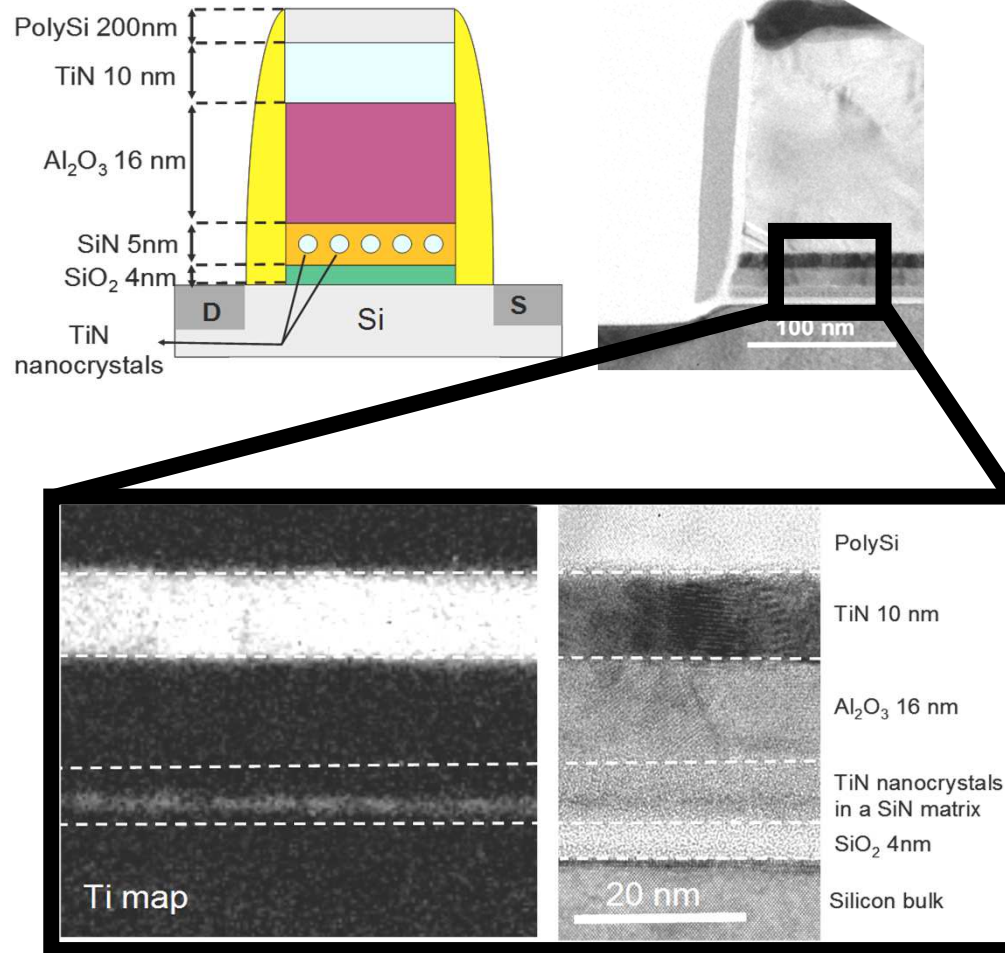
TEM

Density : $7 \cdot 10^{11} \text{ cm}^{-2}$

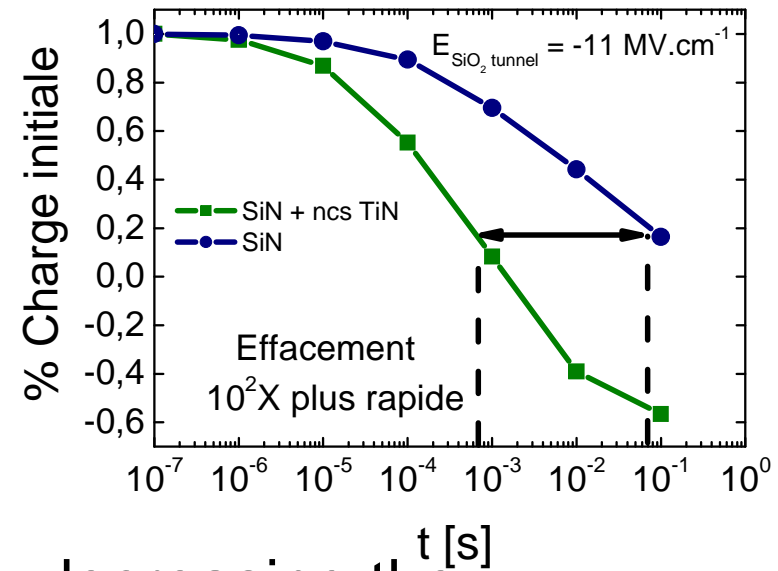
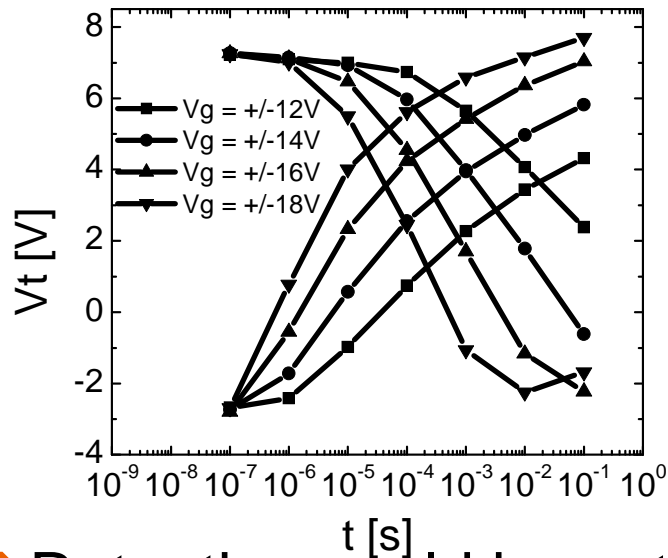
Diameter moyen : 6 nm

Memory devices integrating metallic nanocrystals:

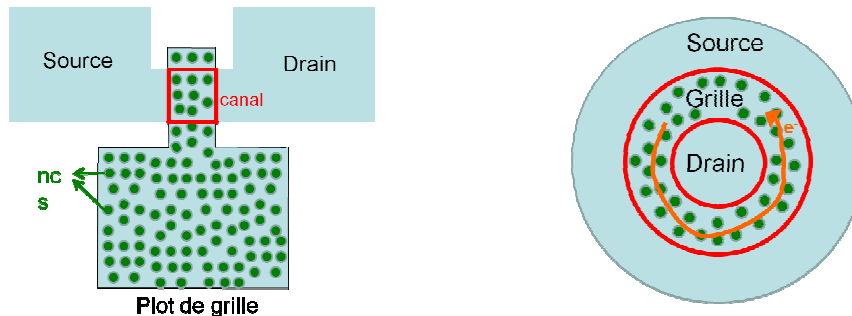
Floating gate = TiN NCs + DCS *passivation* + SiN encapsulation



- Functional devices
- Gain in writing speed, and memory windows



- Retention could be optimized by decreasing the nanocrystals density (lateral leakage of charges)





Conclusions

- CVD allows to grow directly Si, Ge and metallic nanodots
- Control of density and size dispersion possible if nucleation and growth decoupled
- Selective growth possible
- Core / shell nanostructured and passivation possible

- Large scale integration of nanolayers and nanostructures unable by CVD

- Semiconductors, metals, oxydes nanodots



VLS growth and applications of $\text{Si/Si}_{1-x}\text{Ge}_x$ nanowires



OUTLINE

- ❑ Nanocrystals for memory devices

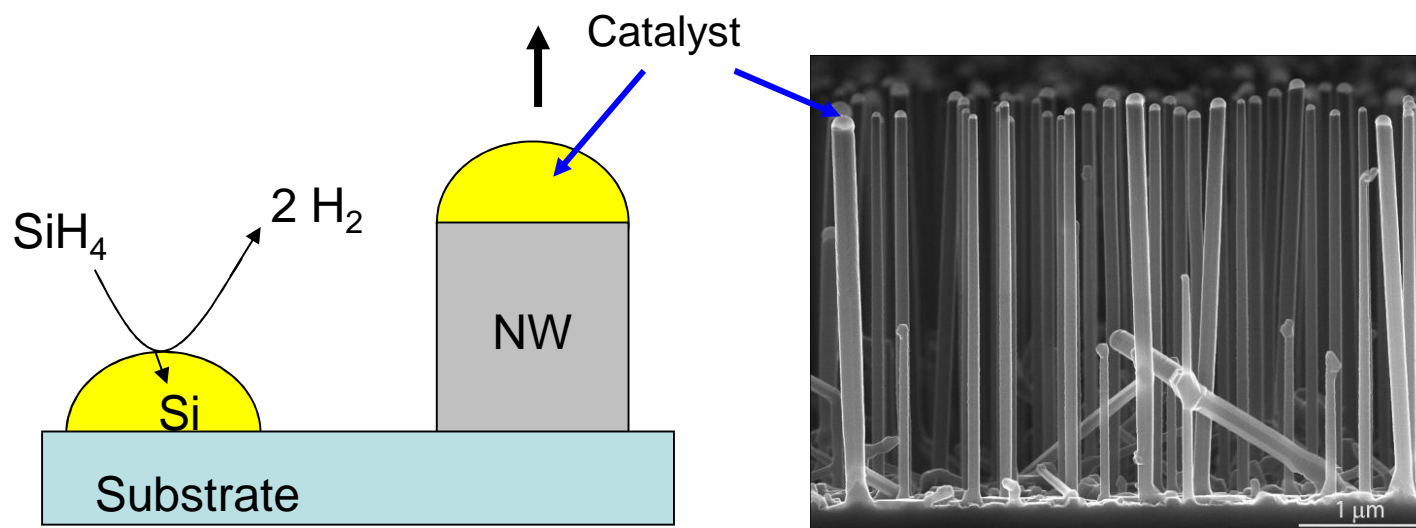
- ❑ Nanowires for low power devices, capacitors and sensors
 - Objective
 - Si/SiGe nanowires catalytic growth
 - Other applications

- ❑ SiGe and InGaAs thin films for NMOS and PMOS FET



Introduction : CVD – VLS nanowires growth

Ellis et Wagner, 1964

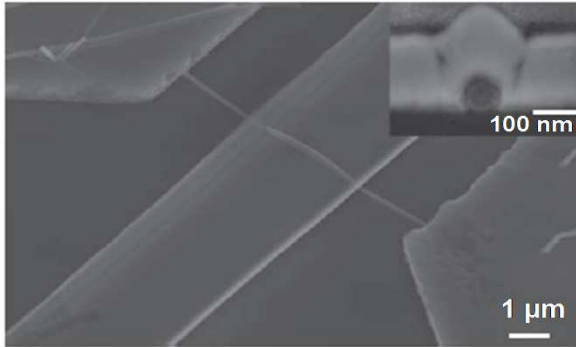


[Oehler10]

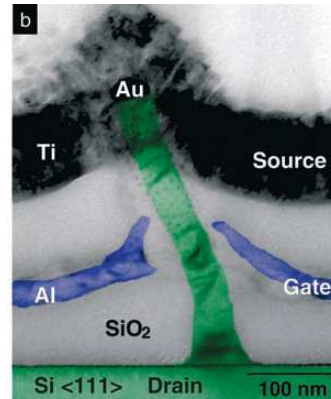
- Crystalline growth possible without any epitaxy relation
- Nanometric diameter without lithographic steps
- Low temperature synthesis < 450°C compatible with back-end process
- High aspect ratio
- High surface/Volume ratio



Transistors

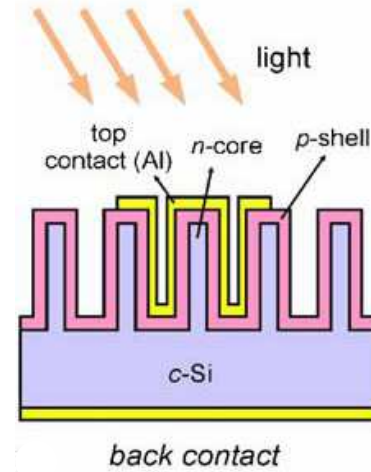


[Garnett09]



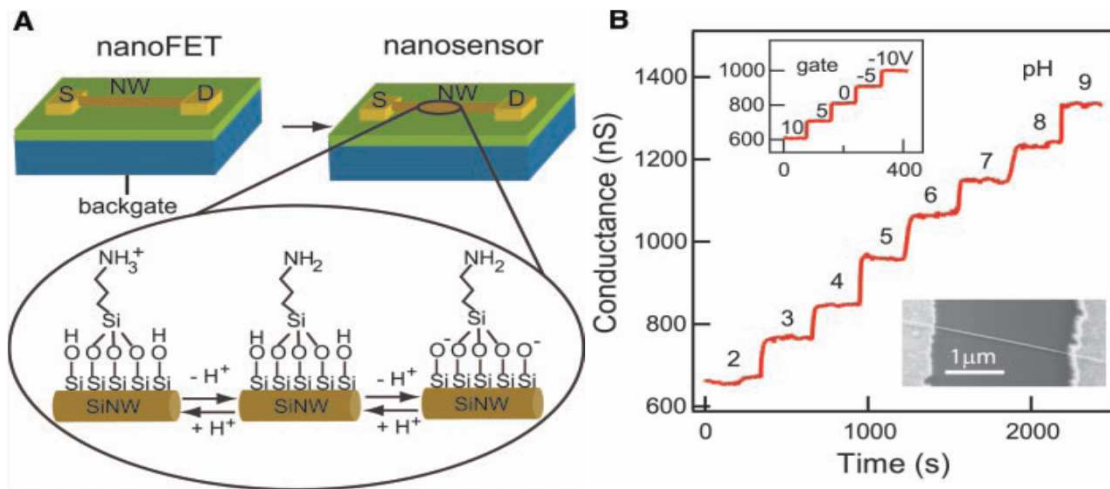
[Schmidt06]

Solar cells



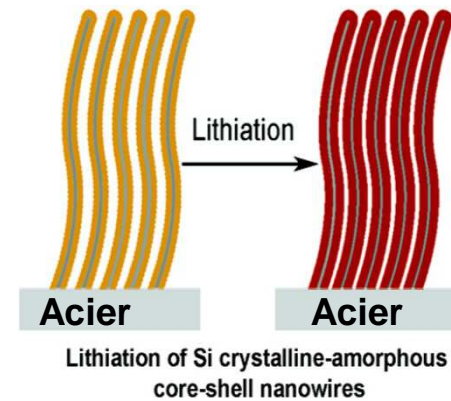
[Gunawan09]

Sensors

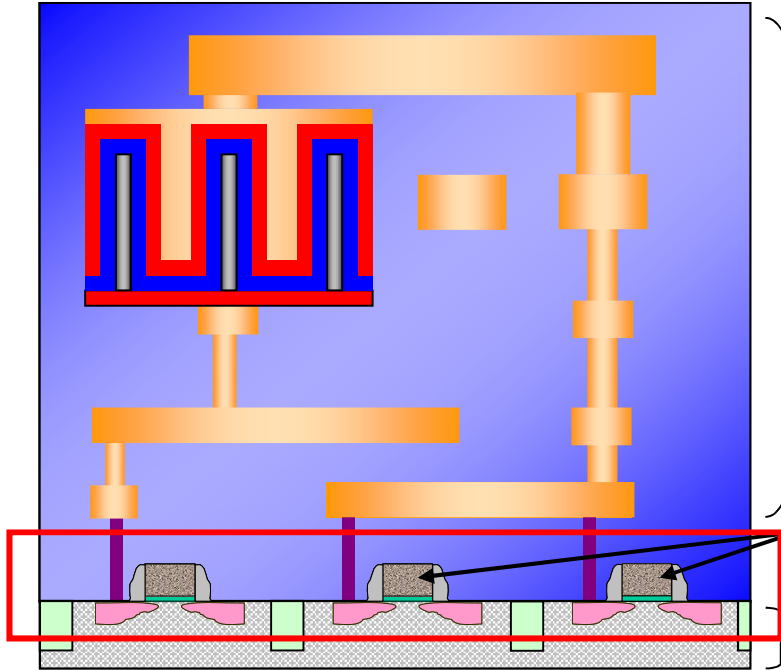


[Cui01]

Batteries



[Cui08]



IC cross section picture

❖ FET in Front End ?

- Precise dimensions
- Aggressive performances
- Metallic interconnections (Back-End-of-line)
- No metallic contamination
- ⇒ Low interest for CVD VLS NWs

❖ Transistors back-end?

- (Front-End-of-line)
- Metallic contamination allowed
- Si Substrate
- Crystalline growth on metal
- ⇒ Challenge (1 NW – 1 device)

❖ High density capacitors in Back End ?

- Use the high surface area available from an assembly of NWs

$$C = \frac{\epsilon_0 \cdot \epsilon_r \cdot S}{e}$$

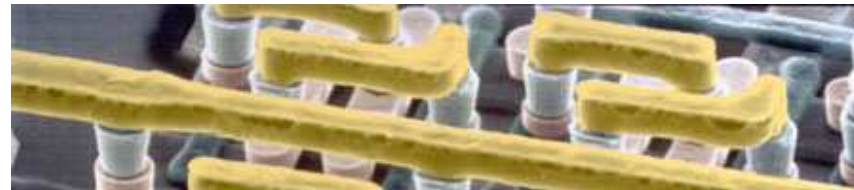
⇒ Challenge



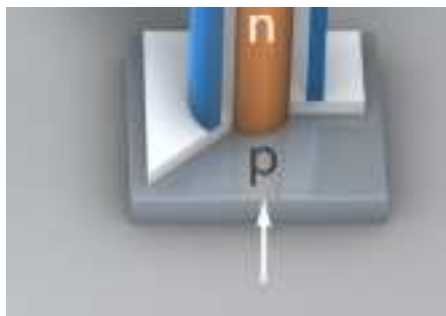
Vertical NWFET

- ❑ Gate all around
 - Improve electrostatic control
- ❑ Compact
- ❑ Integration in interconnection lines

$$C = \frac{S \epsilon_{ox}}{e_{ox}}$$



Reconfigurable interconnection





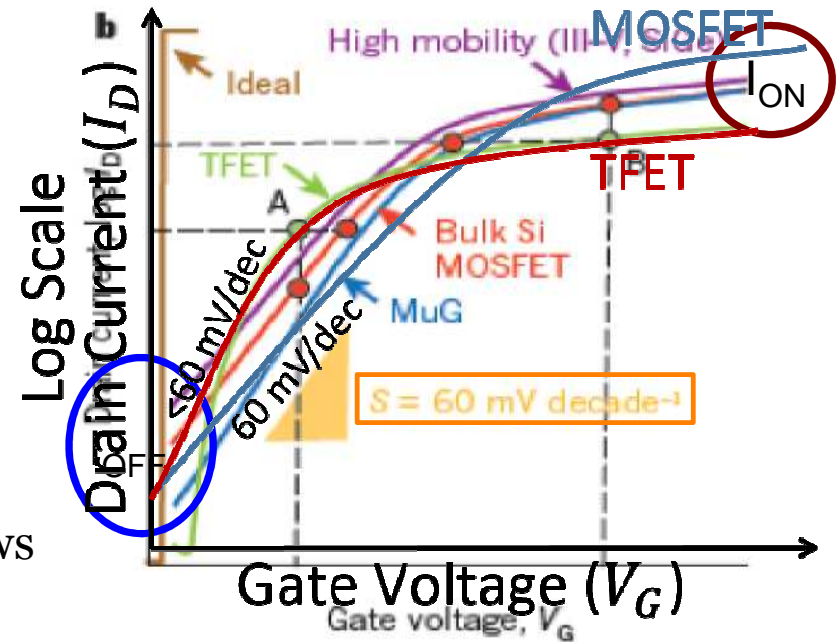
- CMOS subthreshold swing (SS): limitation

$$\frac{k_B T}{q} \ln(10) \sim 60 \text{ mV/dec at } 300 \text{ K}$$

- Scaling down of supply voltage increases the leakage current of MOSFETs (I_{OFF})

➔ Increased power consumption

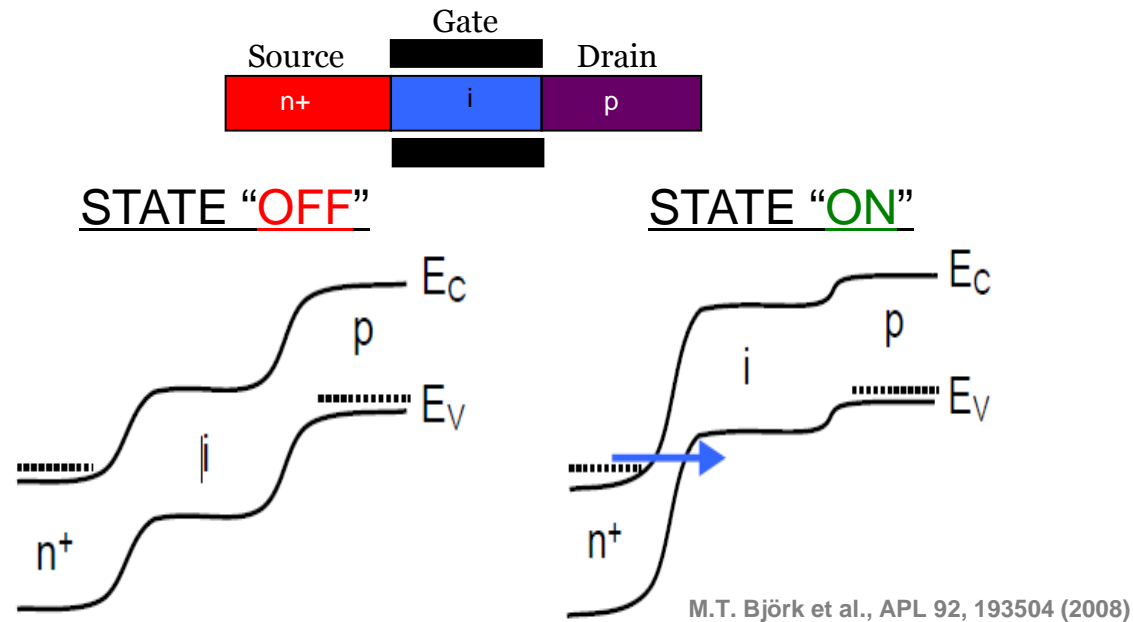
- Interest of steep slope devices. It allows
 - Low threshold voltage
 - LOW I_{OFF}



➔ Potential candidate: Gate all around vertical Tunnel FET

Introduction: TFETs

- TFET is a reverse biased p-i-n gated diode
- The gate voltage V_G modifies channel E_C and E_V enabling **tunneling** at source/channel junction



$$I_{on} \sim T_{tunneling}^{WKB} = \exp\left(-\frac{4\lambda\sqrt{2m^*E_G^{3/2}}}{3qh(\Delta\Phi + E_G)}\right)$$

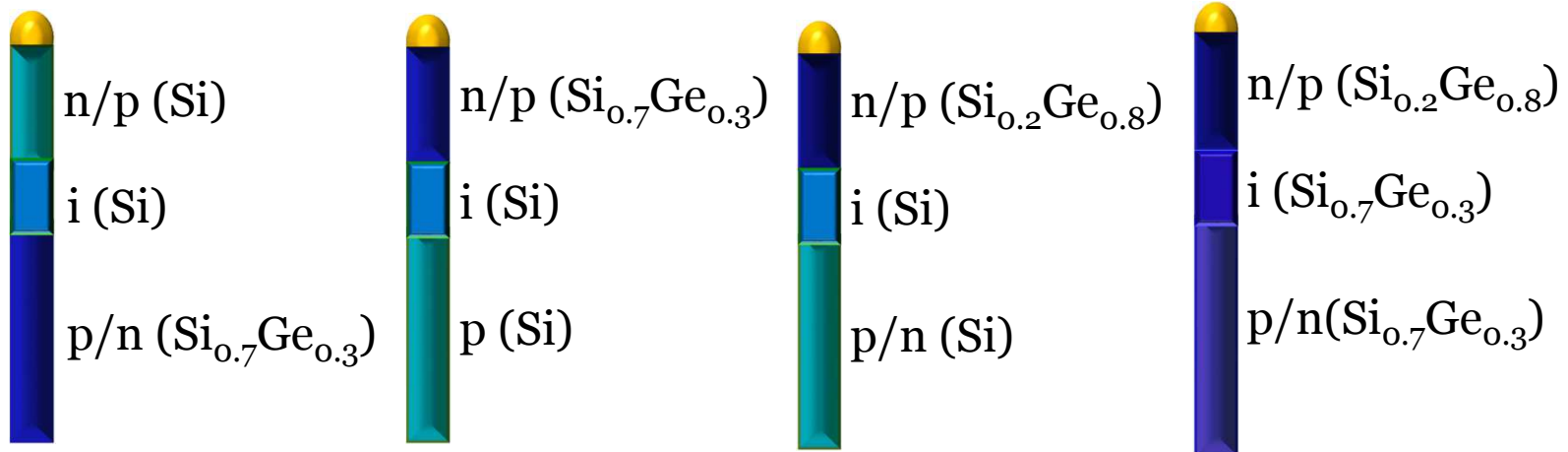
➔ Allows low SS, but **poor** I_{ON}

TFET heterostructures in NWs

Prerequisites for TFET material

- **Low E_g (source) and wide E_g (drain)**
- **Abrupt source-channel junctions**
- **High source doping**

Proposed TFET structures



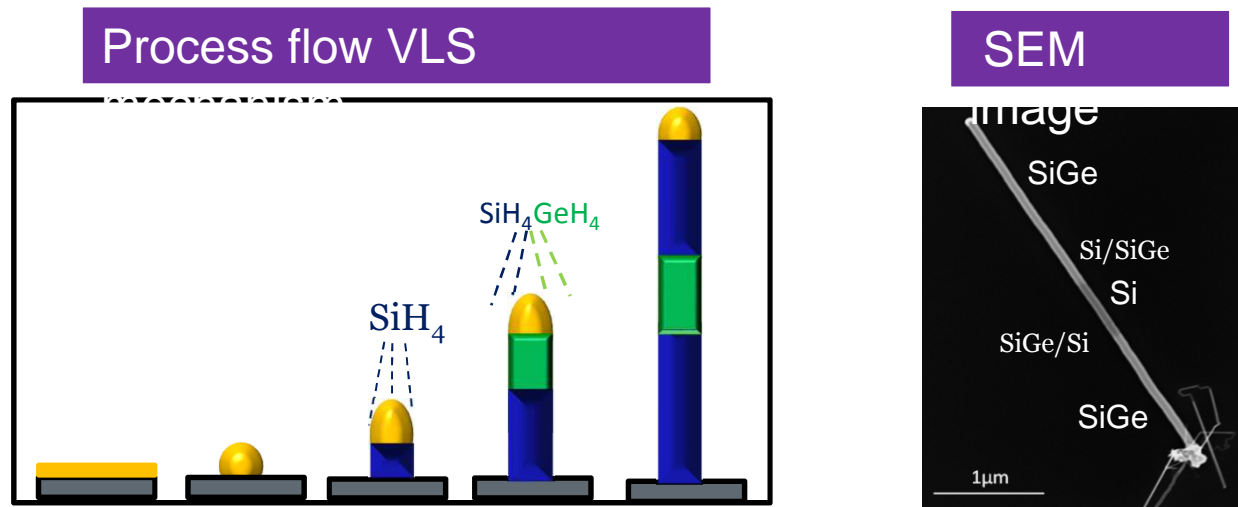
A. TOP DOWN METHOD

- Deposition of Si-SiGe multilayers+Etching

?? Strain relaxation, roughness, defects

B. BOTTOM UP METHOD

- Vapor Liquid Solid mechanism (CVD, MBE, Solid phase synthesis..)



CVD-VLS mechanism allows

- strain relaxation
- low defects

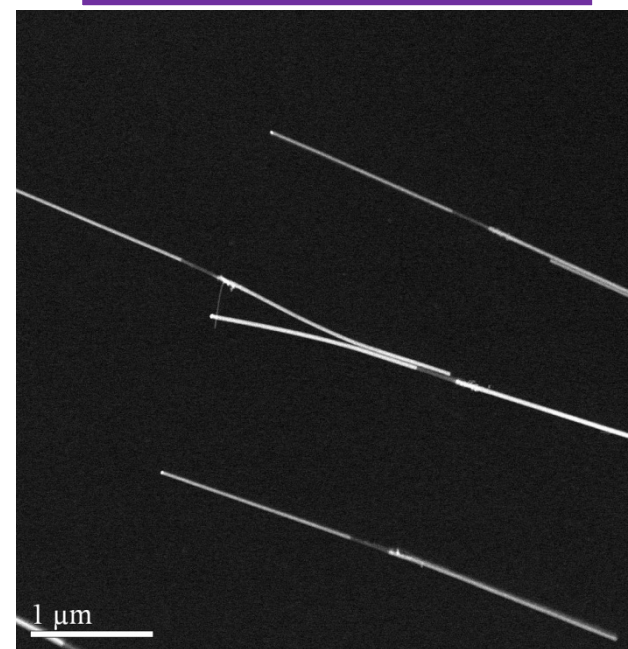
RP-CVD reactor



SiNaPs/CEA/INAC/LTM

- **Gas sources** : SiH_4 , GeH_4 , HCl , H_2 , PH_3 (**n type**), B_2H_6 (**p type**)
- **Temperature** : up to 1100°C
- **Pressure** : from 1 to 10 torr

HAADF-STEM image



Effect of temperature on NW morphology

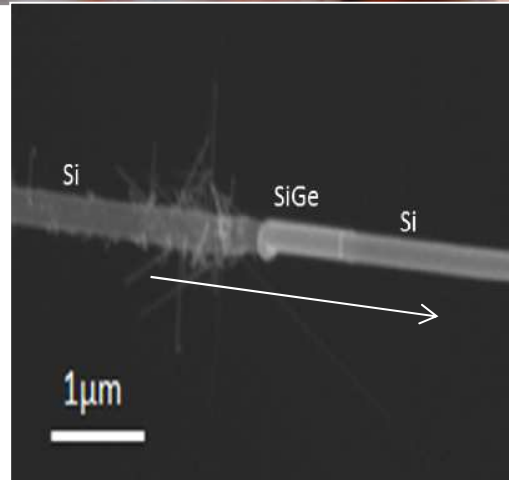
LABORATOIRE DES TECHNOLOGIES
DE LA MICROÉLECTRONIQUE



n ($\text{Si}_{0.3}\text{Ge}_{0.7}$)

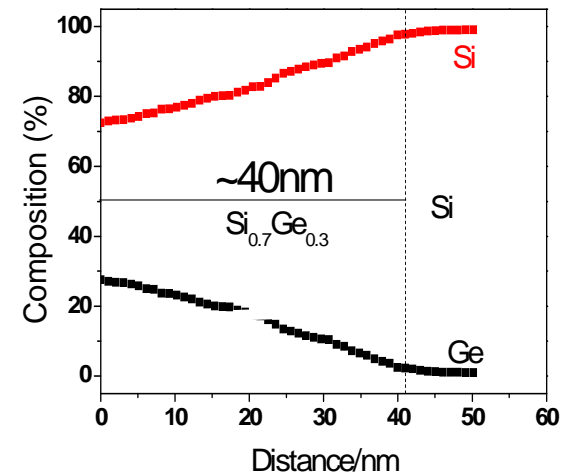
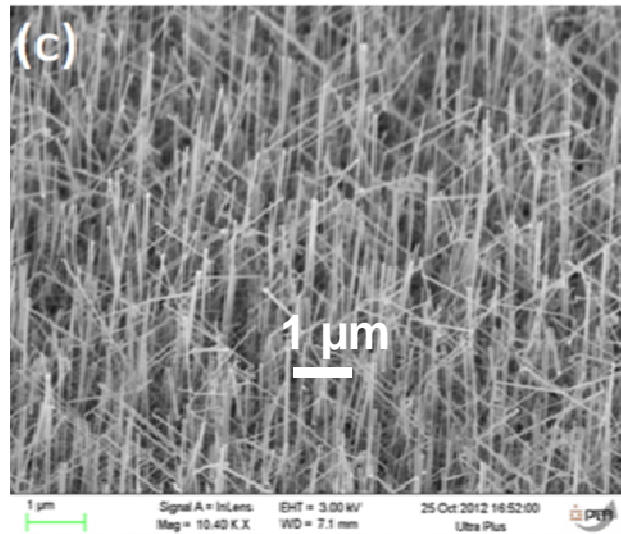
i (Si)

p (Si)



- T_G for Si = 600°C
- T_G for SiGe = 450°C

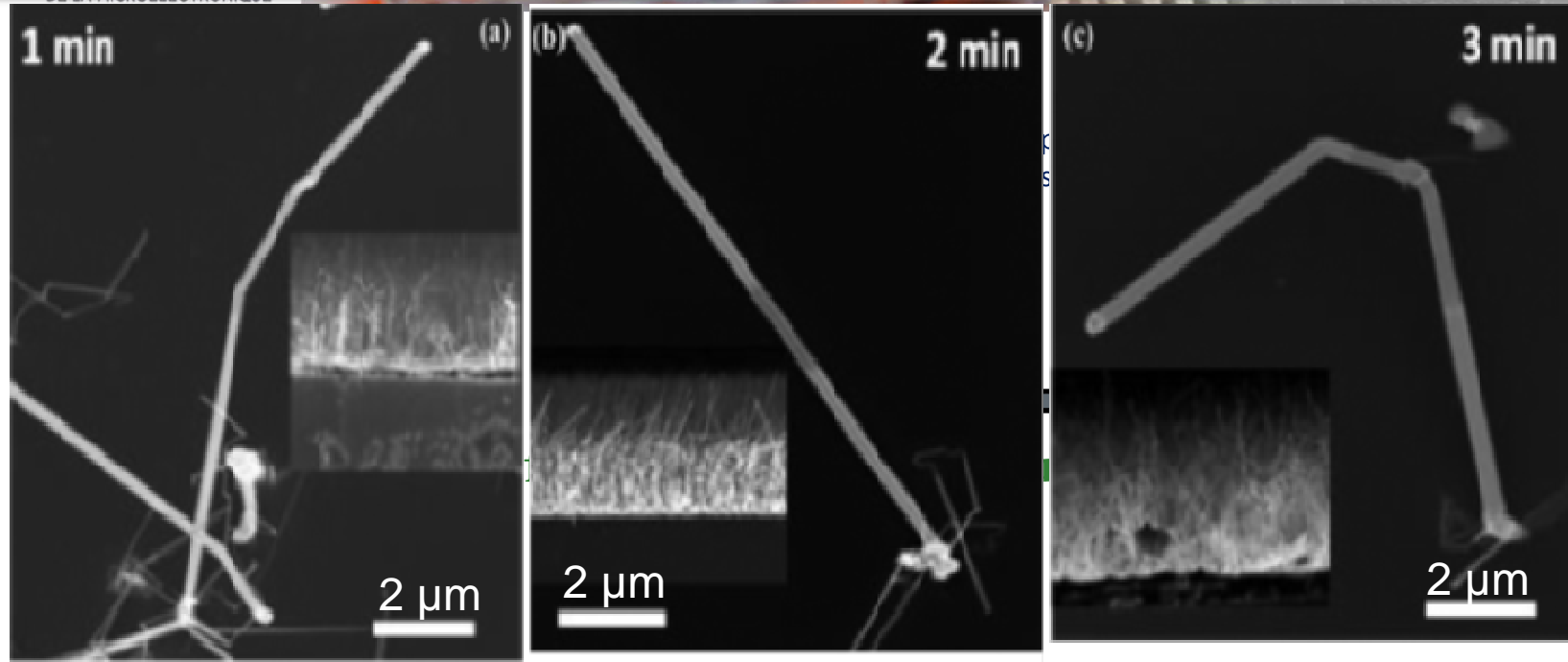
Growth of Si and SiGe at two different temperatures are not favourable



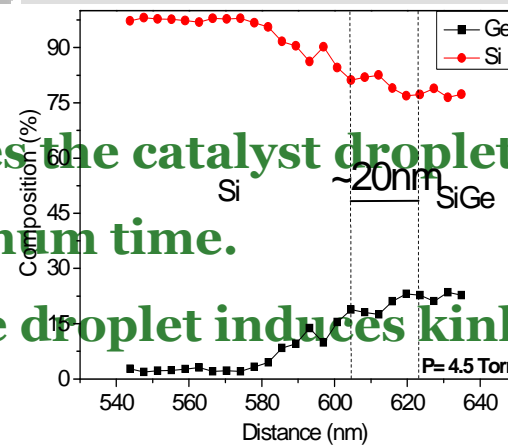
Growth of both segments at 450°C produces high density of NWs

Effect of growth stop on NW morphology

LABORATOIRE DES TECHNOLOGIES
DE LA MICROÉLECTRONIQUE



- Growth stop stabilizes the catalyst droplet and improve abruptness.
- It should be for optimum time.
- Destabilization in the droplet induces kinks or twin boundary.

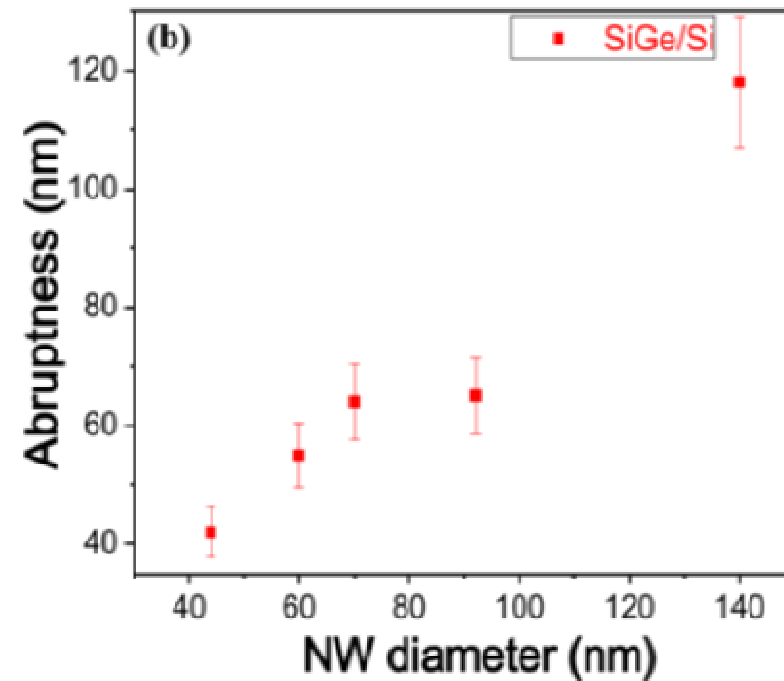
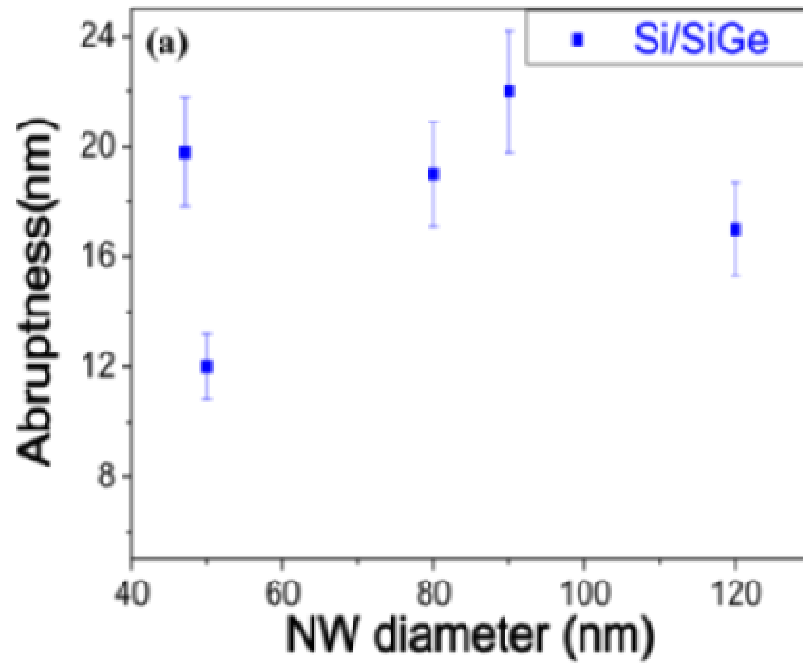


P. Periwal et al JVST A 32 (3) 031101 (2014)

Effect of NW diameter on Si/SiGe and SiGe/Si interface

LABORATOIRE DES TECHNOLOGIES
DE LA MICROÉLECTRONIQUE

For $x=30\%$ and $D=40-120$ nm



- $\text{Si}_{0.7}\text{Ge}_{0.3}/\text{Si}$ interface: linear relation
- $\text{Si}/\text{Si}_{0.7}\text{Ge}_{0.3}$ interface abruptness does not exceed 30 nm.

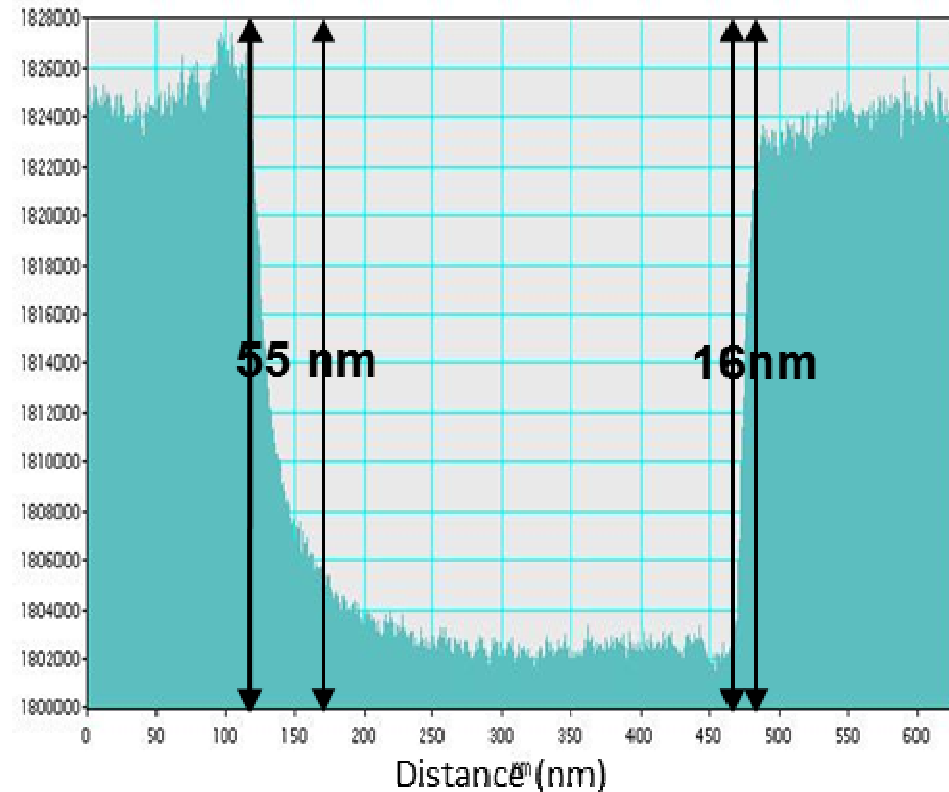
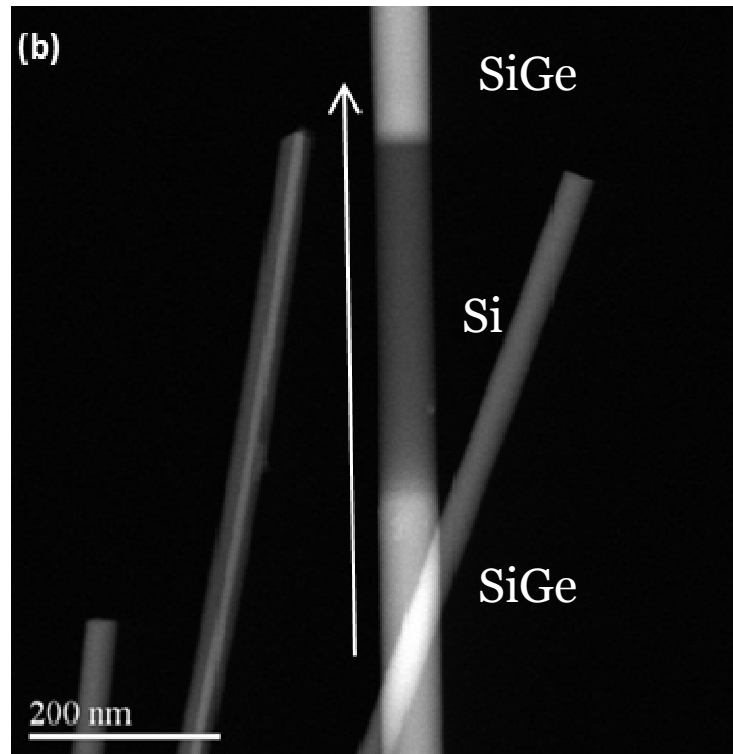
P. Periwal et al NanoLetters 14, 5140 (2014)

Effect of Ge composition in $\text{Si}_{1-x}\text{Ge}_x$ part ($0.3 < x < 0.8$)

LABORATOIRE DES TECHNOLOGIES
DE LA MICROÉLECTRONIQUE

In collaboration with Gilles Patriarche, LPN-Paris

$\text{Si}_{0.4}\text{Ge}_{0.6}$ -Si- $\text{Si}_{0.4}\text{Ge}_{0.6}$ for $D=50-60$ nm

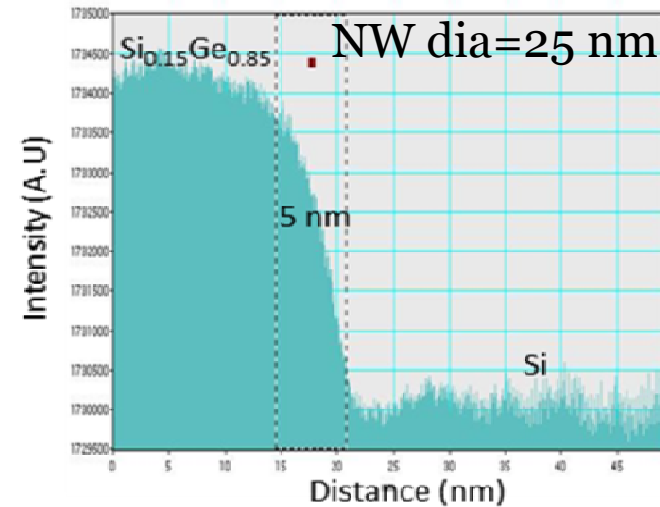
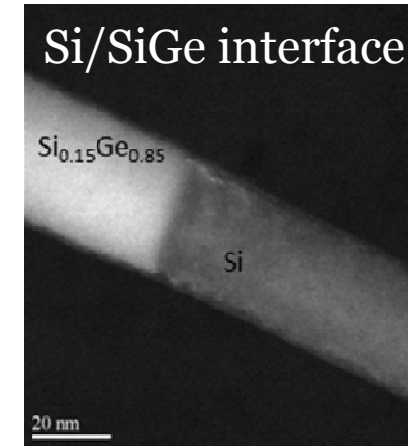
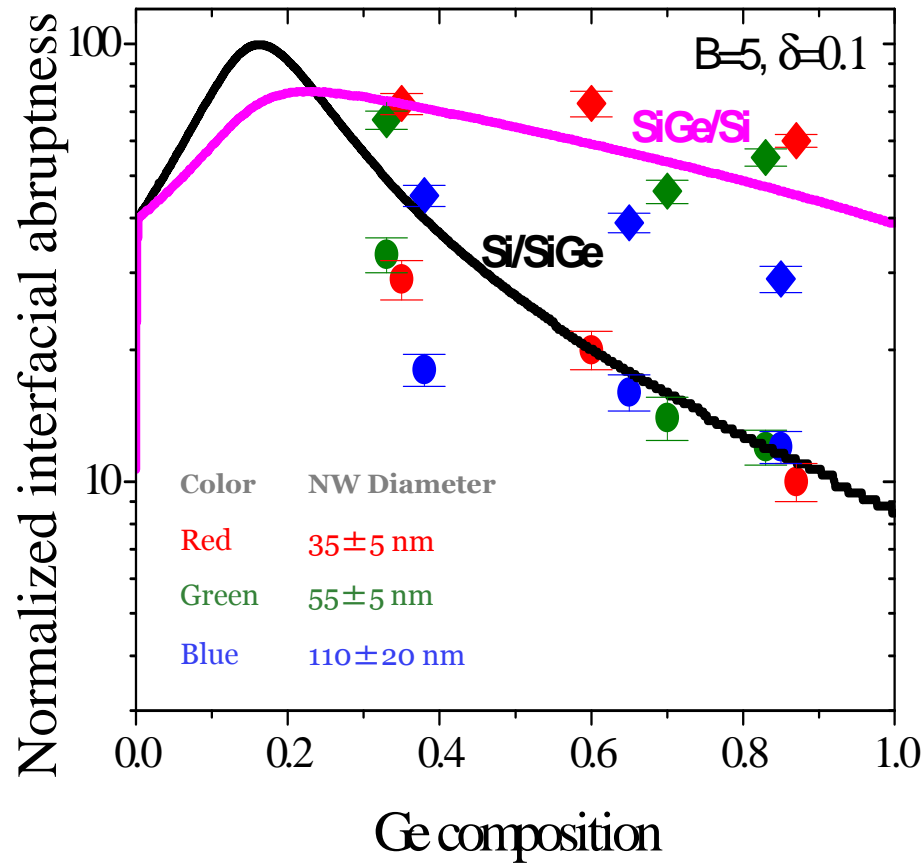


➔ **Asymmetric heterointerfaces:** $\text{Si}_{1-x}\text{Ge}_x/\text{Si}$ is always broader than $\text{Si}/\text{Si}_{1-x}\text{Ge}_x$

P. Periwal et al NanoLetters 14, 5140 (2014)

Modeling & Experimental results

LABORATOIRE DES TECHNOLOGIES
DE LA MICROÉLECTRONIQUE



- Experimental data fits well with the Model
- High Ge & small dia = sharp Si/SiGe interface

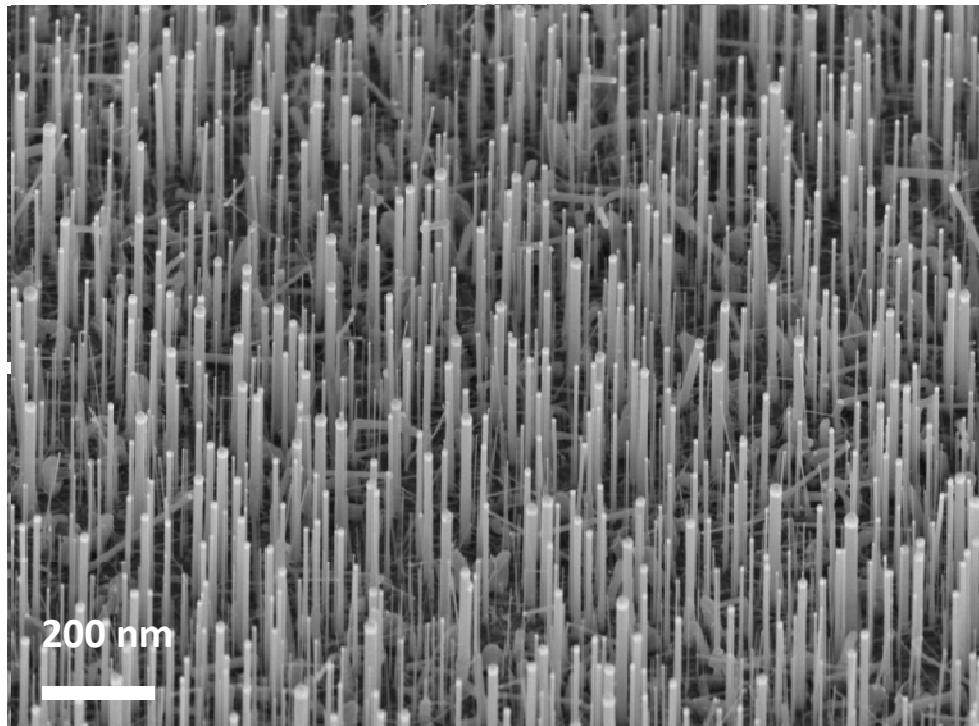
P. Periwal et al NanoLetters 14, 5140 (2014)

Two step growth process: B doped $\text{Si}_{0.7}\text{Ge}_{0.3}$ NWs

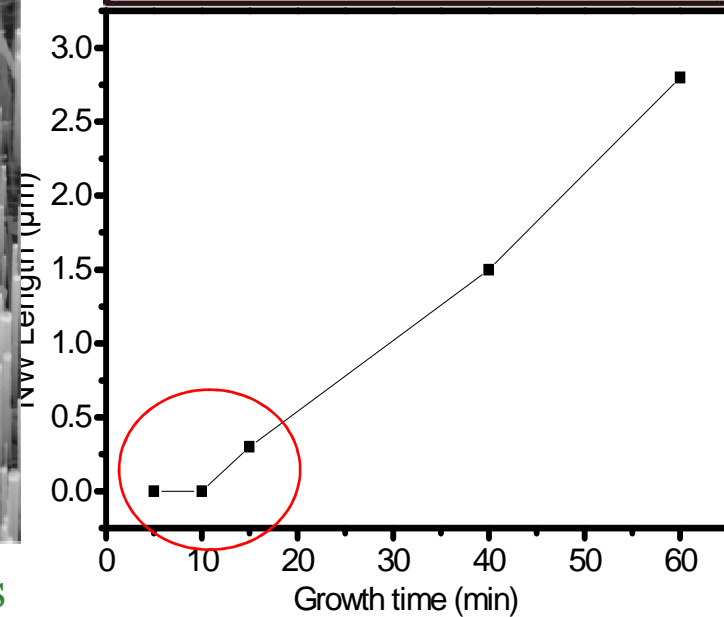
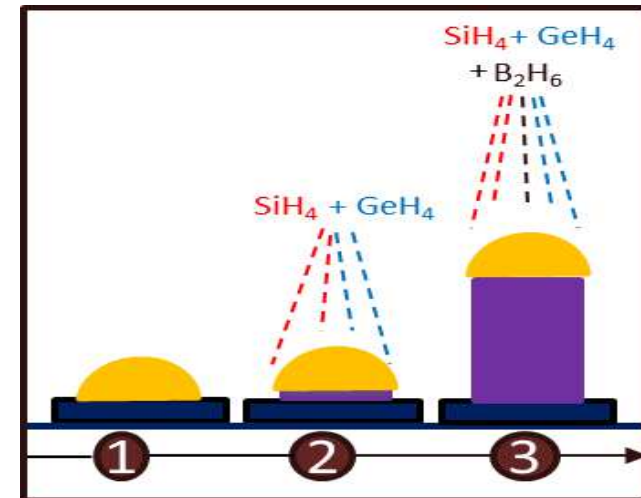
LABORATOIRE DES TECHNOLOGIES
DE LA MICROÉLECTRONIQUE

Two step process:

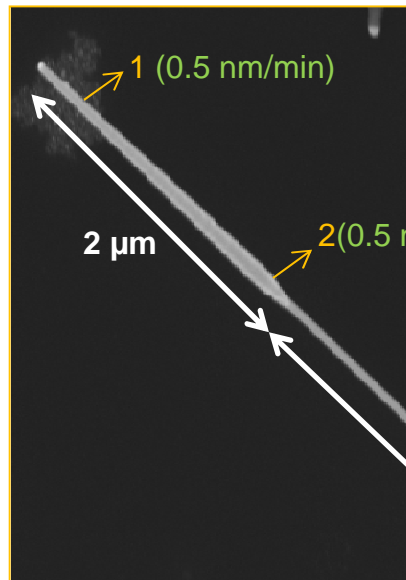
- Continuous flow of SiH_4 , GeH_4 and HCl but no exposure of diborane for few minutes.
- Introduction of diborane gas



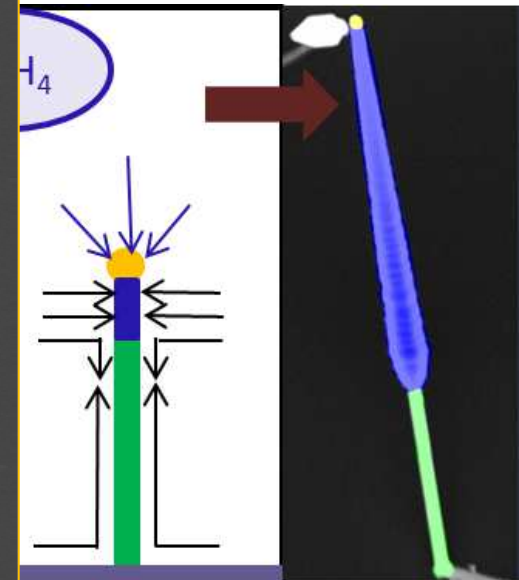
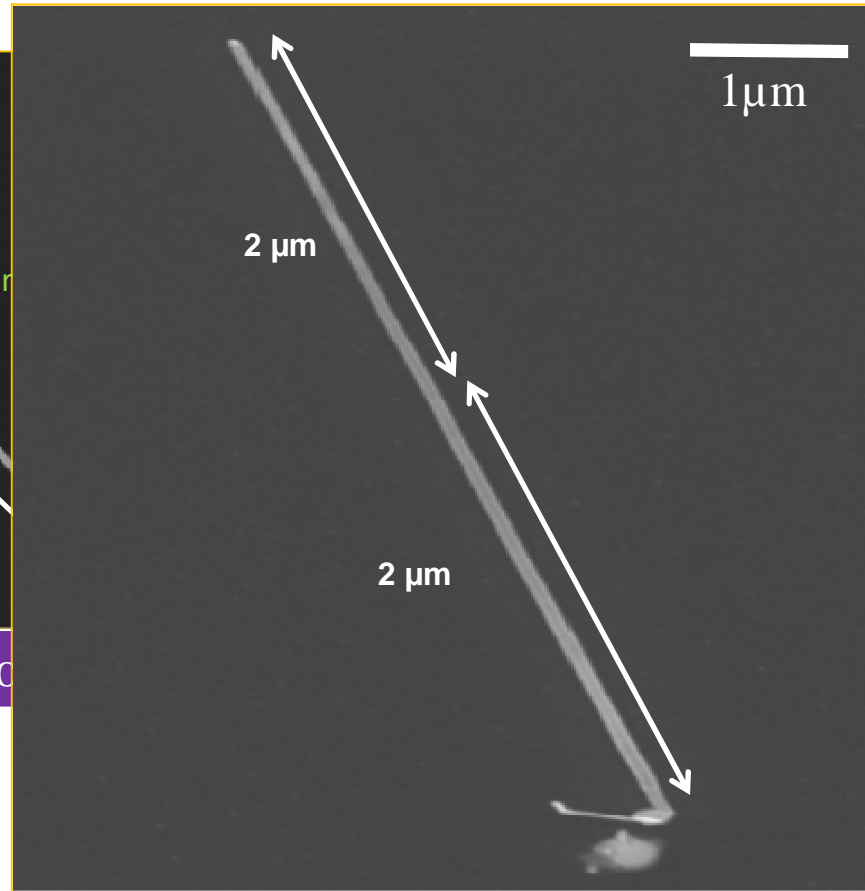
➔ No growth occurs during first 5 minutes



Passivation effect by PH_3 in Ge NWs: Modeling



N+/n junction



Mechanism which takes place

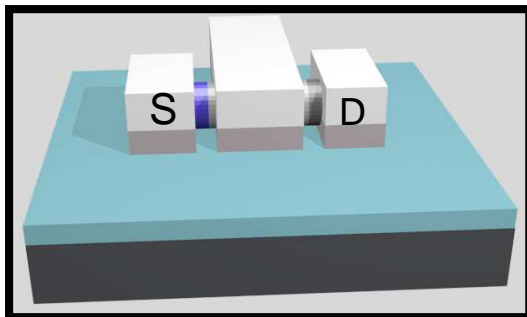
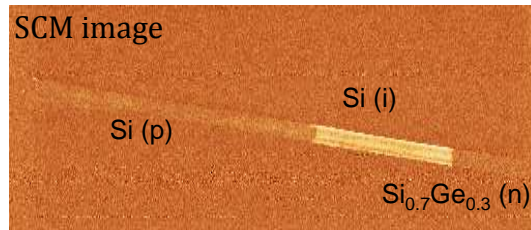
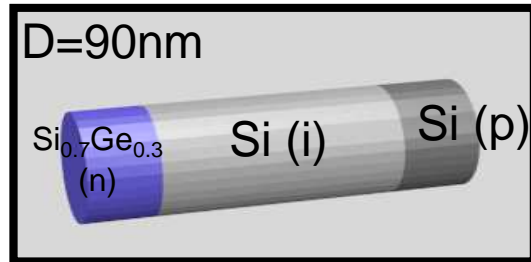
e.

- Mechanism~MBE occurs.

P. Periwal et al APL Mat 2 046105 (2014)

Perspectives: Integration of heterostructure NW in TFET

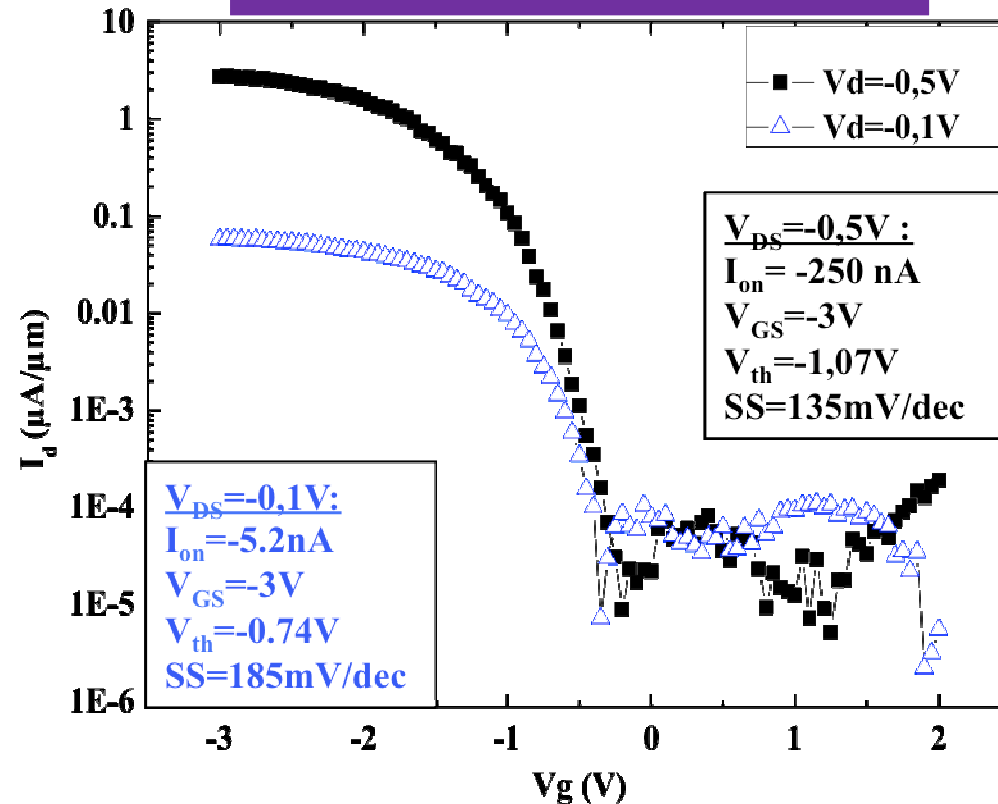
LABORATOIRE DES TECHNOLOGIES
DE LA MICROÉLECTRONIQUE



Device in Ω Gate configuration

➔ Horizontal p-Si/i-Si/n-Si_{0.7}Ge_{0.3} axial heterostructure nanowire
Tunnel FET using Al₂O₃ as gate dielectric represents SS = 135
mV/dec at V_{DS} = -0.5 V

Transfer Characteristics



Thesis Virginie Brouzet (LTM/IMEP) 2015

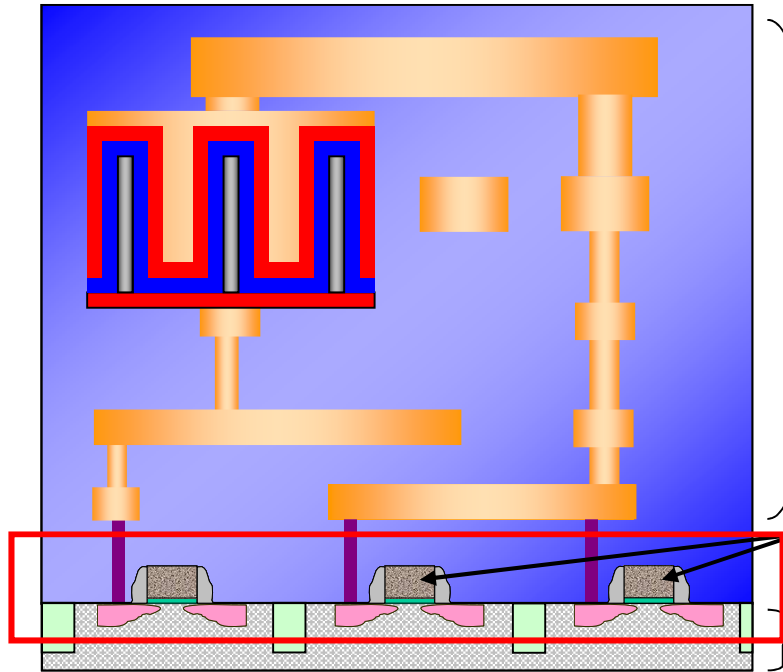


OUTLINE

- ❑ Nanocrystals for memory devices

- ❑ Nanowires for low power devices, capacitors and sensors
 - Low power devices
 - MOS and MIM capacitors
 - Sensors

- ❑ SiGe and InGaAs thin films for NMOS and PMOS FET



IC cross section picture

❖ FET in Front End ?

- Precise dimensions
 - Aggressive performances
 - Metallic interconnections (Back-End-of-line)
 - No metallic contamination
- ⇒ Low interest for CVD VLS NWs

❖ Transistors back-end?

- (Front-End-of-line)
 - Metallic contamination allowed
 - Si Substrate
 - Crystalline growth on metal
- ⇒ Challenge (1 NW – 1 device)

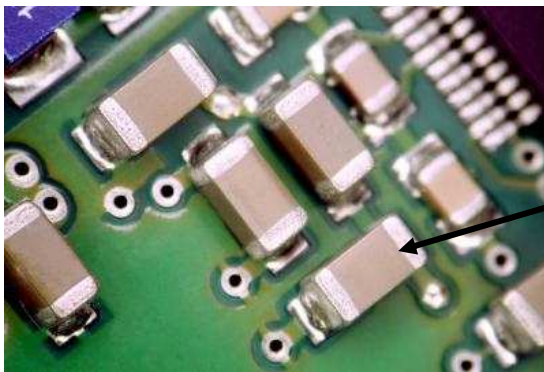
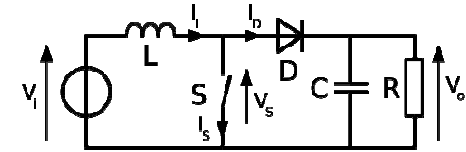
❖ High density capacitors in Back End ?

- Use the high surface area available from an assembly of NWs

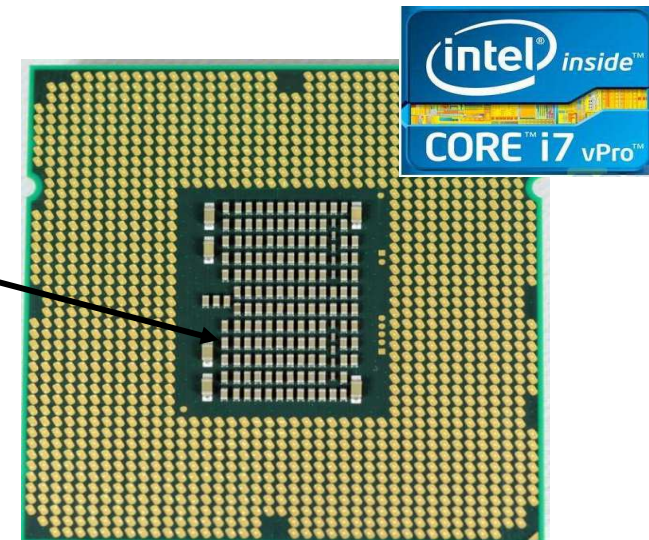
$$C = \frac{\epsilon_0 \cdot \epsilon_r \cdot S}{e}$$

⇒ Challenge

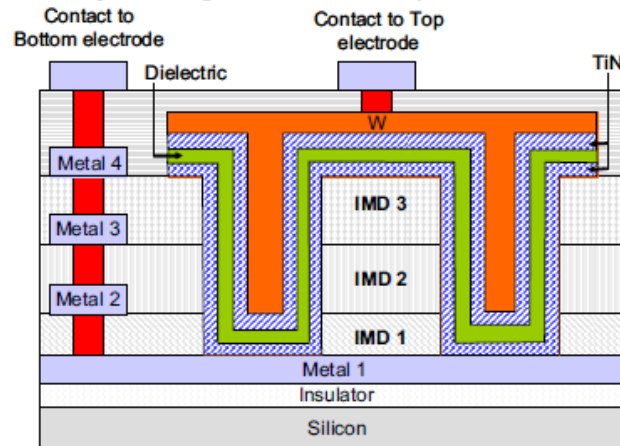
- DC/DC convertor
- **Decoupling capacitor** is a capacitor used to decouple one part of an electrical network (circuit) from another. Noise caused by other circuit elements is shunted through the capacitor, reducing the effect it has on the rest of the circuit.
 - ✓ high capacitance value (1 nF - 1 μF)
 - ✓ Low leakage current
 - ✓ High breakdown voltage (> 10 V)
 - ✓ Low series resistance



Decoupling
capacitors

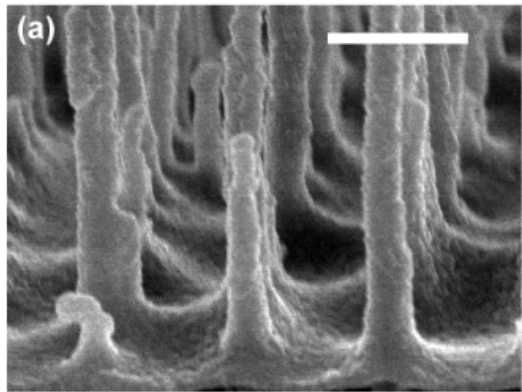


Back-End



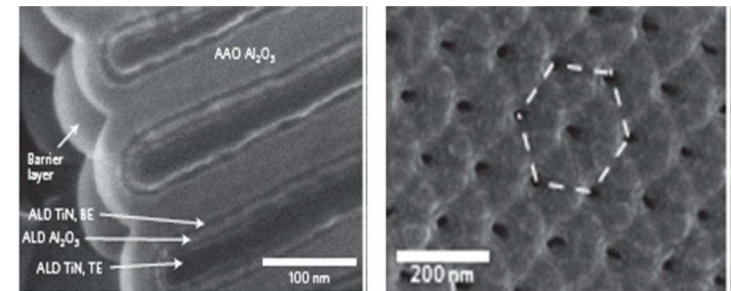
A. Bajolet *et al*, ESSDERC (2005)

$C \sim 4,5 \mu\text{F}/\text{cm}^2$
 $J \sim \text{qq nA}/\text{cm}^2 \text{ à } 1\text{V}$



$C \sim 0.62 \mu\text{F}/\text{cm}^2$
 $J \sim 5 \mu\text{A}/\text{cm}^2 \text{ à } 1\text{V}$

Choi *et al*, Diamond & Related Materials (2009)



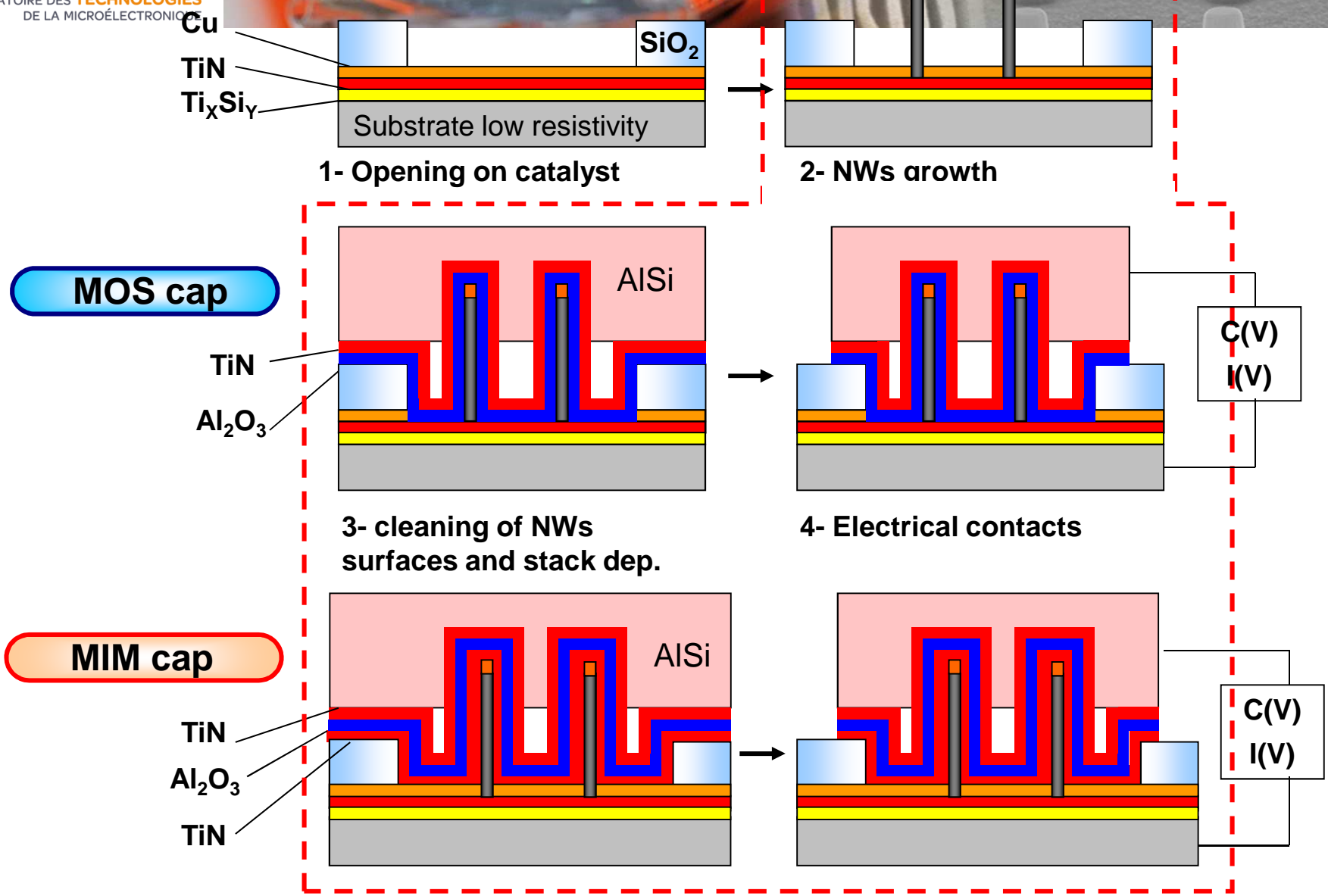
P. Banerjee *et al*, Nat. Nanotech. (2009)

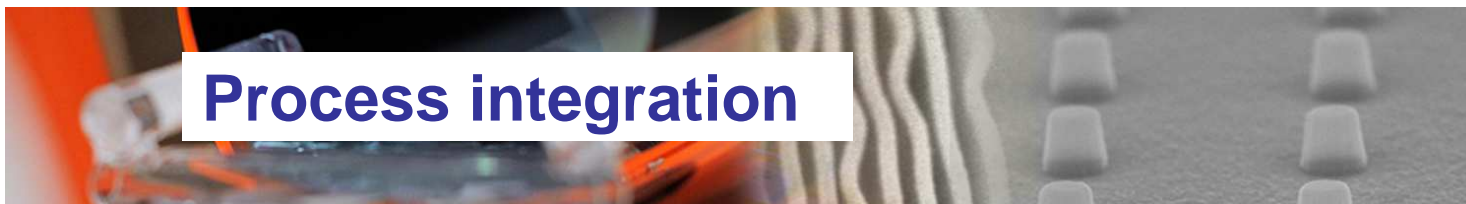
Frequency = 20 Hz

$C \sim 100 \mu\text{F}/\text{cm}^2$
 $J \sim 5 \text{nA}/\text{cm}^2 \text{ à } 2\text{V}$

Process integration

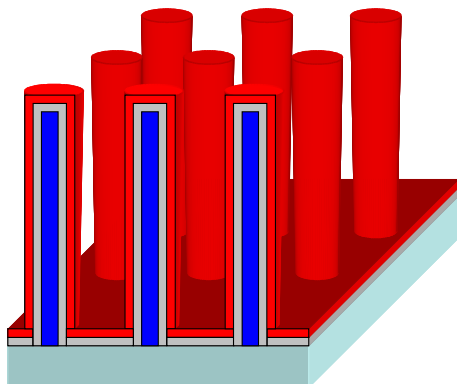
$T < 425^{\circ}\text{C}$





Process integration

Materials choice



- **Dielectric** : ALD alumina

- ✓ Conformal deposition
- ✓ high- κ , $\epsilon_r = 9$
- ✓ High breakdown voltage : 7-10 MV / cm
- ✓ Large band gap : 8,7 eV

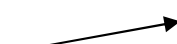
- **Electrodes** : CVD - TiN

- ✓ Conformal deposition
- ✓ Thermodynamically inert with alumina
- ✓ High workfunction : 4,8 eV
- ✗ High resistivity > 200 $\mu\Omega\cdot\text{cm}$

↳ put AlSi for top electrode (2,7 $\mu\Omega\cdot\text{cm}$)

Requirements

- High capacitance density
- Low serie resistance



$$S = 10\,000 \mu\text{m}^2$$

$$10 < C < 20 \mu\text{F}/\text{cm}^2$$

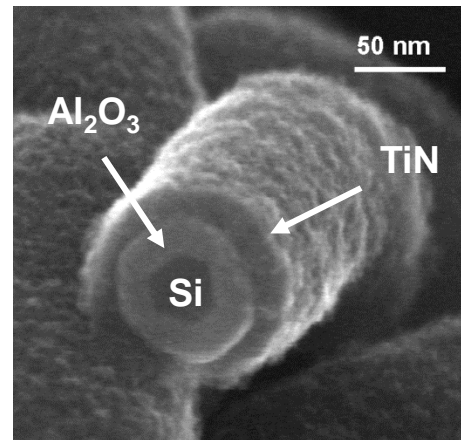
$$R_S \sim 6 \Omega \text{ (MIM) et } R_S \sim 8000 \Omega \text{ (MOS)}$$



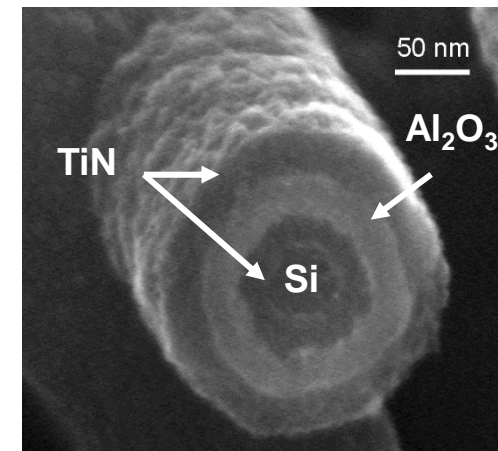
Morphological characterization

MOS

- TiN, 20 nm conformal
- Al₂O₃, 20 nm conformal



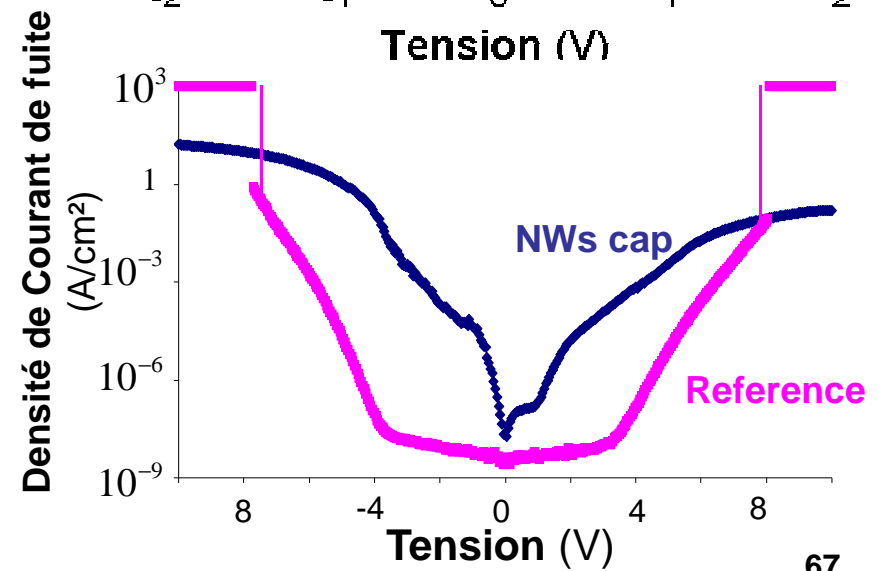
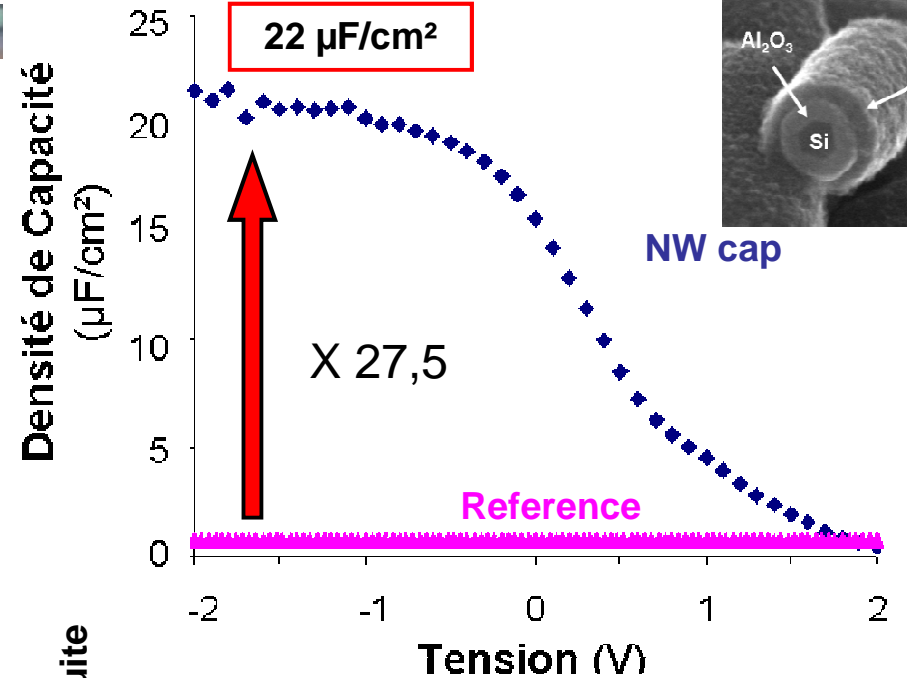
MIM

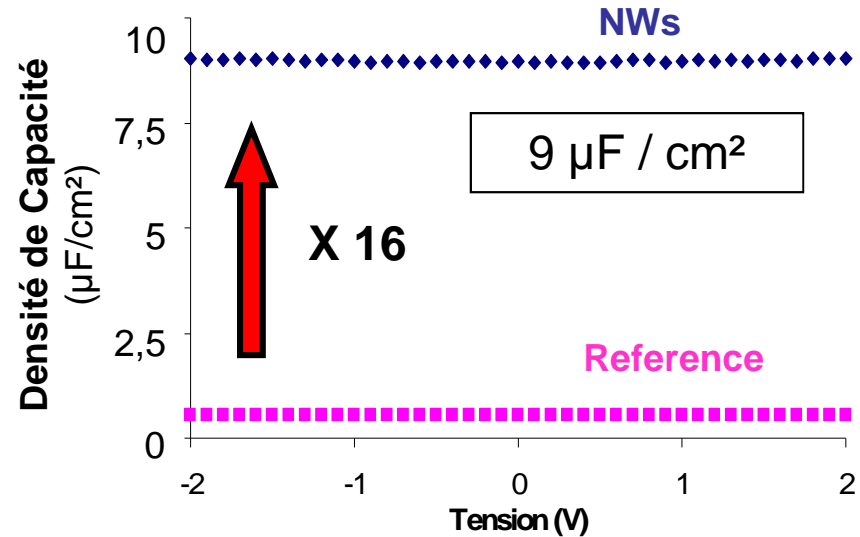
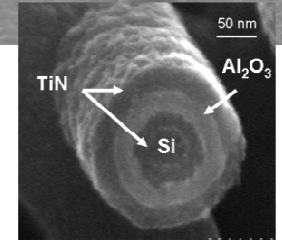


SEM cross section

High capacitance density

- 10 nm alumina
- SI NWs surface cleaning and passivation before ALD deposition
- leakage for NWs capacitors
 - NWs : $49 \mu\text{A}/\text{cm}^2$ à -1V
 - Reference : $6,3 \text{ nA}/\text{cm}^2$
- Lower breakdown voltage





C(V) @ 20 Hz with 15 nm d'alumine

- Gain in capacitance : 16
- decrease of the capacitance from 20 Hz
 - High serie resistance
 - Technological parameters to control



References	[Black04] Gravure	[Choi10] Nanotubes	[Banerjee09] Alum. nanop	Al₂O₃ 15 nm
Density of Capacitance ($\mu\text{F}/\text{cm}^2$) F	3,13	0,62	10	9,6
Density of leakage current de fuite à 1V (nA/cm ²) A	2 500	5 000	5	11
(F/A)	1,25	0,124	2000	873

Industrial requirements for DC/DC converter and decoupling capacitors

	I / C @ 3,6 V	Breakdown V
Specifications Ipdia	$< 7 \times 10^{-12} \text{ A / nF}$	$> 10 \text{ V}$
NW cap 15 nm Al ₂ O ₃	$3,5 \times 10^{-11} \text{ A / nF}$	9 V

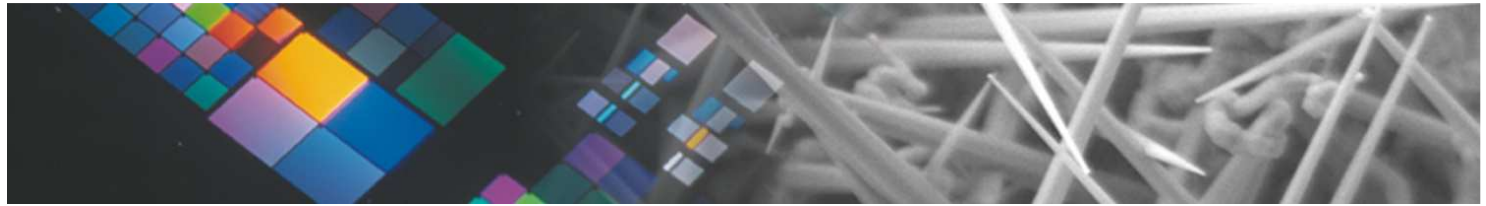


OUTLINE

- ❑ Nanocrystals for memory devices

- ❑ Nanowires for low power devices, capacitors and sensors
 - Low power devices
 - MOS and MIM capacitors
 - Sensors

- ❑ SiGe and InGaAs thin films for NMOS and PMOS FET



Silicon nanonets, Sensors



P. Serre, PhD 2014

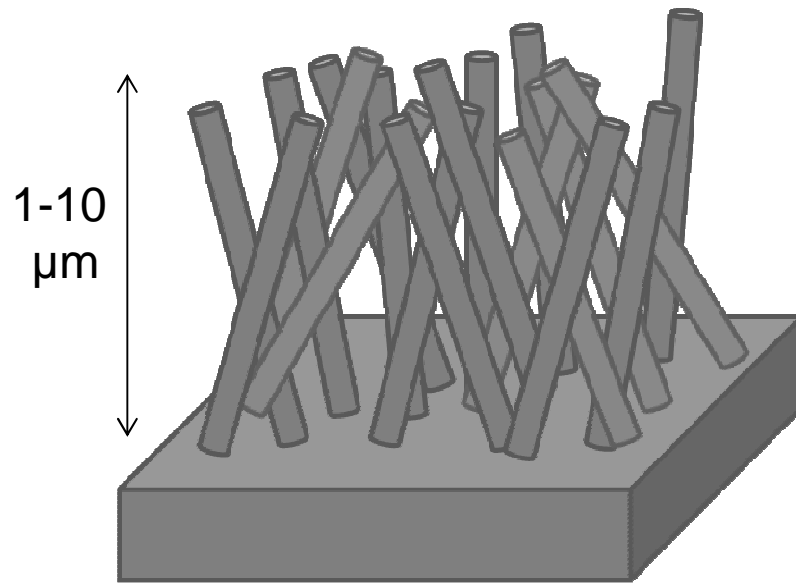
UNIVERSITÉ DE GRENOBLE



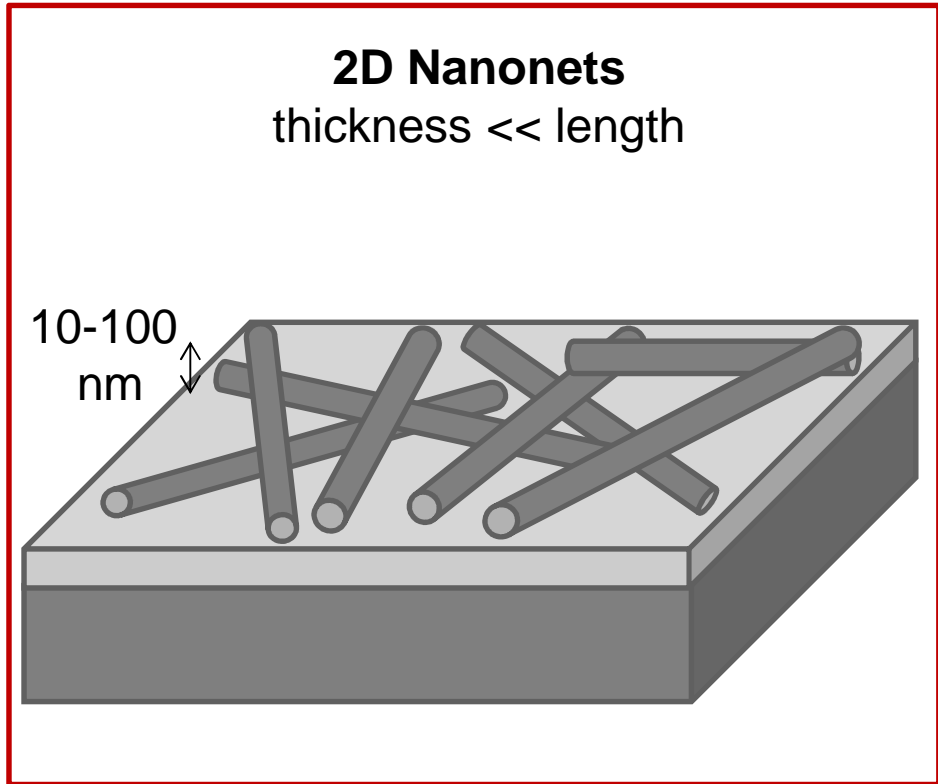
Nanonets

Nanonet = NANOstructured NETwork
Network of 1D (NFs or NTs) randomly oriented

3D Nanonets
thickness \leq length



2D Nanonets
thickness \ll length





Introduction : Si 2D nanonets

Characteristics

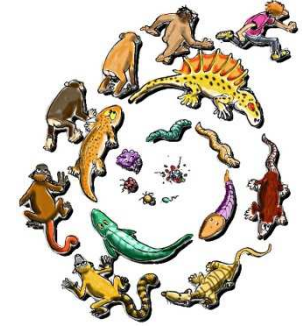
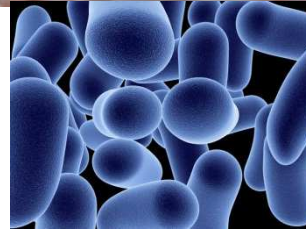
- High aspect ratio
- High specific area
- Electrical conductor
- Optical transparency
- Mechanical flexibility
- Fonctionnalisation possible
- Versatile
- Reproducible

Applications

- Conductive, transparent, flexible electrodes,
 - Solar cells
 - OLED
 - touch screen
- Photodetection
- Chemical and biological sensors

Si Nanonets for detection

Challenges



Health
Medical diagnostic

Evolution

Sensors

Environnement
Water analysis

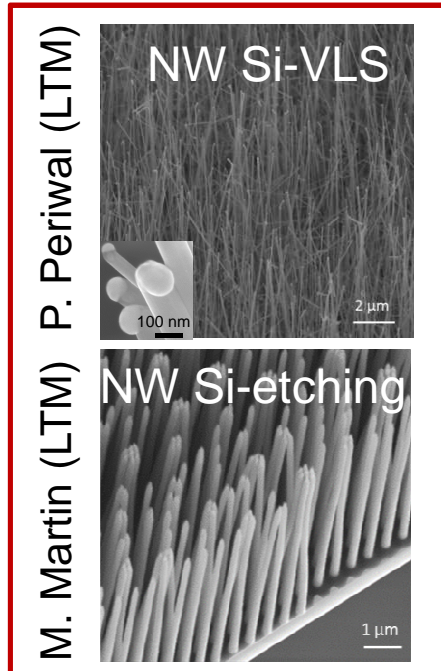
Agroalimentaire
Bacteria detection



- Portable
- Reliable
- Low cost
- Fast response

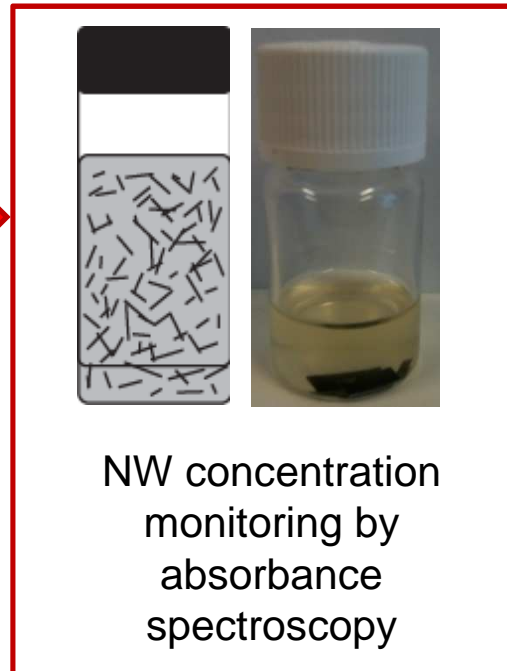
Nanonets fabrication by filtration method

NWs elaboration



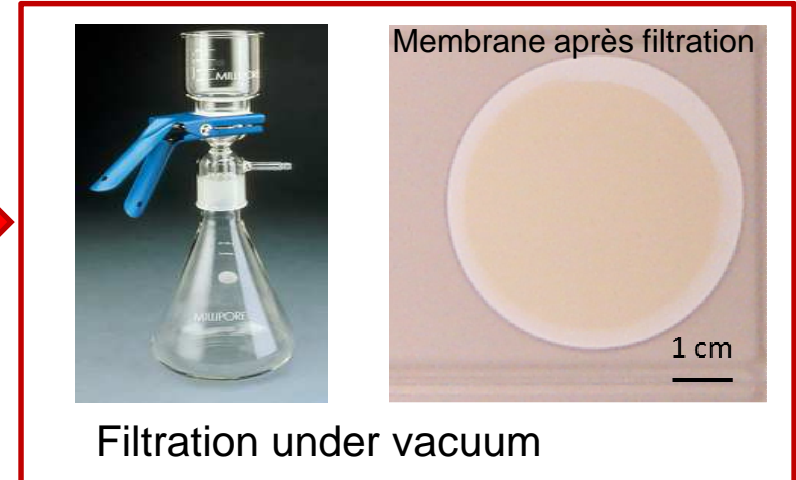
Sonication

Solution

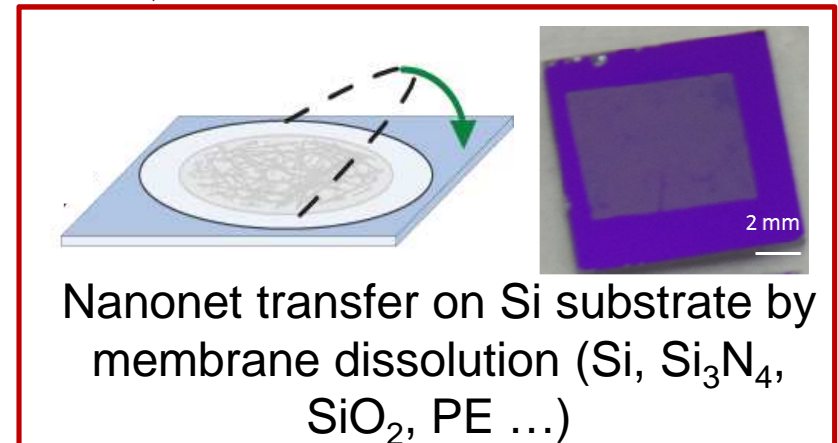


Filtration

Nanonet fabrication



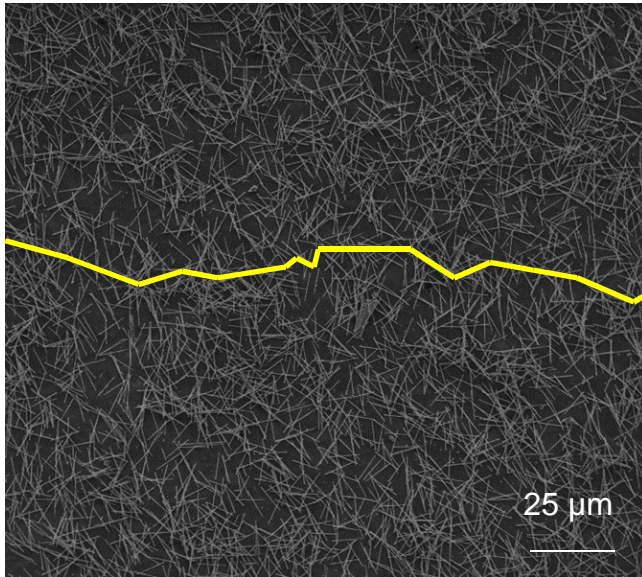
Transfert on substrate



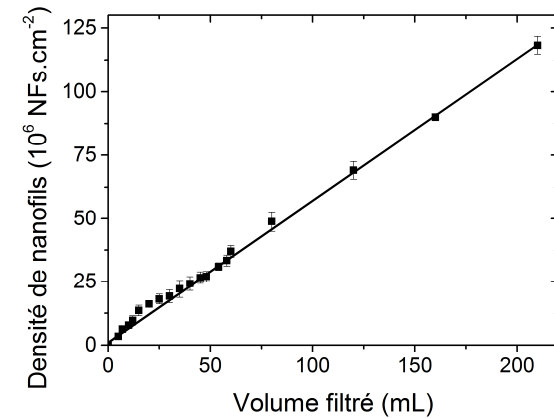
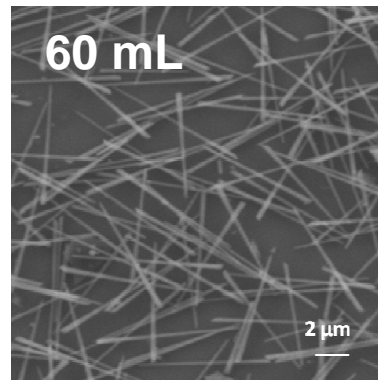
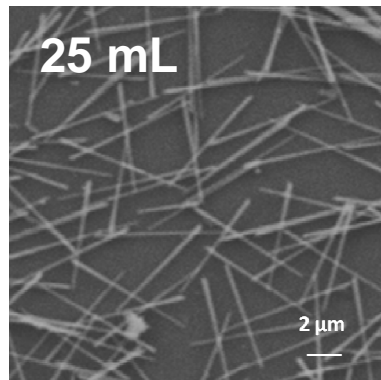
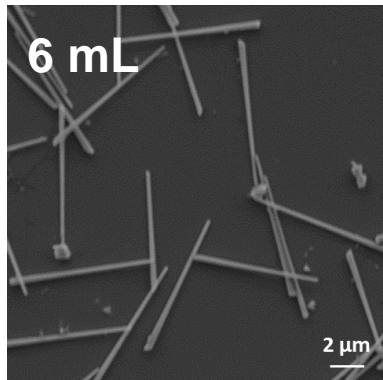
Simple, low cost
RT process
Limited thickness
Large scale

Nanonet morphology

10 μm long NWs



Randomly oriented
Well interconnected
Percolation path
Uniform
Large scale
Good adherence with substrate

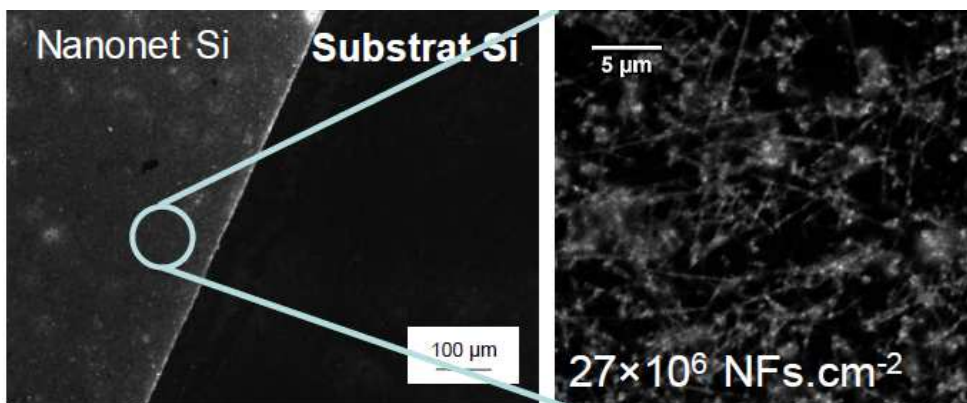


Precise control of
NWs density







ADN hybridation detection by fluorescence

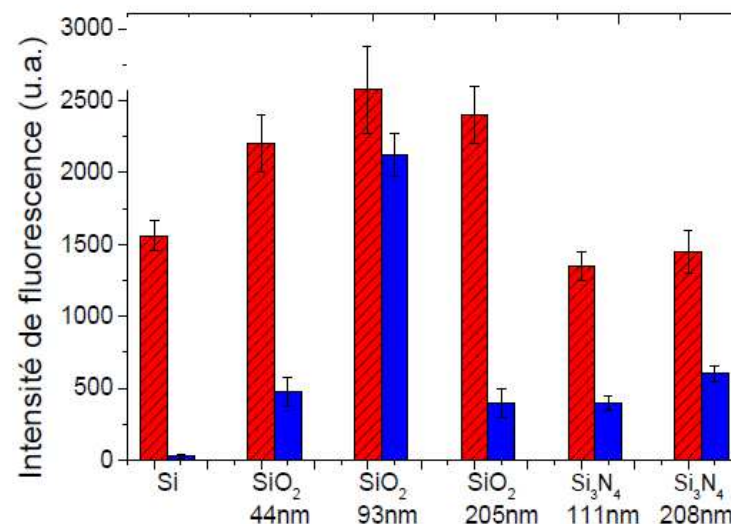


Fluorescence sur les nanonets de Si

Signal de fluorescence discret

P. Serre et al,
Sensors and Actuators B, 182, 390-395 (2013)

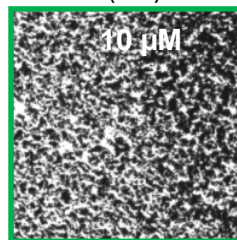
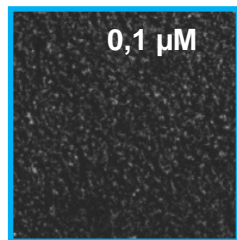
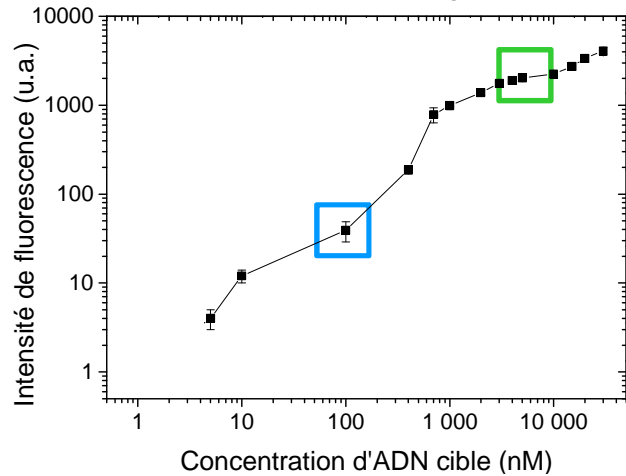
 Avec nanonet de Si
 Substrat plan sans nanonet de Si



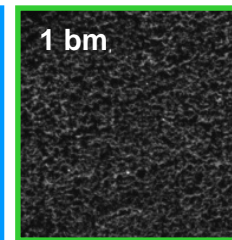
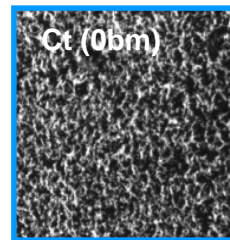
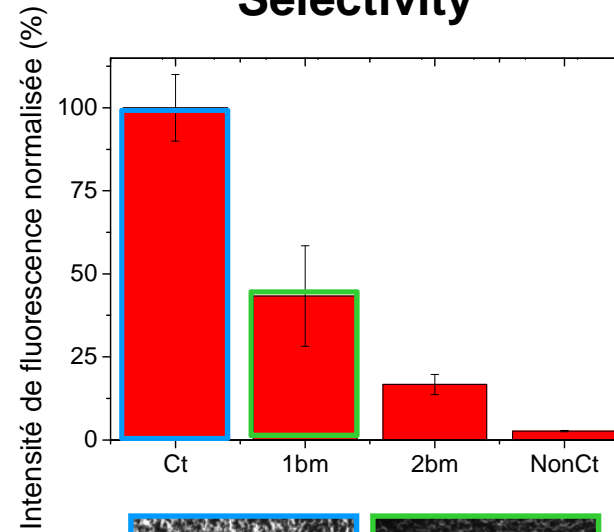
Détection de l'ADN par fluorescence
Immobilisation de l'ADN sur les nanonets de Si

Signal dépend du substrat
Amélioration du signal sur les nanonets de Si par rapport à tous les substrats plans

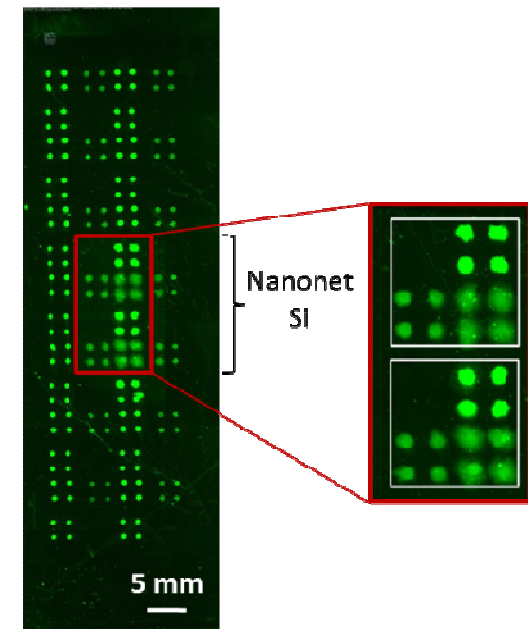
Sensibility



Selectivity



Integration in an DNA dye



P. Serre *et al*,

DNA sensor : sensible, selective.



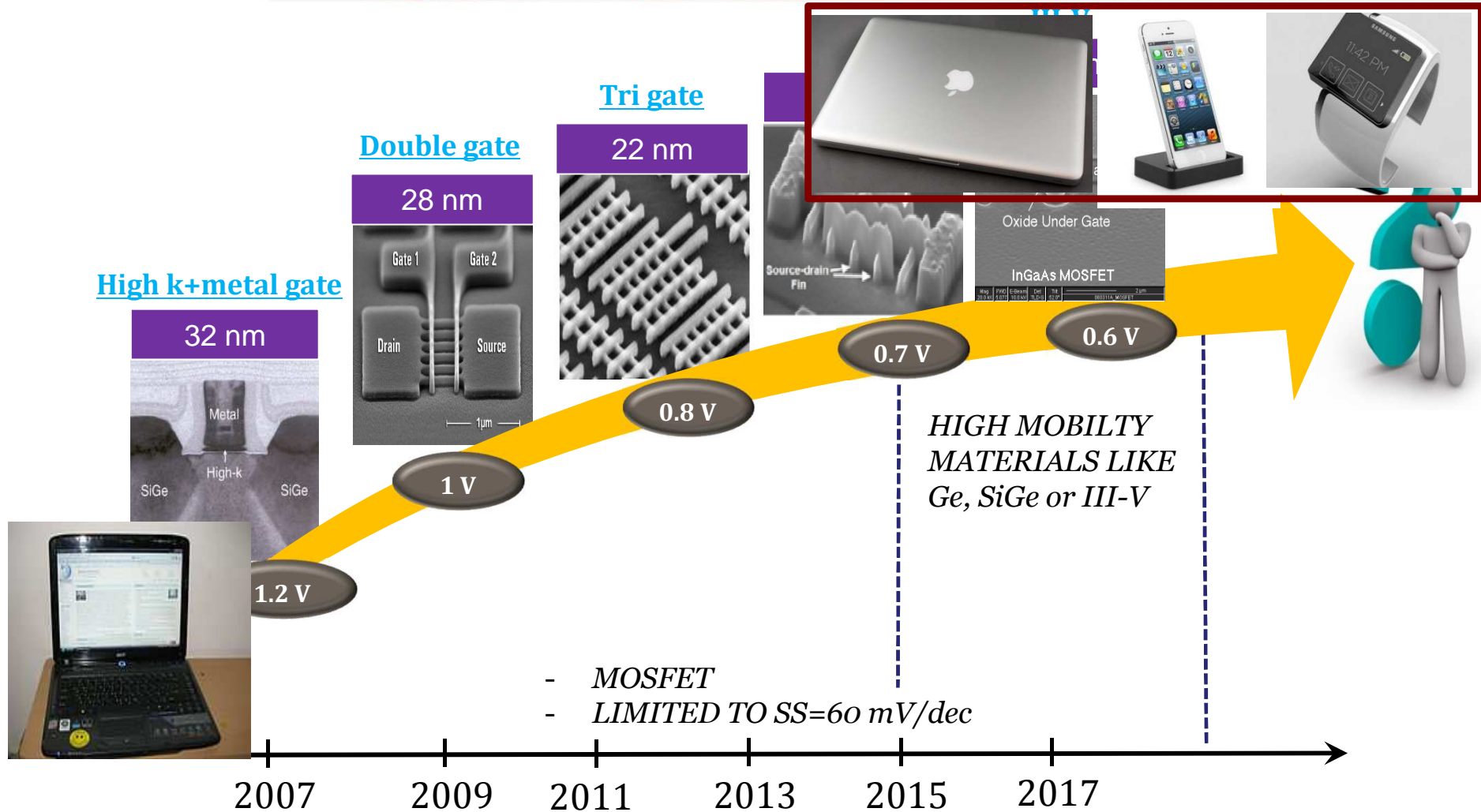
OUTLINE

- ❑ Nanocrystals for memory devices

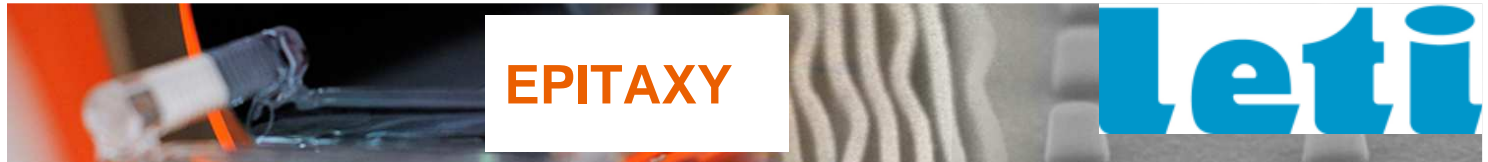
- ❑ Nanowires for low power devices, capacitors and sensors
 - Objective : low power devices
 - Si/SiGe nanowires catalytic growth
 - Other applications

- ❑ SiGe and InGaAs thin films for NMOS and PMOS FET

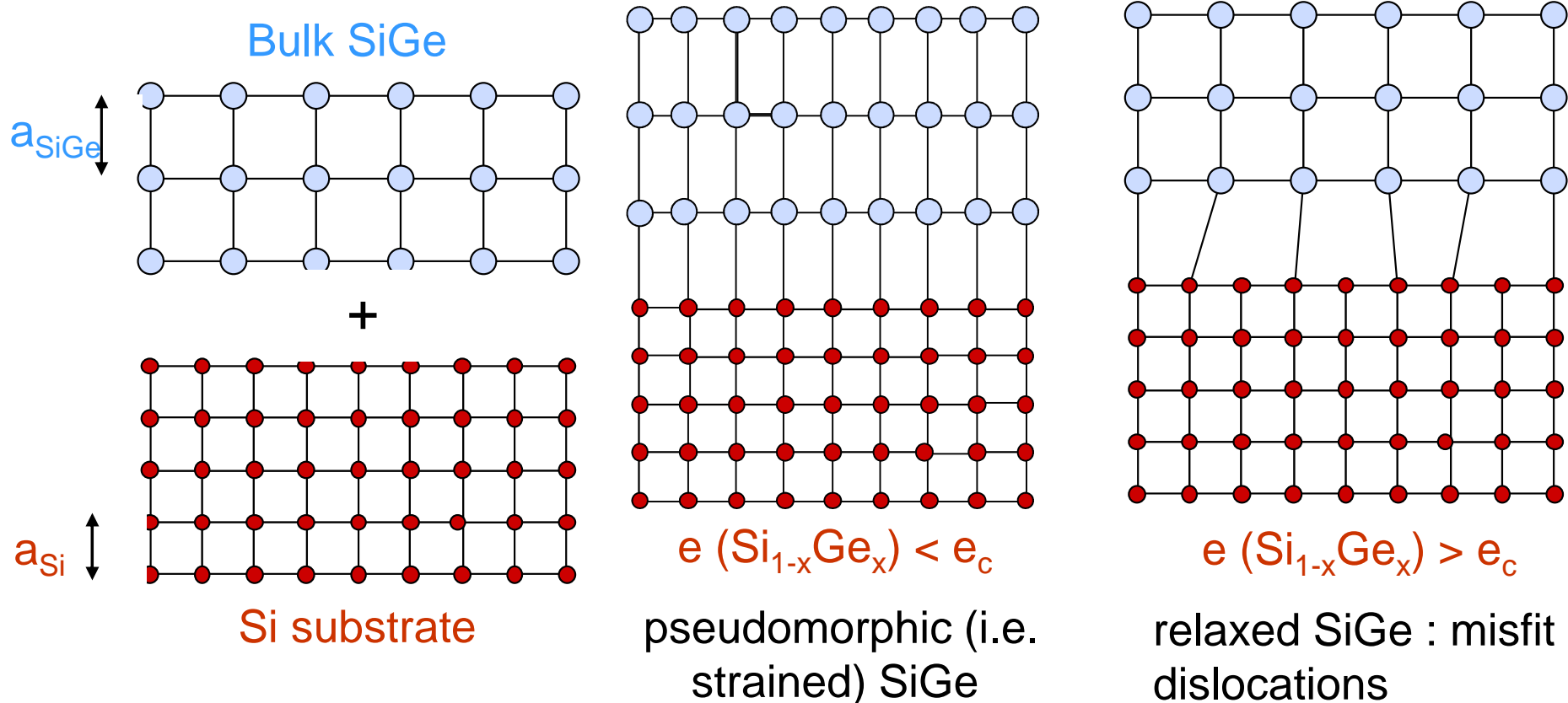
Roadmap of Energy Efficient Devices

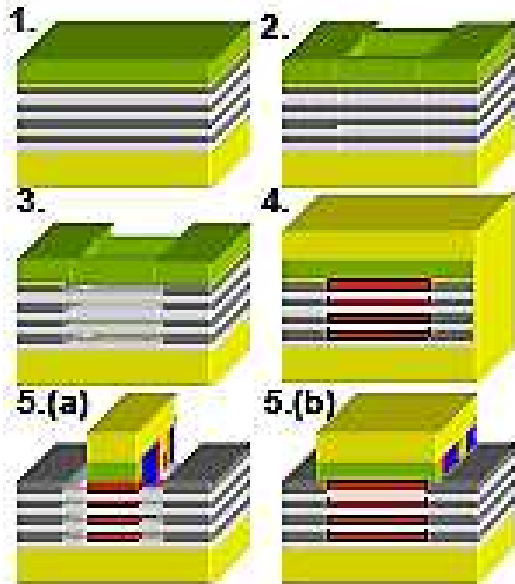


Need of SiGe alloys for future devices and III-V exploration on a Si platform

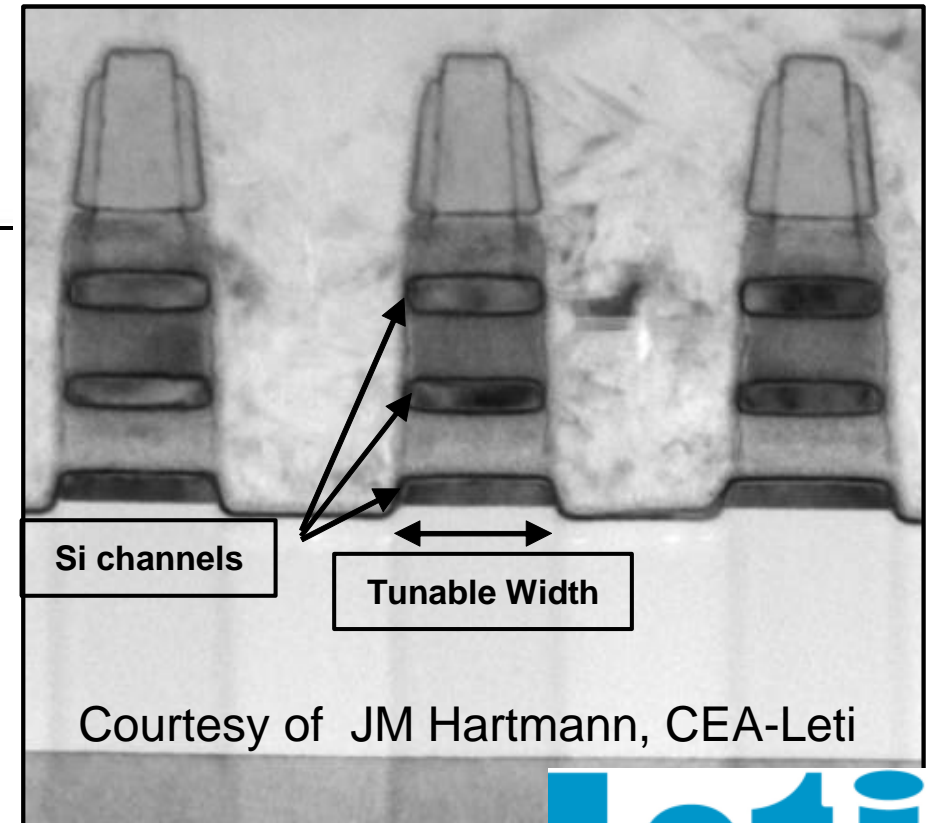
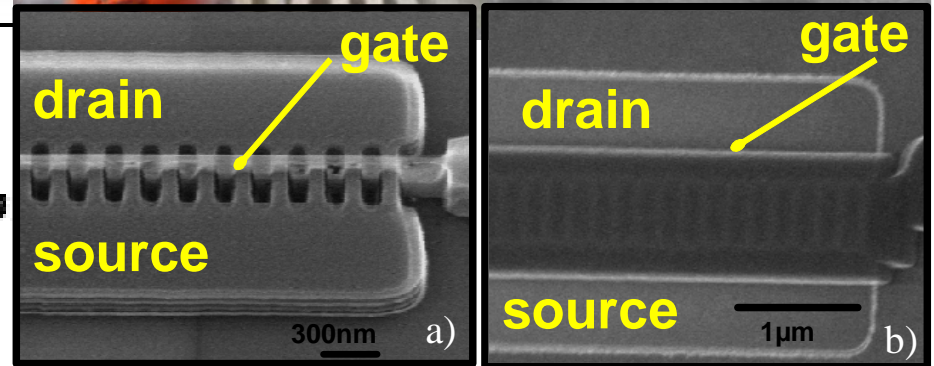


Epitaxy = mono-crystalline layer grown on a mono-crystalline substrate;
homo-epitaxy : layer A (Si) on substrate A (Si);
hetero-epitaxy : layer B (SiGe) on substrate A (Si)
 $a(\text{Si}_{1-x}\text{Ge}_x) = 5.43105 + 0.20050x + 0.0263x^2 \text{ \AA} > a(\text{Si}) = 5.43105 \text{ \AA} \Rightarrow$
Strain accumulation inside the SiGe layer when grown on Si. 2 scenarii :



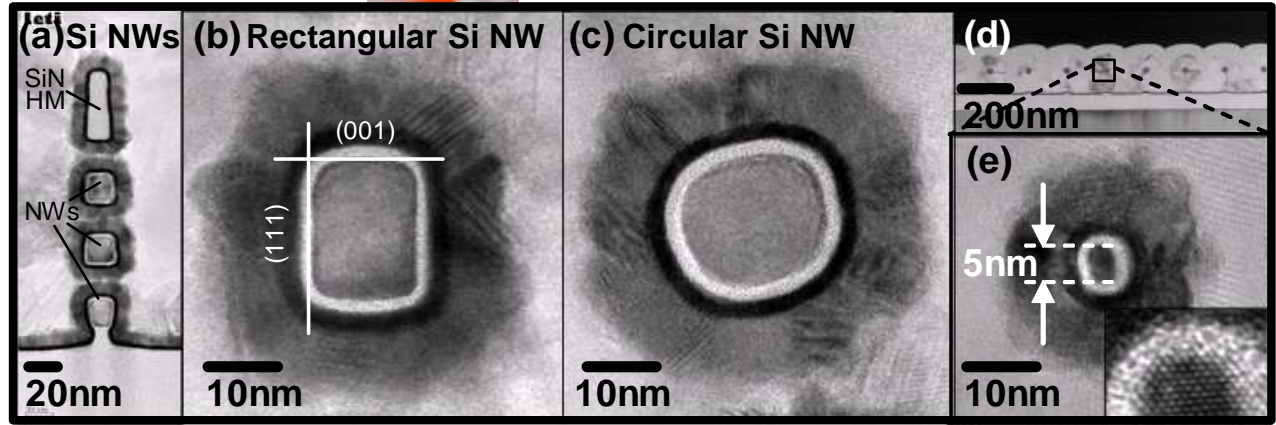


1. Epitaxy of Si/SiGe superlattice
2. Etching (RIE) of multilayer
3. Selective isotropic etching of SiGe
4. Gate stack definition: $\text{HfO}_2/\text{TiN}/\text{poly-Si}$
CMP poly-Si
 SiO_2 hard mask
5. Gate etch (anisotropic+isotropic)
(a) Etched gate (EG)
(b) Plugged gate (PG)

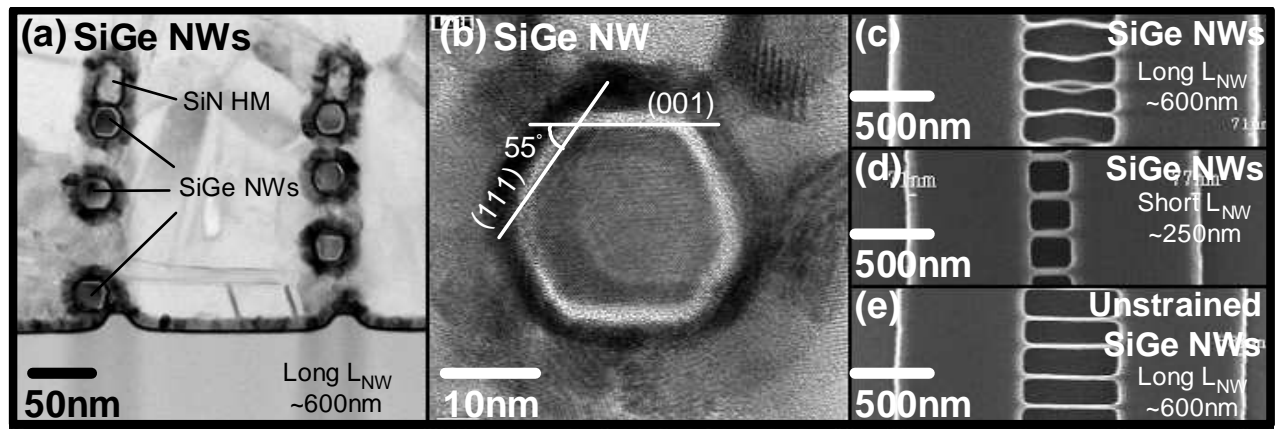


- 1 - Growth of SiGe/Si superlattices on SOI
- 2 - Anisotropic etching of those SL
- 3 - selective plasma etching of SiGe
- 4 - gate stack formation
- 5 - gate etch

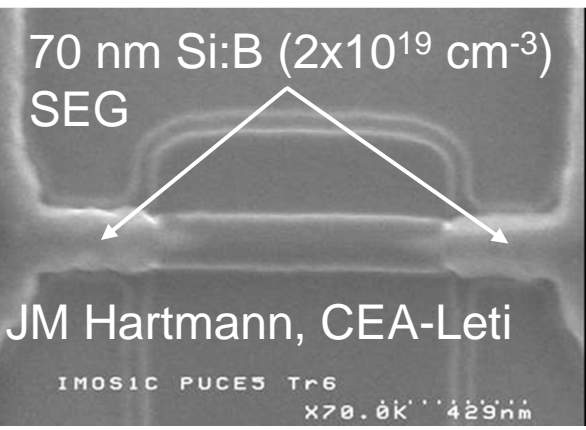
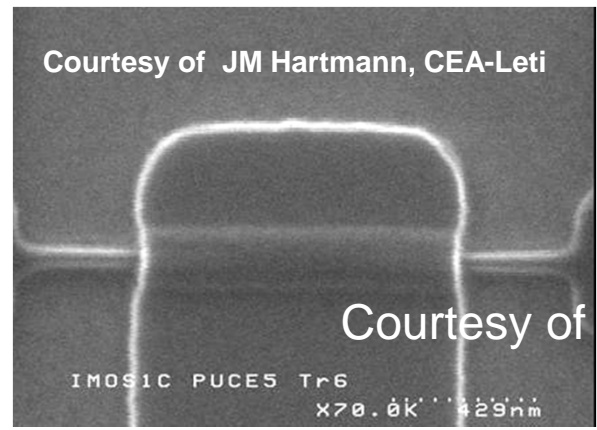
Superior I_{on}/I_{off} trade-offs in MBCFETs :
 nMOS : $2.27 \text{ mA}/\mu\text{m} \Leftrightarrow 16 \text{ pA}/\mu\text{m}$
 pMOS : $1.32 \text{ mA}/\mu\text{m} \Leftrightarrow 16 \text{ pA}/\mu\text{m}$



H₂ bake of square-based Si NWs : rounding. Combined with self-limiting oxydation => very small diameter NWs.



H₂ bake of square-based SiGe NWs : hexagonal section. SEG of thin Si cap to improve hole mobility.



Selective thickening of the access regions of Si NWs

APL 91, 233502 (2007); ECS Trans. 13 (1), 195 (2008) & 27 (7) 471 (2009)

Room temperature properties	Si	Ge	GaAs	InAs	InP	InSb
Electron mobility (cm ² V ⁻¹ s ⁻¹)	1 400	3 900	8 500	40 000	5 400	77 000
Hole mobility (cm ² V ⁻¹ s ⁻¹)	450	1 900	400	500	200	850
Bandgap (eV)	1.12	0.66	1.42	0.35	1.34	0.17
Lattice parameter (Å) Diamond or blende-zinc structure	5.431	5.658	5.653	6.058	5.869	6.749

⇒ **Conduction channel (nMOS) : InGaAs ([In] : 30-70%) on GaAs / Ge / Si when thinking of a monolithic integration on Si**



Challenges : Growth of InGaAs channel on Si(100)

- ❑ Lattice mismatch (Si-GaAs 4%, Si-InAs 10%)
- ❑ Polarity induces antiphase domains
- ❑ Thermal expansion coefficient limits the total thickness before cracks appearing



Antiphase domains

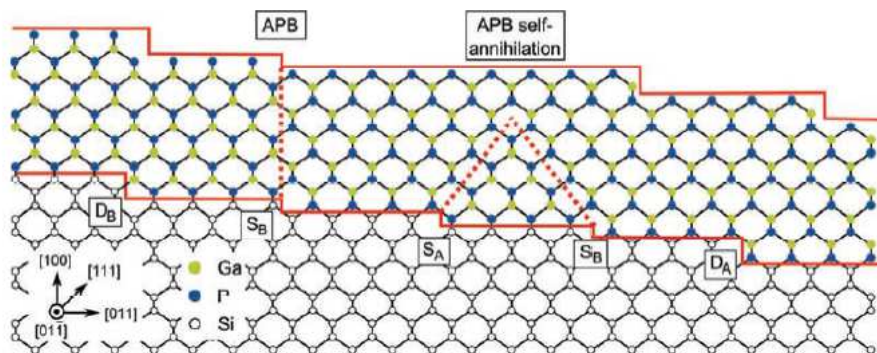
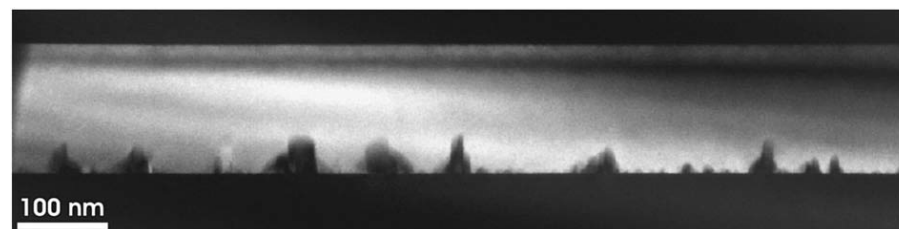


Figure 3: Schematic diagram of the formation of anti-phase disorder due to III-V heteroepitaxy on a Si(100) substrate. Single-layer steps of the Si(100) surface induce anti-phase boundaries (APBs) which penetrate through the film and can be subject to self-annihilation, while double-layer steps on the substrate prevent the formation of APBs during nucleation.



(002) Dark field TEM image in [110] cross section of the GaP/Si heterolayer. Self-annihilation of all antiphase domains leads to antiphase disorder free GaP layer after about 50 nm of overgrowth
 B. Kunert et al. / Thin Solid Films 517 (2008) 140–143

DOESCHER PhD,

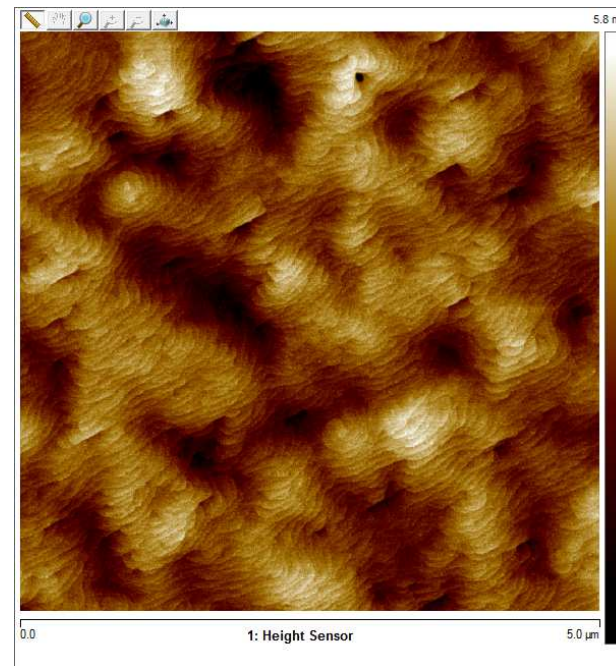
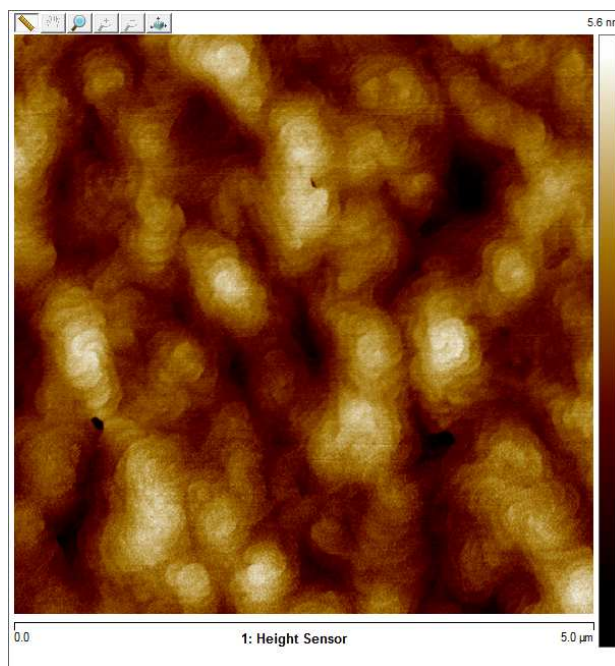
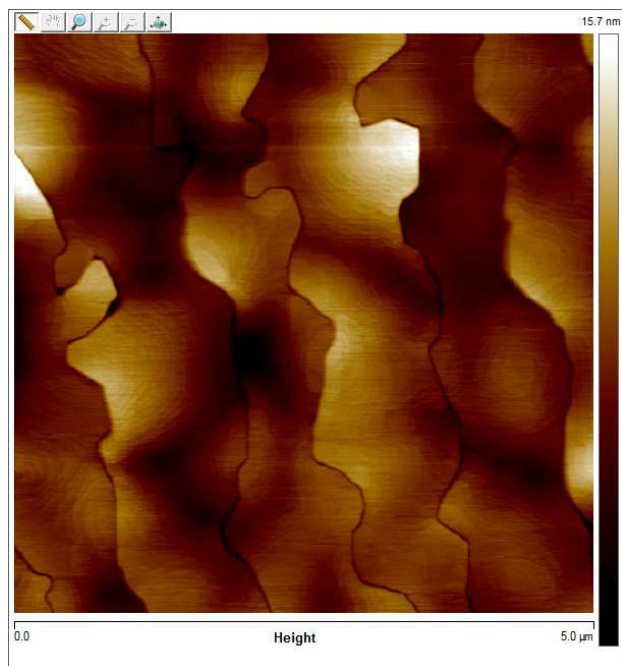
- ❑ **Optimization of GaAs buffer on nominal Si(100)**
- ❑ **Growth of InP on GaAs/Si(100)**
- ❑ **Development of InGaAs growth on InP(100) substrates**



GaAs
RMS roughness : 1,4 nm
APB density = 1,83 μm^{-1}

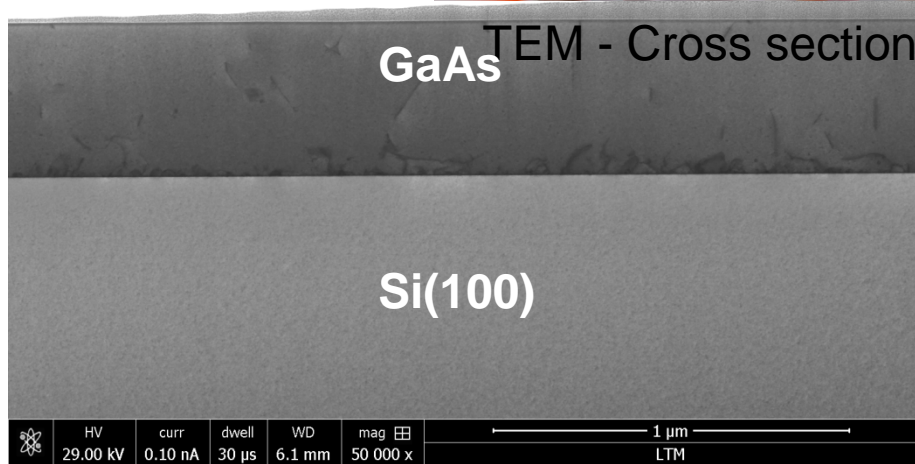
Optimized GaAs
RMS roughness : 0,9 nm

Optimized GaAs
RMS roughness : 0,8 nm

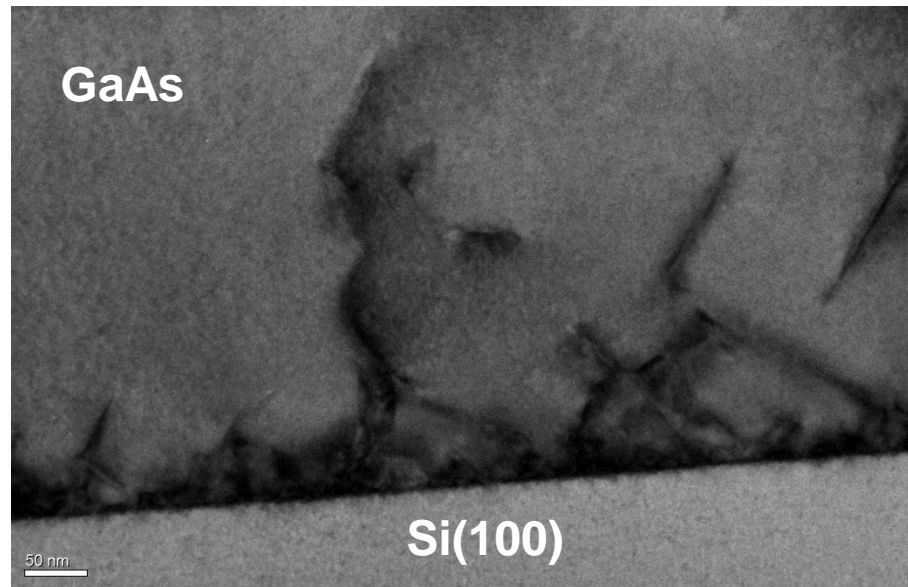
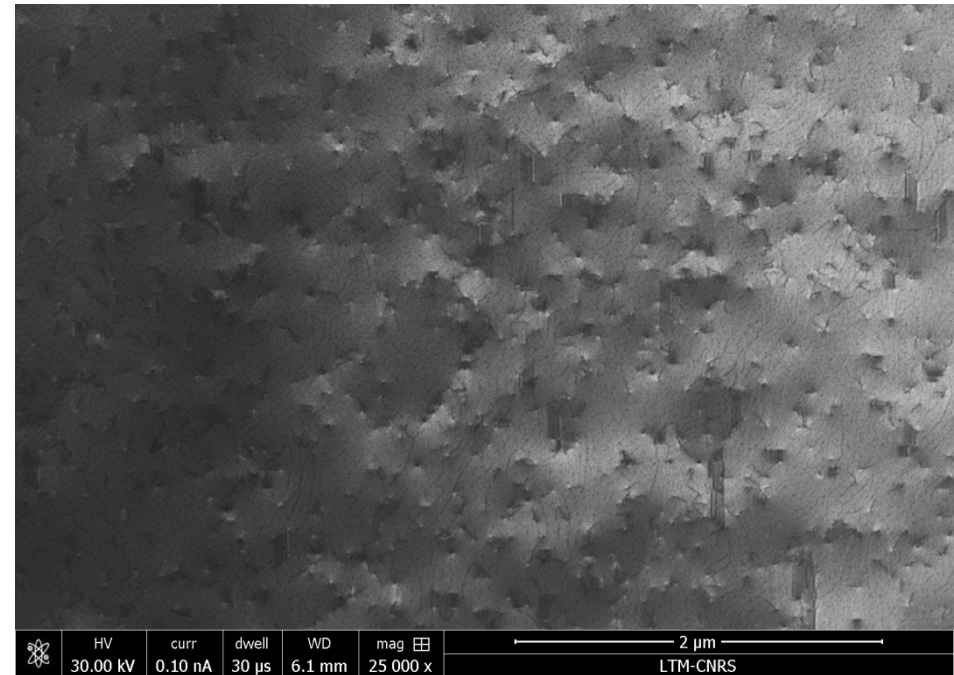




TEM analysis



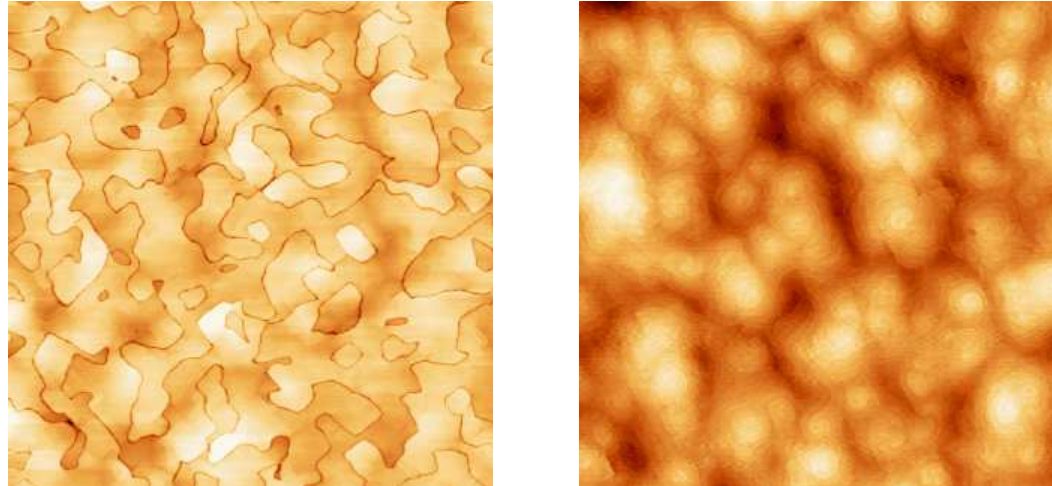
TEM – Top view



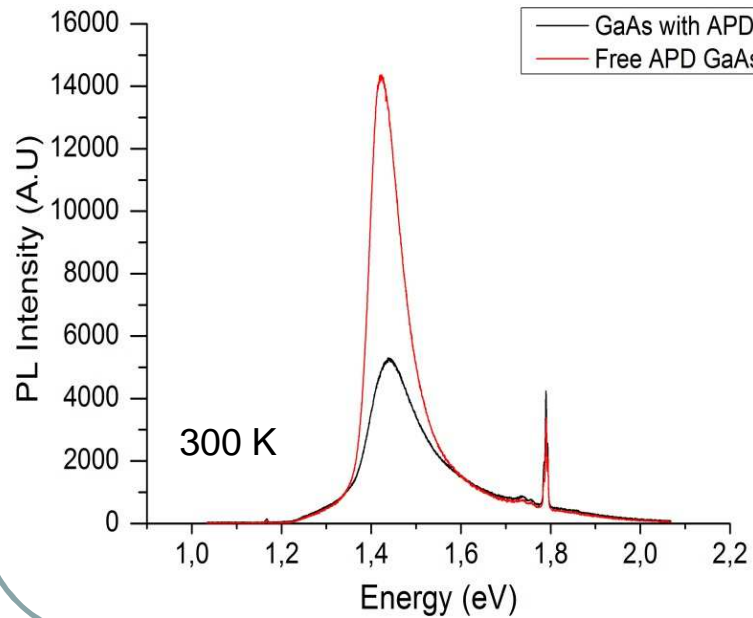
□ Evaluation of dislocation density, 10^9 cm^{-2}

Physical properties of GaAs buffer layer

AFM 5x5 μm^2 pictures



μPL @ RT



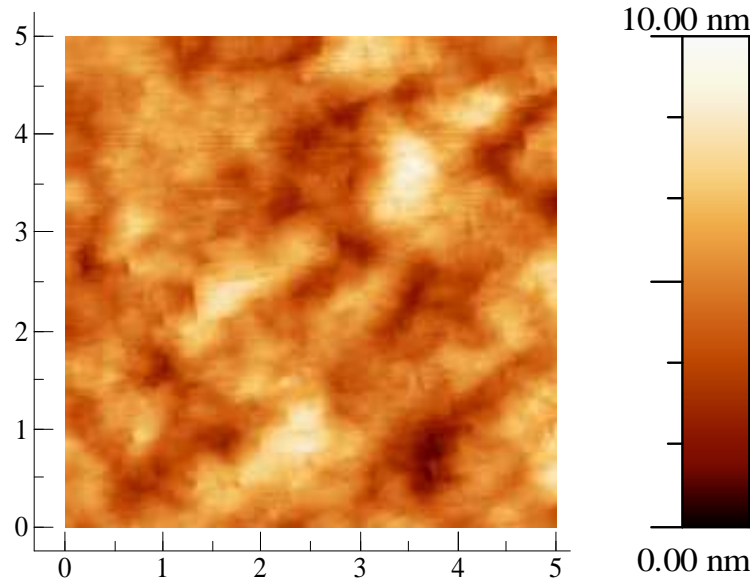
Hall effect measurements @ RT

	Roughness (nm)	APD density (cm^{-1})	μPL peak energy (eV)	FWHM meV	Electron mobility ($\text{cm}^2 \cdot \text{V}^{-1} \cdot \text{s}^{-1}$)
GaAs with APD	1,7	4	1,44	140	200
Free APD GaAs	1	No APD	1,42	87	1600

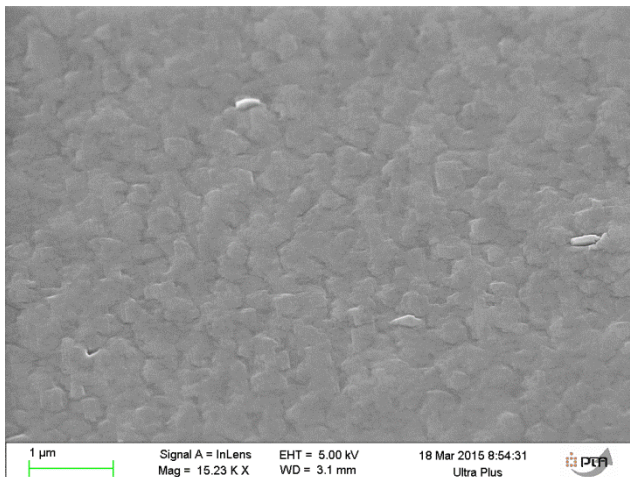
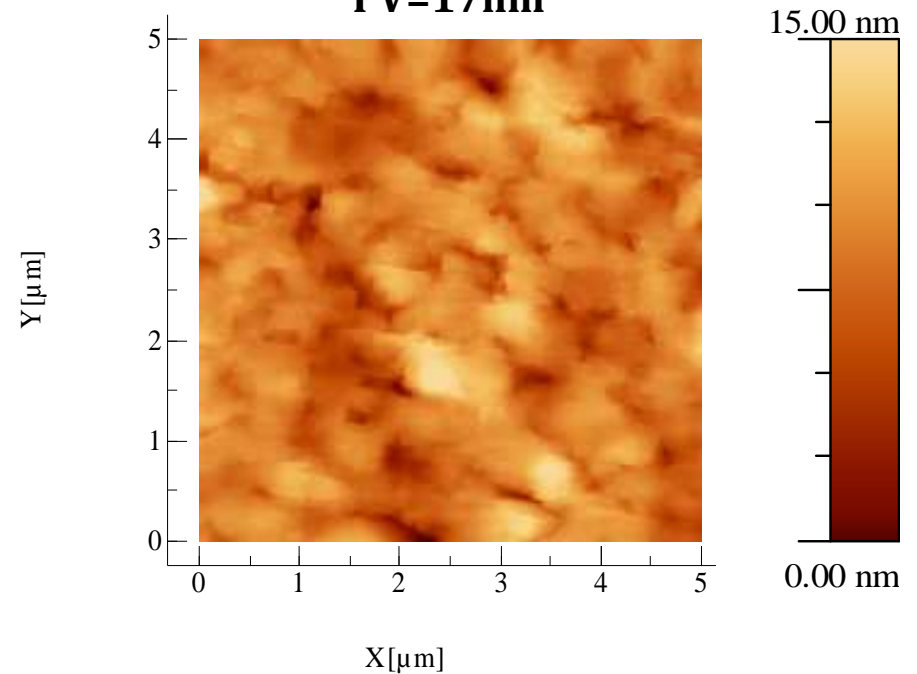
X8
↓

InGaAs/InP buffer/GaAs buffer/Si(100)

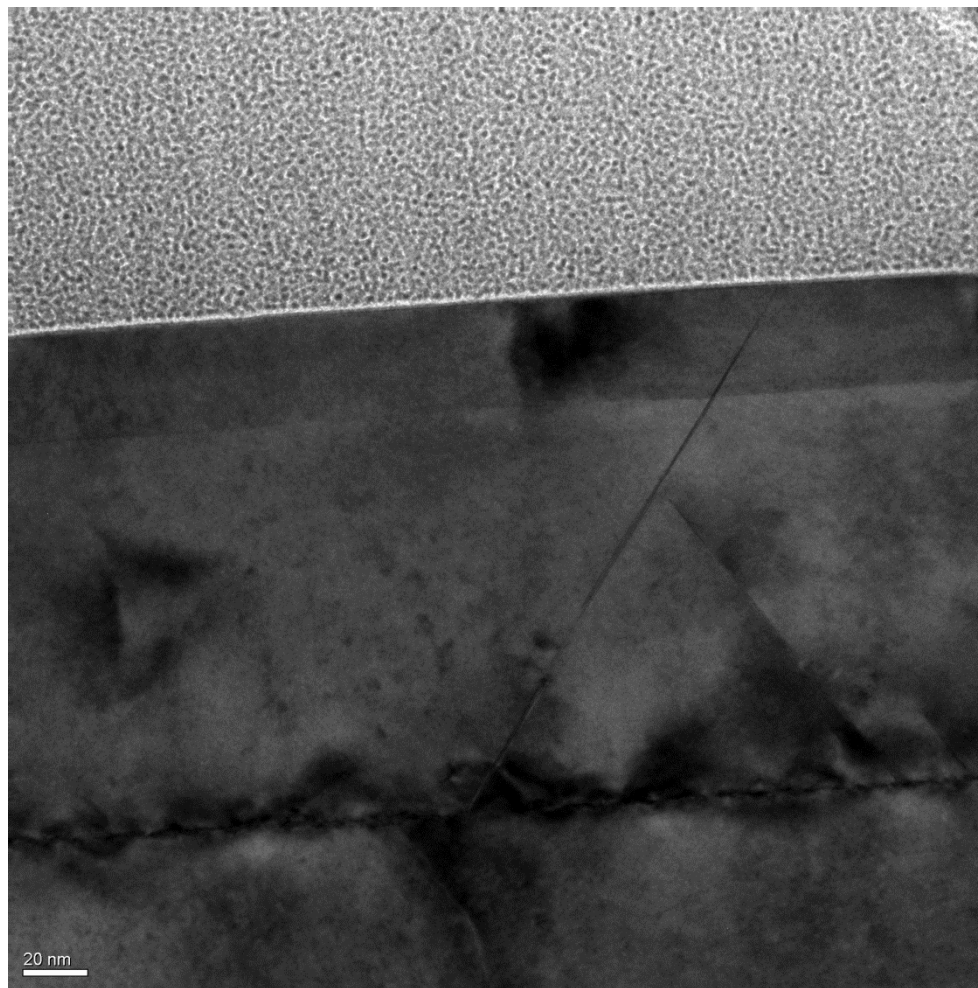
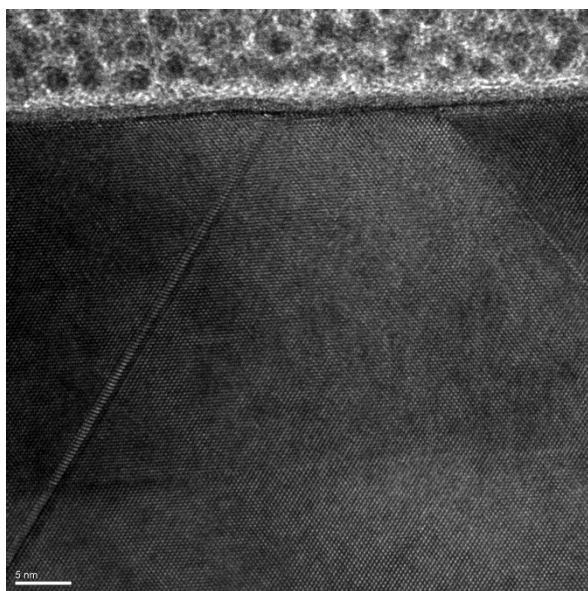
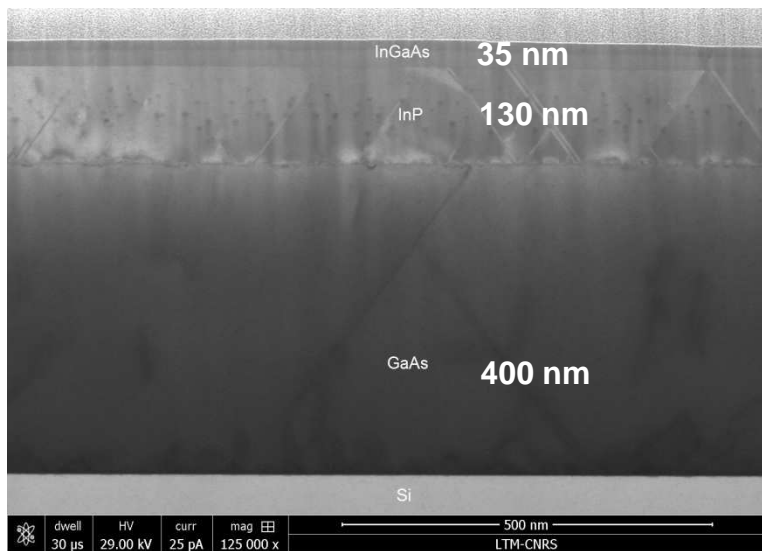
Si(100)/GaAs/InP
 $\sigma = 1,2 \text{ nm}$
PV=9nm



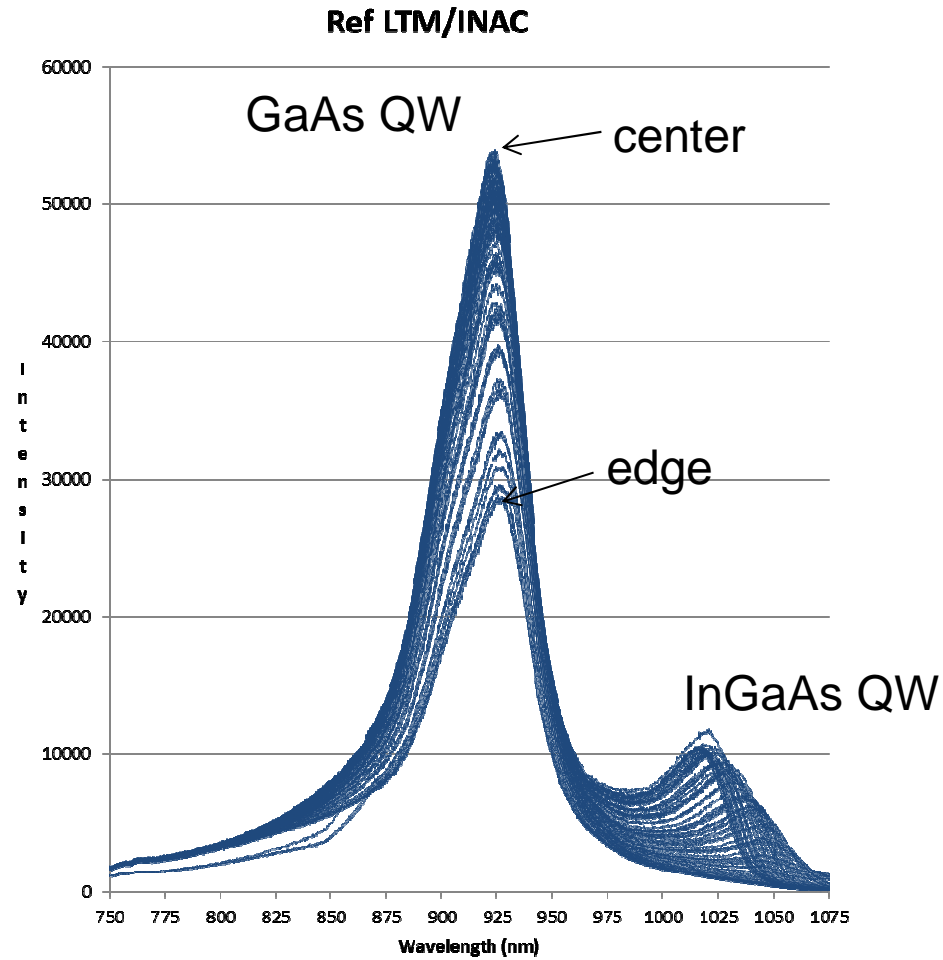
Si(100)/GaAs/InP/In_{0,53}Ga_{0,47}As
 $\sigma = 2,1 \text{ nm}$
PV=17nm



□ Optimization of InGaAs still needed



- GaAs/AlAs/GaAs QW/AlAs/GaAs/InGaAs QW/GaAs/AlAs/GaAs/Si(100)

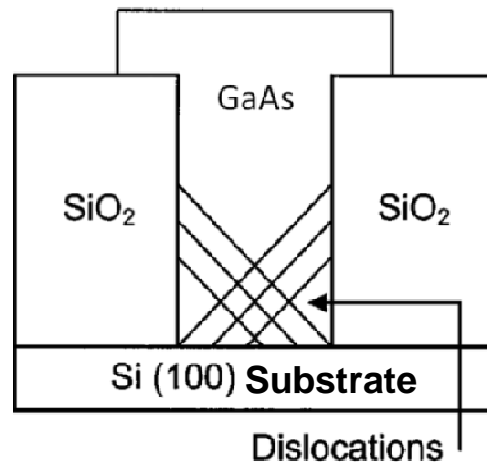
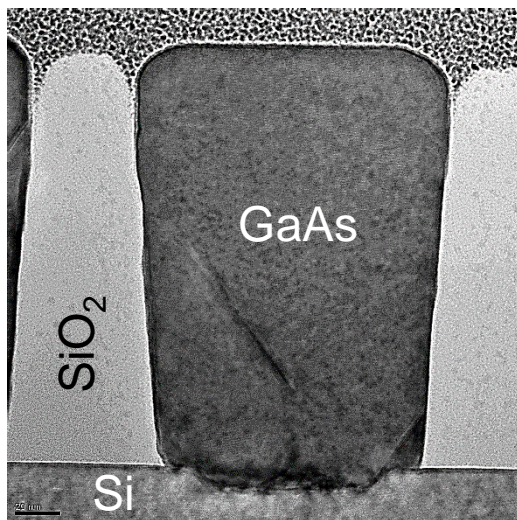
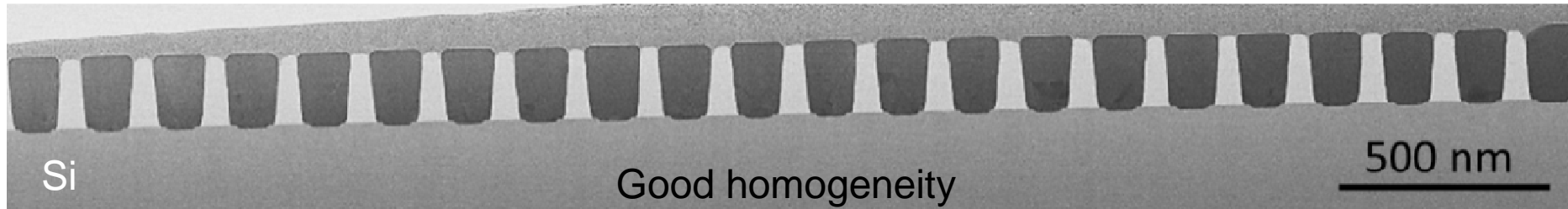


- High dislocation density (10^9 cm^{-2}), to be improved

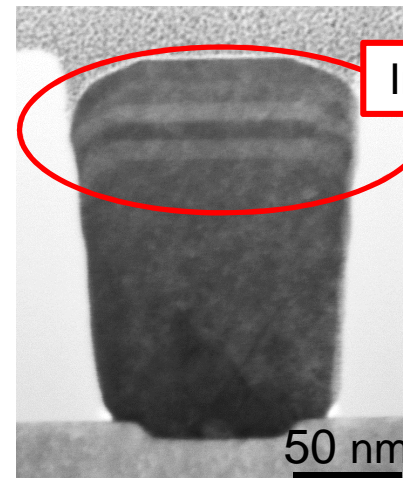


Aspect Ratio Trapping : selective epitaxial growth

GaAs selective epitaxial growth in SiO₂ patterns (STEM cross sectional views)



Amber Wave



InGaAs QW

To measure the material quality :

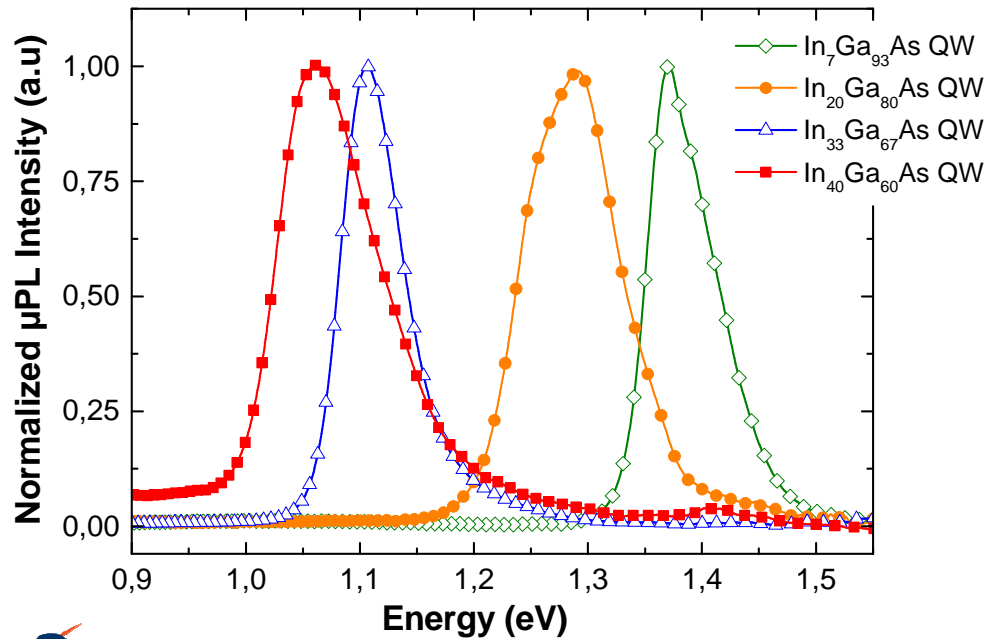
- Growth of InGaAs/AlGaAs quantum well in the top region : optical measurements

Annihilation of anti-phase boundaries, emerging dislocations, stacking fault



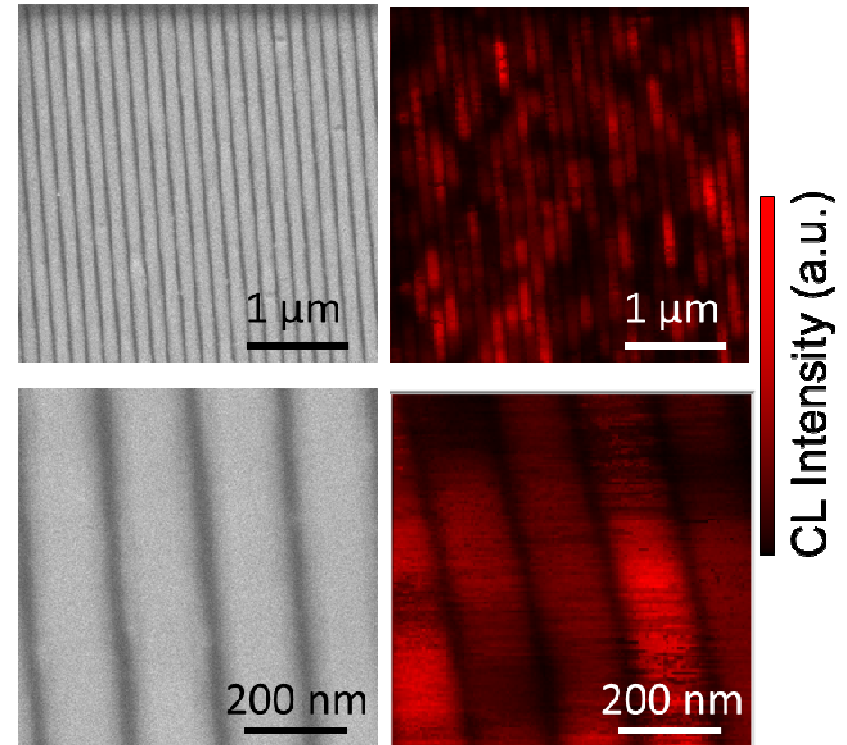
Optical measurements

- μ PL at room temperature



R. Cipro et al., Appl. Phys. Lett. **104**, 262103 (2014)

- Cathodolum. mapping at low temperature (top view)



- Room temperature μ PL signal with FWHM of 60 meV is seen on pattern with dimension <200 nm
- Non radiative recombination centers degrade the luminescence



InGaAs MOSFET on 300 mm wafers

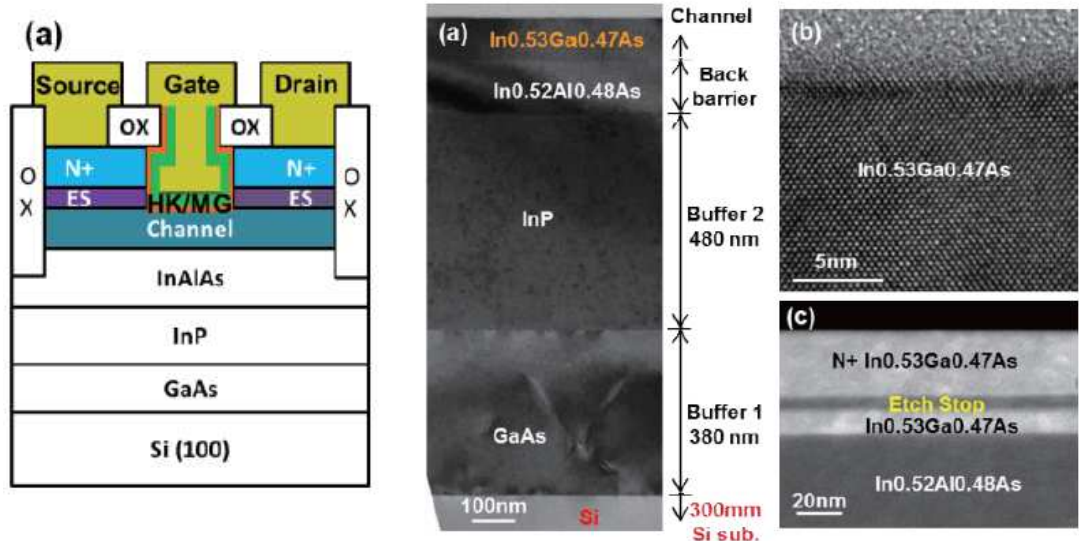


Fig. 1 (a) XTEM images of InGaAs channel with InAlAs barrier on Si. The metamorphic GaAs/InP buffer has thickness of $\sim 0.86 \mu\text{m}$, (b) HRTEM image of top InGaAs channel. (c) HAADF image of InGaAs device structure on GaAs/InP platform.

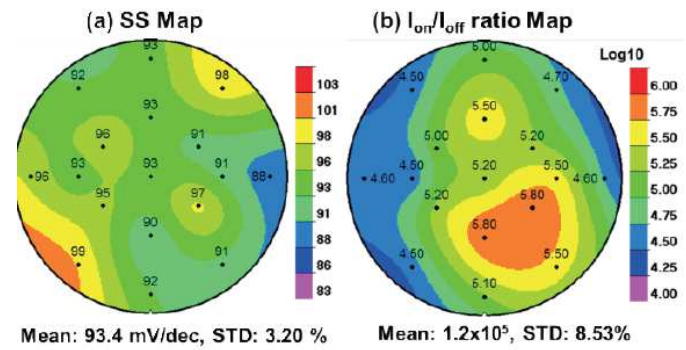


Fig. 8 The (a) SS and (b) I_{on}/I_{off} ratio map across 300mm wafer, respectively. The good uniformity with low SS(AVE) of 93 mV/dec and high I_{on}/I_{off} (AVE) ratio of 1.2×10^5 .

M.L. Huang et al. , TSMC,
VLSI Symposium 2015



InAs/InGaSb/OI NMOS and PMOSFET

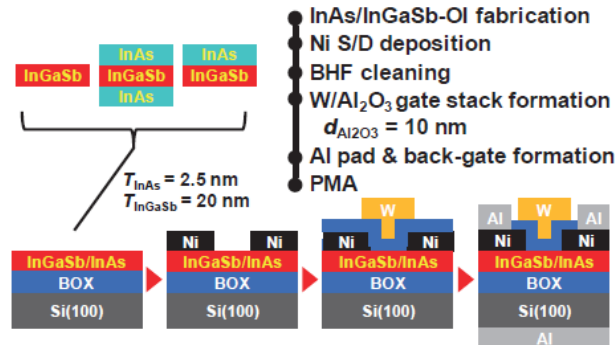


Fig. 10 Fabrication process flow of the front-gate InAs/InGaSb-OI CMOS on Si with single-layer InGaSb, InAs/InGaSb/InAs QW, and InAs/InGaSb hetero-channel.

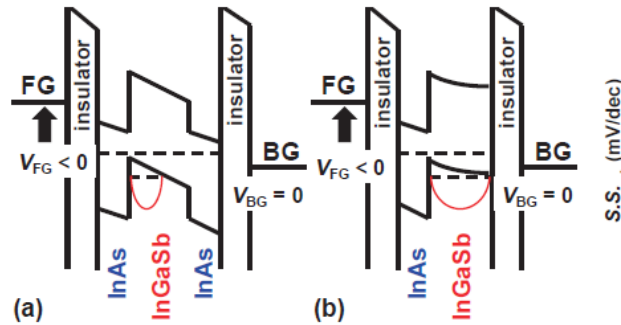


Fig. 15 Band diagram of the (a) QW and (b) hetero channel InGaSb-OI under $V_{FG} < 0$ and $V_{BG} = 0V$.

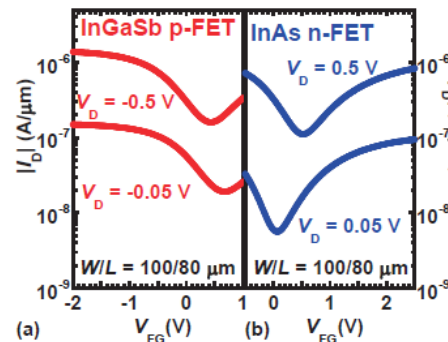


Fig. 18 I_D - V_G curves of the (a) InGaSb-OI p-MOSFET and (b) the InAs-OI n-MOSFET.

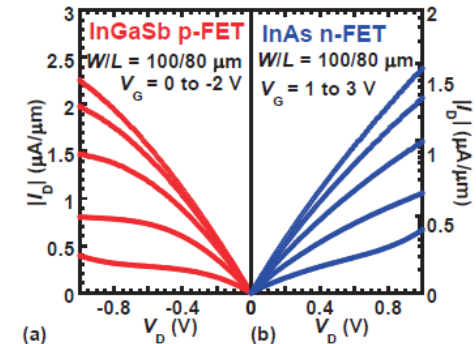


Fig. 19 I_D - V_D curves of the (a) InGaSb-OI p-MOSFET and (b) the InAs-OI n-MOSFET.

K. Nishi, et al. University of Tokyo,
VLSI Symposium 2015



InGaAs-OI FinFET by selective + lateral epitaxy

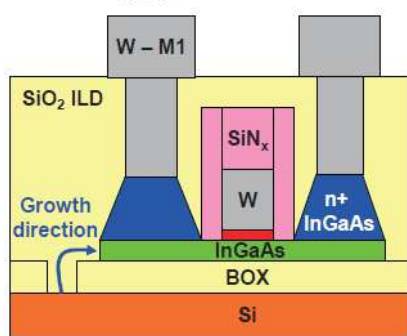


Fig. 8: Schematic of the fabricated gate-first InGaAs MOSFETs highlighting the InGaAs growth direction from the Si seed.

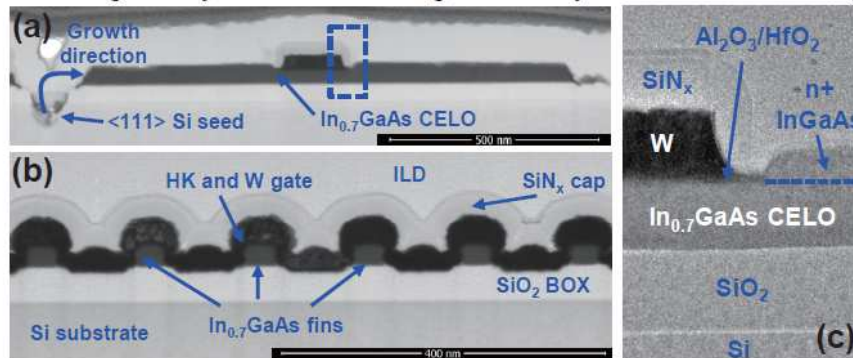


Fig. 9: Cross-sectional TEM images of a self-aligned InGaAs-OI FinFET integrated on Si by CELO. Views are (a,c) across the gate and (b) across the 25nm x 35nm fins. Standard gate-first process [8] with raised source/drain could be applied seamlessly thanks to the excellent InGaAs thermal stability.

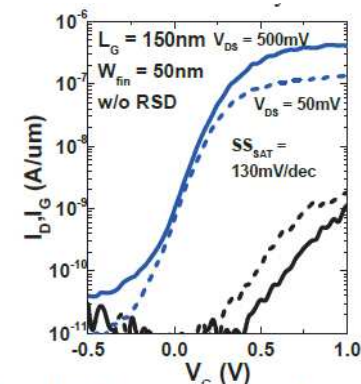


Fig. 10: Transfer an InGaAs FinFET without RSD showing an excellent I_{ON}/I_{OFF} ratio above 10^4 decades suggesting a low background doping.

❑ CNRS-LTM staff

➤ M. Martin, J. Moeyart, F. Bassani, B. Salem, S. David, C. Ternon...

❑ CEA -Leti, T. Ernst, H. Boutry, P. Mur, F. Martin, JM. Hartmann ...

❑ CNRS, UJF, Renatech, PTA, ANR, European founding,

❑ PhD works :

➤ NCS : F. Mazen, J. Dufourcq, G. Gay

➤ NWS / F. Dhalluin, A. Potié, G. Rosaz, P. Periwal, PH Morel, F. Oelher, P. Serre

➤ III-V/Si : R. Cipro, R. Alcotte, V. Gorbenko, M. Billaud,